Tensor network methods for lattice gauge theories

Krzysztof Cichy
Adam Mickiewicz University, Poznań, Poland

in collaboration with:
Mari Carmen Bañuls (MPQ Garching)
J. Ignacio Cirac (MPQ Garching)
Karl Jansen (DESY Zeuthen)
Stefan Kühn (MPQ Garching, Perimeter Institute)
Hana Saito (DESY Zeuthen)

Talk outline

1. Introduction
   - Motivation
   - Schwinger model, $N_f = 1, 2$
2. Review of results
   - Abelian case (Schwinger model (2D)):
     - ⋆ $N_f = 1$, $T = 0$: spectrum
     - ⋆ $N_f = 1$, $T > 0$: chiral condensate
     - ⋆ $N_f = 2$, $T = 0$: non-zero chemical potential
   - Non-Abelian case ($SU(2)$ (2D)):
     - ⋆ $N_f = 1$, $T = 0$: spectrum
     - ⋆ $N_f = 1$, $T = 0$: entanglement entropy
3. Summary

Based on:

- M. C. Bañuls, K.C., K. Jansen and J. I. Cirac, "The mass spectrum of the Schwinger model with Matrix Product States," JHEP **1311** (2013) 158, [arXiv:1305.3765 [hep-lat]]
- M. C. Bañuls, K.C., J. I. Cirac, K. Jansen and H. Saito, "Thermal evolution of the Schwinger model with Matrix Product Operators," Phys. Rev. **D92** (2015) 034519, [arXiv:1505.00279 [hep-lat]]
- M. C. Bañuls, K.C., K. Jansen and H. Saito, "Chiral condensate in the Schwinger model with Matrix Product Operators," Phys. Rev. **D93** (2016) 094512, [arXiv:1603.05002 [hep-lat]]
- M. C. Bañuls, K.C., J. I. Cirac, K. Jansen and S. Kühn, "Density Induced Phase Transitions in the Schwinger Model: A Study with Matrix Product States," Phys. Rev. Lett. **118** (2017) 071601, [arXiv:1611.00705 [hep-lat]]
- M. C. Bañuls, K.C., J.I. Cirac, K. Jansen and S. Kühn, "Efficient basis formulation for 1+1 dimensional SU(2) lattice gauge theory: Spectral calculations with matrix product states," Phys. Rev. **X7** (2017) 041046 [arXiv:1707.06434 [hep-lat]]

Recent review:

- M. C. Bañuls, K.C., J.I. Cirac, K. Jansen and S. Kühn, "Tensor Networks and their use for Lattice Gauge Theories," PoS LATTICE2018 (2018) 022 [arXiv:1810.12838 [hep-lat]]

Active area of research – LFT

- DMRG approach, Schwinger model – T. Byrnes et al. [Phys.Rev. **D66** (2002) 013002]
- DMRG, 2d $\lambda\phi^4$ – T. Sugihara [JHEP **0405** (2004) 007]
- MPS, Z(2) LGT – T. Sugihara [JHEP **0507** (2005) 022]
- Atomic Quantum Simulation of LGTs – D. Banerjee et al.[PRL 109 (2012) 175302, PRL 110 (2013) 125303]
- MPS, Schwinger model spectrum – M.C. Bañuls et al. [JHEP **1311** (2013) 158]
- Optical Abelian LGTs – L. Tagliacozzo et al. [Annals Phys. 330 (2013) 160]
- MPS, 2d $\lambda\phi^4$ – A. Milsted et al. [Phys.Rev. **D88**, 085030 (2013)]
- TN, quantum link models – E. Rico et al. [PRL 112 (2014) 201601]
- MPS, Schwinger model – B. Buyens et al. [PRL 113 (2014) 091601]
- Grassmann TRG, Schwinger model – Y. Shimizu et al. [Phys.Rev. D90 (2014) 014508]
- Lattice Gauge Tensor Networks – P. Silvi et al. [New J.Phys. 16 (2014) no.10, 103015]
- Tensor Networks for LGTs with continuous groups – L. Tagliacozzo et al. [Phys.Rev. X4 (2014) 041024]
- Gauging quantum states – J. Haegeman et al., [Phys.Rev. X5 (2015) 011024]
- LGTs for Quantum Simulations – E. Zohar, M. Burrello [Phys.Rev. D91 (2015) 054506]
- MPS, Schwinger model $T > 0$ – M.C. Bañuls et al. [Phys.Rev. **D92** (2015) 034519, Phys.Rev. **D93** (2016) 094512]
- Fermionic PEPS with U(1) gauge symmetry – E. Zohar et al. [Annals Phys. 363 (2015) 385-439]
- MPS, SU(2) gauge theory spectrum and entanglement – S. Kühn et al. [JHEP 1507 (2015) 130]
- MPS, Schwinger model real-time dynamics – T. Pichler et al. [Phys.Rev. X6 (2016) 011023], B. Buyens et al. [Phys.Rev. X6 (2016) no.4, 041040]
- PEPS with non-Abelian symmetries – E. Zohar et al. [Annals Phys. 374 (2016) 84]
- MPS, Schwinger model $T > 0$ – B. Buyens et al. [Phys.Rev. D94 (2016) 085018]
- MPS, $N_f = 2$ Schwinger model with chemical potential – M.C. Bañuls et al. [PRL **118** (2017) 071601]
- Schwinger model with iMPS – K. Zapp, R. Orus [Phys.Rev. D95 (2017) 114508]
- MPS, SU(2) gauge theory at finite density – P. Silvi et al. [Quantum 1, 9 (2017)]
- topological defects in QFT – E. Gillmann, A. Rajantie [Phys.Rev. D96 (2017) 094509]
- MPS, SU(2) gauge theory spectrum and entanglement – M.C. Bañuls et al. [Phys. Rev. **X7** (2017) 041046]
- classification of MPS with gauge symmetry – I. Kull et al. [Annals Phys. 386 (2017) 199]
- combining TNS with MC – E. Zohar, J.I. Cirac [Phys.Rev. D97 (2018) 034510]
- Gaussian states for 1+1d U(1), SU(2) – P. Sala et al. [Phys.Rev. D98, 034505]
- fermionic PEPS for LGTs – E. Zohar [arXiv:1807.01294]
- 2d Thirring model – M.C. Bañuls et al. [arXiv:1810.12038]
- 2d O(3) model – F. Bruckmann et al. [arXiv:1812.00944]
- compact 1D QCD at finite density – P. Silvi et al. [arXiv:1901.04403]

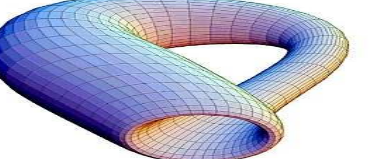

Active area of research – LFT

- DMRG approach, Schwinger model – T. Byrnes et al. [Phys.Rev. **D66** (2002) 013002]
- DMRG, 2d $\lambda\phi^4$ – T. Sugihara [JHEP **0405** (2004) 007]
- MPS, Z(2) LGT – T. Sugihara [JHEP **0507** (2005) 022]
- Atomic Quantum Simulation of LGTs – D. Banerjee et al.[PRL 109 (2012) 175302, PRL 110 (2013) 125303]
- MPS, Schwinger model spectrum – M.C. Bañuls et al. [JHEP **1311** (2013) 158]
- Optical Abelian LGTs – L. Tagliacozzo et al. [Annals Phys. 330 (2013) 160]
- MPS, 2d $\lambda\phi^4$ – A. Milsted et al. [Phys.Rev. **D88**, 085030 (2013)]
- TN, quantum link models – E. Rico et al. [PRL 112 (2014) 201601]
- MPS, Schwinger model – B. Buyens et al. [PRL 113 (2014) 091601]
- Grassmann TRG, Schwinger model – Y. Shimizu et al. [Phys.Rev. D90 (2014) 014508]
- Lattice Gauge Tensor Networks – P. Silvi et al. [New J.Phys. 16 (2014) no.10, 103015]
- Tensor Networks for LGTs with continuous groups – L. Tagliacozzo et al. [Phys.Rev. X4 (2014) 041024]
- Gauging quantum states – J. Haegeman et al., [Phys.Rev. X5 (2015) 011024]
- LGTs for Quantum Simulations – E. Zohar, M. Burrello [Phys.Rev. D91 (2015) 054506]
- MPS, Schwinger model $T > 0$ – M.C. Bañuls et al. [Phys.Rev. **D92** (2015) 034519, Phys.Rev. **D93** (2016) 094512]
- Fermionic PEPS with U(1) gauge symmetry – E. Zohar et al. [Annals Phys. 363 (2015) 385-439]
- MPS, SU(2) gauge theory spectrum and entanglement – S. Kühn et al. [JHEP 1507 (2015) 130]
- MPS, Schwinger model real-time dynamics – T. Pichler et al. [Phys.Rev. X6 (2016) 011023], B. Buyens et al. [Phys.Rev. X6 (2016) no.4, 041040]
- PEPS with non-Abelian symmetries – E. Zohar et al. [Annals Phys. 374 (2016) 84]
- MPS, Schwinger model $T > 0$ – B. Buyens et al. [Phys.Rev. D94 (2016) 085018]
- MPS, $N_f = 2$ Schwinger model with chemical potential – M.C. Bañuls et al. [PRL **118** (2017) 071601]
- Schwinger model with iMPS – K. Zapp, R. Orus [Phys.Rev. D95 (2017) 114508]
- MPS, SU(2) gauge theory at finite density – P. Silvi et al. [Quantum 1, 9 (2017)]
- topological defects in QFT – E. Gillmann, A. Rajantie [Phys.Rev. D96 (2017) 094509]
- MPS, SU(2) gauge theory spectrum and entanglement – M.C. Bañuls et al. [Phys. Rev. **X7** (2017) 041046]
- classification of MPS with gauge symmetry – I. Kull et al. [Annals Phys. 386 (2017) 199]
- combining TNS with MC – E. Zohar, J.I. Cirac [Phys.Rev. D97 (2018) 034510]
- Gaussian states for 1+1d U(1), SU(2) – P. Sala et al. [Phys.Rev. D98, 034505]
- fermionic PEPS for LGTs – E. Zohar [arXiv:1807.01294]
- 2d Thirring model – M.C. Bañuls et al. [arXiv:1810.12038]
- 2d O(3) model – F. Bruckmann et al. [arXiv:1812.00944]
- compact 1D QCD at finite density – P. Silvi et al. [arXiv:1901.04403]

Sorry, certainly still incomplete...

Motivation

- The motivation for applying TN methods to LQCD comes mostly from the sign problem that appears for certain parameter regimes of MC simulations.

Motivation

- The motivation for applying TN methods to LQCD comes mostly from the sign problem that appears for certain parameter regimes of MC simulations.
- The (Euclidean) QCD path integral: $Z = \int D\bar{\psi} D\psi DU \; e^{-S_{gauge}[U] - S_{ferm}[\psi,\bar{\psi},U]}$.

Motivation

- The motivation for applying TN methods to LQCD comes mostly from the sign problem that appears for certain parameter regimes of MC simulations.
- The (Euclidean) QCD path integral: $Z = \int D\bar{\psi} D\psi DU \; e^{-S_{gauge}[U] - S_{ferm}[\psi,\bar{\psi},U]}$.
  static properties, zero baryon density: no sign problem! $\Rightarrow$ tremedous successes

Motivation

- The motivation for applying TN methods to LQCD comes mostly from the sign problem that appears for certain parameter regimes of MC simulations.
- The (Euclidean) QCD path integral: $Z = \int D\bar{\psi} D\psi DU \; e^{-S_{gauge}[U] - S_{ferm}[\psi,\bar{\psi},U]}$.
  static properties, zero baryon density: no sign problem! $\Rightarrow$ tremedous successes
  real-time dynamics: impossible in Euclidean spacetime...

Motivation

- The motivation for applying TN methods to LQCD comes mostly from the sign problem that appears for certain parameter regimes of MC simulations.
- The (Euclidean) QCD path integral: $Z = \int D\bar{\psi} D\psi DU \; e^{-S_{gauge}[U] - S_{ferm}[\psi,\bar{\psi},U]}$.
  static properties, zero baryon density: no sign problem! $\Rightarrow$ tremedous successes
  real-time dynamics: impossible in Euclidean spacetime...
  finite baryon density: mild or severe sign problem; at the same time huge physical significance of this regime

- The motivation for applying TN methods to LQCD comes mostly from the sign problem that appears for certain parameter regimes of MC simulations.
- The (Euclidean) QCD path integral: $Z = \int D\bar{\psi} D\psi DU \; e^{-S_{gauge}[U] - S_{ferm}[\psi,\bar{\psi},U]}$.
static properties, zero baryon density: no sign problem! $\Rightarrow$ tremedous successes
real-time dynamics: impossible in Euclidean spacetime...
finite baryon density: mild or severe sign problem; at the same time huge physical significance of this regime

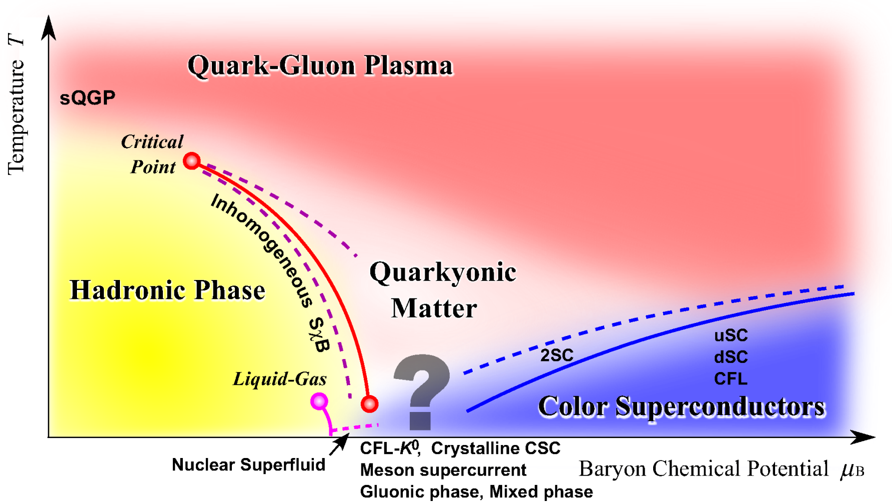

[K. Fukushima, T. Hatsuda, Rep. Prog. Phys. 74 (2011) 14001]

Motivation

- The motivation for applying TN methods to LQCD comes mostly from the sign problem that appears for certain parameter regimes of MC simulations.
- The (Euclidean) QCD path integral: $Z = \int D\bar{\psi} D\psi DU \; e^{-S_{gauge}[U] - S_{ferm}[\psi,\bar{\psi},U]}$.
static properties, zero baryon density: no sign problem! $\Rightarrow$ tremedous successes
real-time dynamics: impossible in Euclidean spacetime...
finite baryon density: mild or severe sign problem; at the same time huge physical significance of this regime

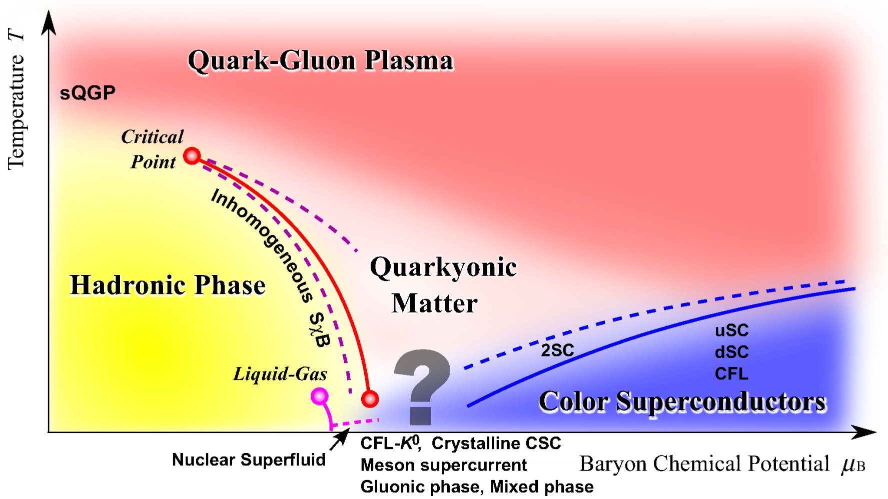

[K. Fukushima, T. Hatsuda, Rep. Prog. Phys. 74 (2011) 14001]

- Ways to alleviate the (mild) sign problem:

- The motivation for applying TN methods to LQCD comes mostly from the sign problem that appears for certain parameter regimes of MC simulations.
- The (Euclidean) QCD path integral: $Z = \int D\bar{\psi} D\psi DU \; e^{-S_{gauge}[U] - S_{ferm}[\psi,\bar{\psi},U]}$.
  static properties, zero baryon density: no sign problem! $\Rightarrow$ tremedous successes
  real-time dynamics: impossible in Euclidean spacetime...
  finite baryon density: mild or severe sign problem; at the same time huge physical significance of this regime

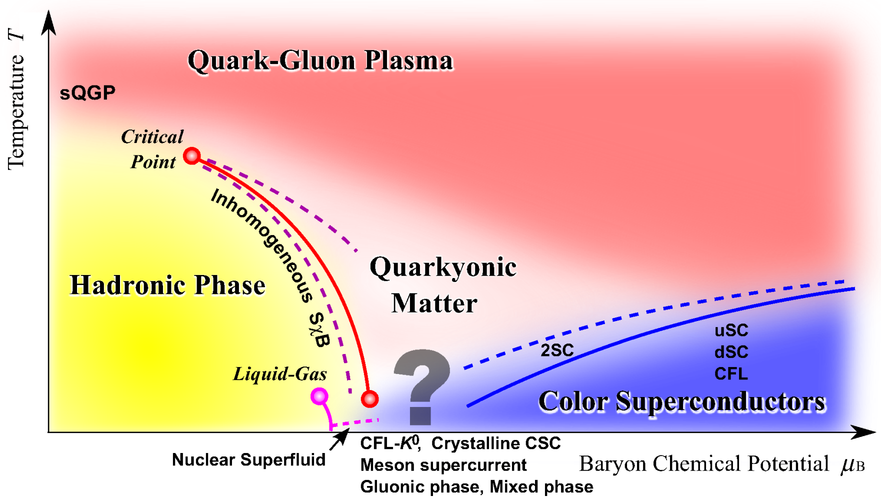

[K. Fukushima, T. Hatsuda, Rep. Prog. Phys. 74 (2011) 14001]

- Ways to alleviate the (mild) sign problem: reweighting, Taylor expansion, analytic continuation from imaginary μ, ...

Motivation

- The motivation for applying TN methods to LQCD comes mostly from the sign problem that appears for certain parameter regimes of MC simulations.
- The (Euclidean) QCD path integral: $Z = \int D\bar{\psi} D\psi DU \; e^{-S_{gauge}[U]-S_{ferm}[\psi,\bar{\psi},U]}$.
  static properties, zero baryon density: no sign problem! $\Rightarrow$ tremedous successes
  real-time dynamics: impossible in Euclidean spacetime...
  finite baryon density: mild or severe sign problem; at the same time huge physical significance of this regime

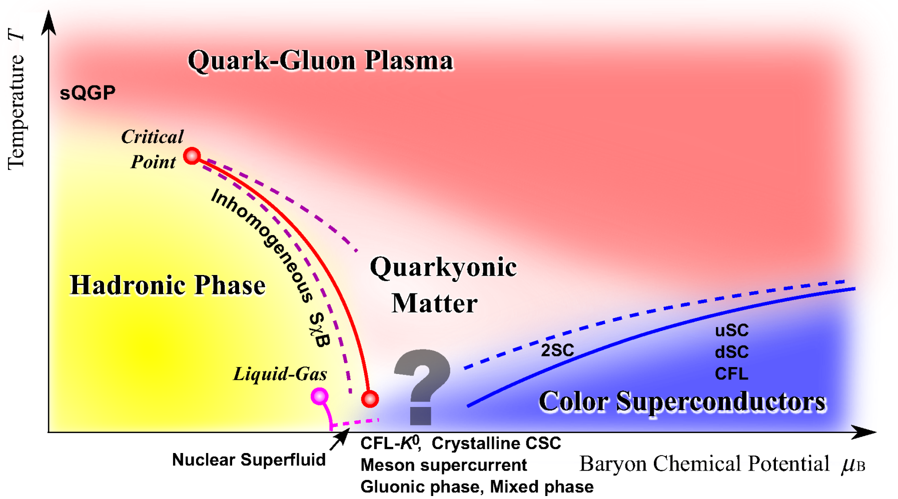

[K. Fukushima, T. Hatsuda, Rep. Prog. Phys. 74 (2011) 14001]

- Ways to alleviate the (mild) sign problem: reweighting, Taylor expansion, analytic continuation from imaginary μ, ...
  – **basically hopeless...**

- The motivation for applying TN methods to LQCD comes mostly from the sign problem that appears for certain parameter regimes of MC simulations.
- The (Euclidean) QCD path integral: $Z = \int D\bar{\psi} D\psi DU \; e^{-S_{gauge}[U] - S_{ferm}[\psi,\bar{\psi},U]}$.
  static properties, zero baryon density: no sign problem! $\Rightarrow$ tremedous successes
  real-time dynamics: impossible in Euclidean spacetime...
  finite baryon density: mild or severe sign problem; at the same time huge physical significance of this regime

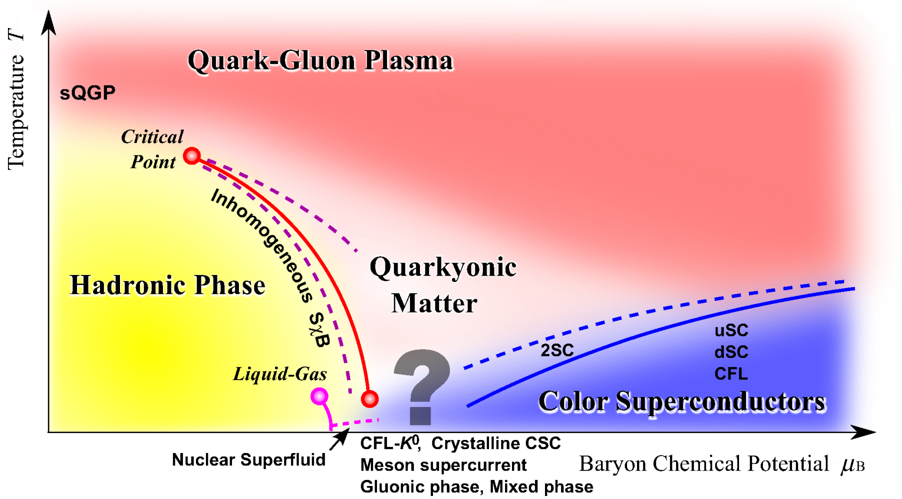

[K. Fukushima, T. Hatsuda, Rep. Prog. Phys. 74 (2011) 14001]

- Ways to alleviate the (mild) sign problem: reweighting, Taylor expansion, analytic continuation from imaginary μ, ...
  – **basically hopeless...**
- Smarter ways:

Motivation

- The motivation for applying TN methods to LQCD comes mostly from the sign problem that appears for certain parameter regimes of MC simulations.
- The (Euclidean) QCD path integral: $Z = \int D\bar{\psi} D\psi DU \; e^{-S_{gauge}[U] - S_{ferm}[\psi,\bar{\psi},U]}$.
  static properties, zero baryon density: no sign problem! $\Rightarrow$ tremedous successes
  real-time dynamics: impossible in Euclidean spacetime...
  finite baryon density: mild or severe sign problem; at the same time huge physical significance of this regime

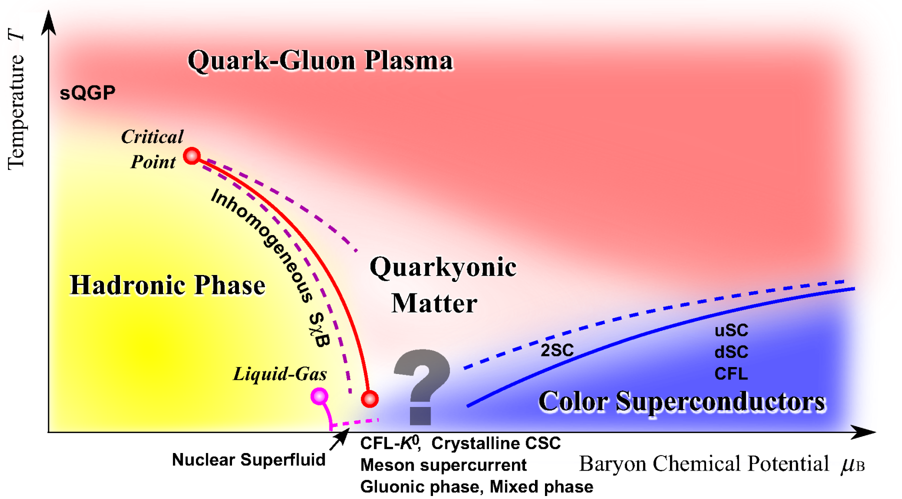

[K. Fukushima, T. Hatsuda, Rep. Prog. Phys. 74 (2011) 14001]

- Ways to alleviate the (mild) sign problem: reweighting, Taylor expansion, analytic continuation from imaginary μ, ...
  – **basically hopeless...**
- Smarter ways:
  Lefschetz thimbles, complex Langevin, ...

Motivation

- The motivation for applying TN methods to LQCD comes mostly from the sign problem that appears for certain parameter regimes of MC simulations.
- The (Euclidean) QCD path integral: $Z = \int D\bar{\psi} D\psi DU \; e^{-S_{gauge}[U] - S_{ferm}[\psi,\bar{\psi},U]}$.
  static properties, zero baryon density: no sign problem! $\Rightarrow$ tremedous successes
  real-time dynamics: impossible in Euclidean spacetime...
  finite baryon density: mild or severe sign problem; at the same time huge physical significance of this regime

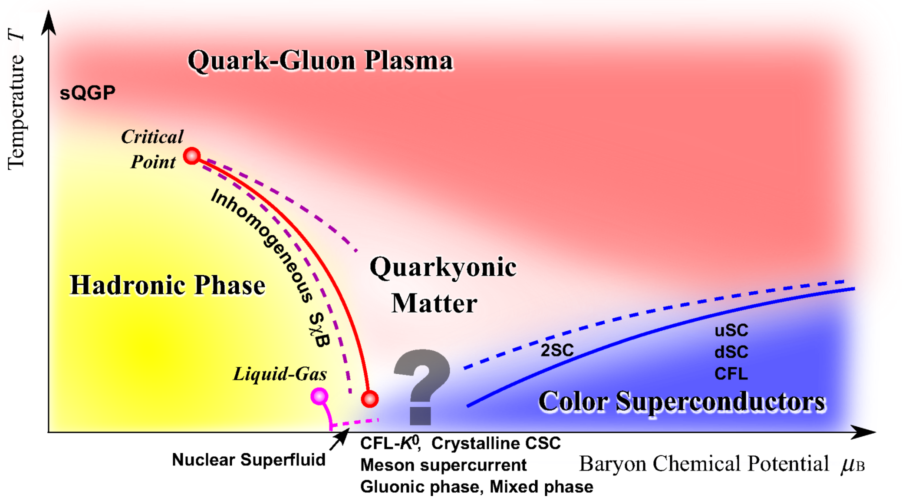

[K. Fukushima, T. Hatsuda, Rep. Prog. Phys. 74 (2011) 14001]

- Ways to alleviate the (mild) sign problem: reweighting, Taylor expansion, analytic continuation from imaginary μ, ...
  – **basically hopeless...**
- Smarter ways:
  Lefschetz thimbles, complex Langevin, ...
  – **interesting progress and hope for good results for regimes with severe sign problem!**

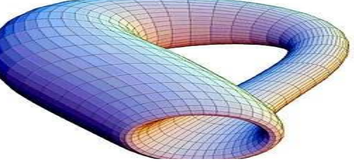

Motivation

- The motivation for applying TN methods to LQCD comes mostly from the sign problem that appears for certain parameter regimes of MC simulations.
- The (Euclidean) QCD path integral: $Z = \int D\bar{\psi} D\psi DU \; e^{-S_{gauge}[U] - S_{ferm}[\psi,\bar{\psi},U]}$.
  static properties, zero baryon density: no sign problem! $\Rightarrow$ tremedous successes
  real-time dynamics: impossible in Euclidean spacetime...
  finite baryon density: mild or severe sign problem; at the same time huge physical significance of this regime

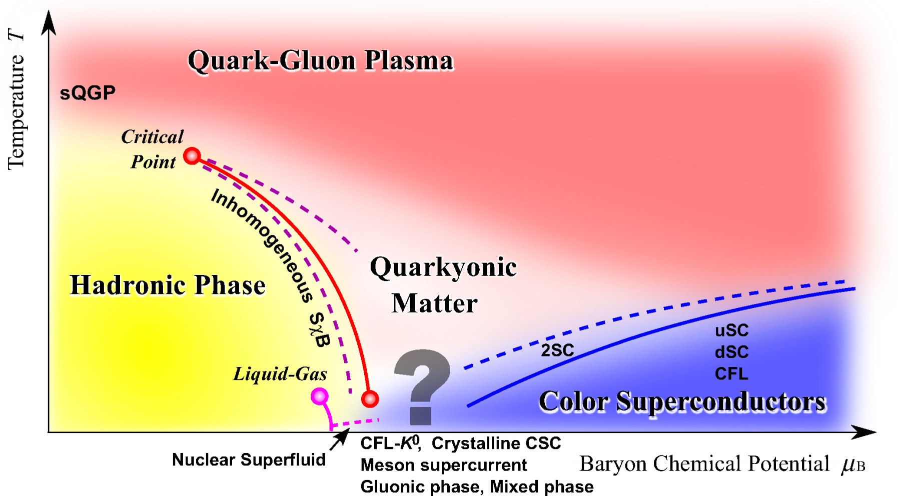

[K. Fukushima, T. Hatsuda, Rep. Prog. Phys. 74 (2011) 14001]

- Ways to alleviate the (mild) sign problem: reweighting, Taylor expansion, analytic continuation from imaginary μ, ...
  – **basically hopeless...**
- Smarter ways:
  Lefschetz thimbles, complex Langevin, ...
  – **interesting progress and hope for good results for regimes with severe sign problem!**
- Still: **alternative approaches wanted!**

Motivation

- The motivation for applying TN methods to LQCD comes mostly from the sign problem that appears for certain parameter regimes of MC simulations.
- The (Euclidean) QCD path integral: $Z = \int D\bar{\psi} D\psi DU \; e^{-S_{gauge}[U] - S_{ferm}[\psi,\bar{\psi},U]}$.
  static properties, zero baryon density: no sign problem! $\Rightarrow$ tremedous successes
  real-time dynamics: impossible in Euclidean spacetime...
  finite baryon density: mild or severe sign problem; at the same time huge physical significance of this regime

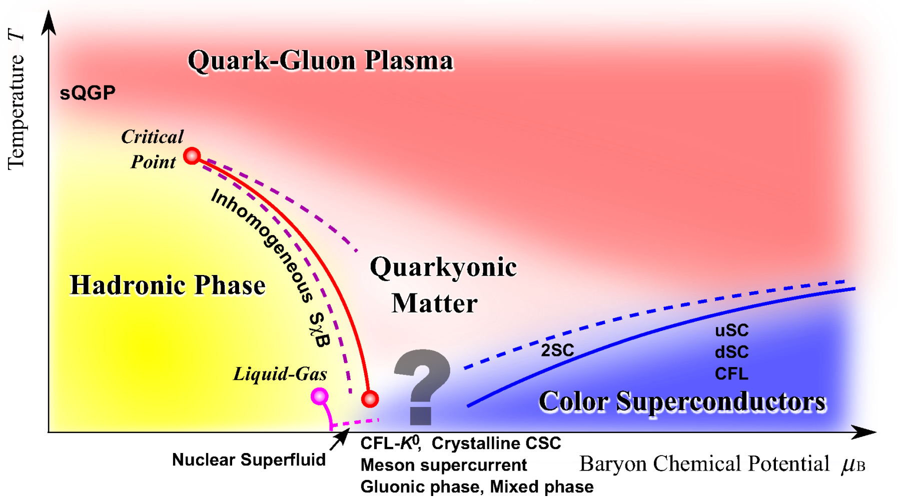

[K. Fukushima, T. Hatsuda, Rep. Prog. Phys. 74 (2011) 14001]

- Ways to alleviate the (mild) sign problem: reweighting, Taylor expansion, analytic continuation from imaginary μ, ...
  – **basically hopeless...**
- Smarter ways:
  Lefschetz thimbles, complex Langevin, ...
  – **interesting progress and hope for good results for regimes with severe sign problem!**
- Still: **alternative approaches wanted!**
  Tensor Networks?

Our main toy model: the Schwinger model (QED in 1+1d)

[J. S. Schwinger, Phys. Rev. **128** (1962) 2425]

$$\mathcal{L} = -\frac{1}{4} F_{\mu\nu} F^{\mu\nu} + \bar{\psi}(i \not{\partial} - g \not{A} - m)\psi$$

The Schwinger model

Our main toy model: the Schwinger model (QED in 1+1d)
[J. S. Schwinger, Phys. Rev. **128** (1962) 2425]

$$\mathcal{L} = -\frac{1}{4} F_{\mu\nu} F^{\mu\nu} + \bar{\psi}(i \not{\partial} - g \not{A} - m)\psi$$

- Simplest gauge theory, but physics still surprisingly rich.

The Schwinger model

Our main toy model: the Schwinger model (QED in 1+1d)

[J. S. Schwinger, Phys. Rev. **128** (1962) 2425]

$$\mathcal{L} = -\frac{1}{4} F_{\mu\nu} F^{\mu\nu} + \bar{\psi}(i \not{\partial} - g \not{A} - m)\psi$$

- Simplest gauge theory, but physics still surprisingly rich.
- In several aspects resembles much more complex theories (QCD):
  - ⋆ confinement,
  - ⋆ chiral symmetry breaking (via anomaly, not spontaneous),
  - ⋆ non-perturbative generation of mass gap.

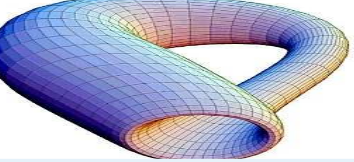

The Schwinger model

Our main toy model: the Schwinger model (QED in 1+1d)

[J. S. Schwinger, Phys. Rev. **128** (1962) 2425]

$$\mathcal{L} = -\frac{1}{4} F_{\mu\nu} F^{\mu\nu} + \bar{\psi}(i \not{\partial} - g \not{A} - m)\psi$$

- Simplest gauge theory, but physics still surprisingly rich.
- In several aspects resembles much more complex theories (QCD):
  - ⋆ confinement,
  - ⋆ chiral symmetry breaking (via anomaly, not spontaneous),
  - ⋆ non-perturbative generation of mass gap.
- Massless case analytically solvable ⇒ precise checks possible.

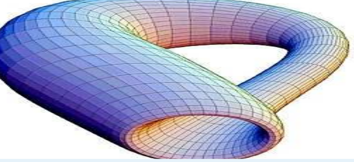

The Schwinger model

Our main toy model: the Schwinger model (QED in 1+1d)
[J. S. Schwinger, Phys. Rev. **128** (1962) 2425]

$$\mathcal{L} = -\frac{1}{4}F_{\mu\nu}F^{\mu\nu} + \bar{\psi}(i\,\not{\partial} - g\,\not{A} - m)\psi$$

- Simplest gauge theory, but physics still surprisingly rich.
- In several aspects resembles much more complex theories (QCD):
  - ⋆ confinement,
  - ⋆ chiral symmetry breaking (via anomaly, not spontaneous),
  - ⋆ non-perturbative generation of mass gap.
- Massless case analytically solvable ⇒ precise checks possible.
- Standard toy model for testing lattice techniques.

The Schwinger model

Our main toy model: the Schwinger model (QED in 1+1d)

[J. S. Schwinger, Phys. Rev. **128** (1962) 2425]

$$\mathcal{L} = -\frac{1}{4}F_{\mu\nu}F^{\mu\nu} + \bar{\psi}(i\,\not{\partial} - g\,\not{A} - m)\psi$$

- Simplest gauge theory, but physics still surprisingly rich.
- In several aspects resembles much more complex theories (QCD):
  - ⋆ confinement,
  - ⋆ chiral symmetry breaking (via anomaly, not spontaneous),
  - ⋆ non-perturbative generation of mass gap.
- Massless case analytically solvable ⇒ precise checks possible.
- Standard toy model for testing lattice techniques.

Formulation of the model:

The Schwinger model

Our main toy model: the Schwinger model (QED in 1+1d)
[J. S. Schwinger, Phys. Rev. **128** (1962) 2425]

$$\mathcal{L} = -\frac{1}{4}F_{\mu\nu}F^{\mu\nu} + \bar{\psi}(i\not\partial - g\not A - m)\psi$$

- Simplest gauge theory, but physics still surprisingly rich.
- In several aspects resembles much more complex theories (QCD):
  - ⋆ confinement,
  - ⋆ chiral symmetry breaking (via anomaly, not spontaneous),
  - ⋆ non-perturbative generation of mass gap.
- Massless case analytically solvable ⇒ precise checks possible.
- Standard toy model for testing lattice techniques.

Formulation of the model:
- staggered discretization,

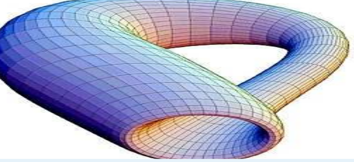

The Schwinger model

Our main toy model: the Schwinger model (QED in 1+1d)
[J. S. Schwinger, Phys. Rev. **128** (1962) 2425]

$$\mathcal{L} = -\frac{1}{4} F_{\mu\nu} F^{\mu\nu} + \bar{\psi}(i \not{\partial} - g \not{A} - m)\psi$$

- Simplest gauge theory, but physics still surprisingly rich.
- In several aspects resembles much more complex theories (QCD):
  - ⋆ confinement,
  - ⋆ chiral symmetry breaking (via anomaly, not spontaneous),
  - ⋆ non-perturbative generation of mass gap.
- Massless case analytically solvable ⇒ precise checks possible.
- Standard toy model for testing lattice techniques.

Formulation of the model:
- staggered discretization,
- Jordan-Wigner transformation to spin-1/2 variables.

Multi-flavour Schwinger model as a spin model

$$H = -xi^{N_f-1} \sum_{f=0}^{N_f-1} \sum_{n=0}^{N-2} \Big[\sigma^+_{N_f n+f} \sigma^z_{N_f n+f+1} \dots \sigma^z_{N_f n+N_f+f-1} \sigma^-_{N_f n+N_f+f} +$$

$$(-1)^{N_f-1} \sigma^-_{N_f n+f} \sigma^z_{N_f n+f+1} \dots \sigma^z_{N_f n+N_f+f-1} \sigma^+_{N_f n+N_f+f} \Big] +$$

$$+ \sum_{k=0}^{N_f N-1} \alpha_1(k) 1 + \sum_{k=0}^{N_f N-1} \alpha(k) \sigma^z_k + \sum_{k=0}^{N_f N-1} \sum_{k'=k+1}^{N_f N-1} \beta'(k') \sigma^z_k \sigma^z_{k'},$$

with:

$$\alpha_1(k) = \frac{l_0^2}{N_f} \left(1 - \delta_{k/F, N-1}\right) + l_0 \left(1 - (k/N_f)\%2\right) + \frac{1}{2} M_{k\%N_f} + \frac{1}{8}(N + N_f - 1) + \xi,$$

$$\alpha(k) = l_0(N - k/N_f - 1) + \frac{\widetilde{\mu}_{k\%N_f}}{2} + \frac{1}{2} M_{k\%N_f} (-1)^{k/N_f} + \frac{N_f}{4} \left(N - k/N_f - (k/N_f)\%2\right),$$

$$\beta'(k) = \frac{1}{2} \left(N - k/N_f - 1 + 2\xi\right),$$

HOPPING TERM

$$H = -x i^{N_f-1} \sum_{f=0}^{N_f-1} \sum_{n=0}^{N-2} \Big[\sigma^+_{N_f n+f} \sigma^z_{N_f n+f+1} \cdots \sigma^z_{N_f n+N_f+f-1} \sigma^-_{N_f n+N_f+f} +$$

HOPPING TERM H.c.

$$(-1)^{N_f-1} \sigma^-_{N_f n+f} \sigma^z_{N_f n+f+1} \cdots \sigma^z_{N_f n+N_f+f-1} \sigma^+_{N_f n+N_f+f} \Big] +$$

$$+ \sum_{k=0}^{N_f N-1} \alpha_1(k) 1 + \sum_{k=0}^{N_f N-1} \alpha(k) \sigma^z_k + \sum_{k=0}^{N_f N-1} \sum_{k'=k+1}^{N_f N-1} \beta'(k') \sigma^z_k \sigma^z_{k'},$$

with:

$$\alpha_1(k) = \frac{l_0^2}{N_f}\left(1 - \delta_{k/F,N-1}\right) + l_0\left(1 - (k/N_f)\%2\right) + \frac{1}{2} M_{k\%N_f} + \frac{1}{8}(N + N_f - 1) + \xi,$$

$$\alpha(k) = l_0(N - k/N_f - 1) + \frac{\widetilde{\mu}_{k\%N_f}}{2} + \frac{1}{2} M_{k\%N_f} (-1)^{k/N_f} + \frac{N_f}{4}\left(N - k/N_f - (k/N_f)\%2\right),$$

$$\beta'(k) = \frac{1}{2}\left(N - k/N_f - 1 + 2\xi\right),$$

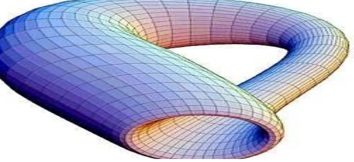

Multi-flavour Schwinger model as a spin model

HOPPING TERM

$$H = -xi^{N_f-1}\sum_{f=0}^{N_f-1}\sum_{n=0}^{N-2}\Big[\sigma^+_{N_f n+f}\sigma^z_{N_f n+f+1}\cdots\sigma^z_{N_f n+N_f+f-1}\sigma^-_{N_f n+N_f+f}+$$

HOPPING TERM H.c.

$$(-1)^{N_f-1}\sigma^-_{N_f n+f}\sigma^z_{N_f n+f+1}\cdots\sigma^z_{N_f n+N_f+f-1}\sigma^+_{N_f n+N_f+f}\Big]+$$

$$+\sum_{k=0}^{N_f N-1}\alpha_1(k)\mathbb{1}+\sum_{k=0}^{N_f N-1}\alpha(k)\sigma^z_k+\sum_{k=0}^{N_f N-1}\sum_{k'=k+1}^{N_f N-1}\beta'(k')\sigma^z_k\sigma^z_{k'},$$

INHOMOGENEOUS OFFSET

with:

$$\alpha_1(k) = \frac{l_0^2}{N_f}\left(1-\delta_{k/F,N-1}\right)+l_0\left(1-(k/N_f)\%2\right)+\frac{1}{2}M_{k\%N_f}+\frac{1}{8}(N+N_f-1)+\xi,$$

$$\alpha(k) = l_0(N-k/N_f-1)+\frac{\widetilde{\mu}_{k\%N_f}}{2}+\frac{1}{2}M_{k\%N_f}(-1)^{k/N_f}+\frac{N_f}{4}\left(N-k/N_f-(k/N_f)\%2\right),$$

$$\beta'(k) = \frac{1}{2}\left(N-k/N_f-1+2\xi\right),$$

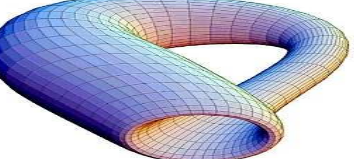

Multi-flavour Schwinger model as a spin model

HOPPING TERM

$$H = -x i^{N_f-1} \sum_{f=0}^{N_f-1} \sum_{n=0}^{N-2} \Big[\sigma^+_{N_f n+f} \sigma^z_{N_f n+f+1} \cdots \sigma^z_{N_f n+N_f+f-1} \sigma^-_{N_f n+N_f+f} +$$

HOPPING TERM H.c.

$$(-1)^{N_f-1} \sigma^-_{N_f n+f} \sigma^z_{N_f n+f+1} \cdots \sigma^z_{N_f n+N_f+f-1} \sigma^+_{N_f n+N_f+f} \Big] +$$

$$+ \sum_{k=0}^{N_f N-1} \alpha_1(k) \mathbb{1} + \sum_{k=0}^{N_f N-1} \alpha(k) \sigma^z_k + \sum_{k=0}^{N_f N-1} \sum_{k'=k+1}^{N_f N-1} \beta'(k') \sigma^z_k \sigma^z_{k'},$$

INHOMOGENEOUS OFFSET — INHOMOGENEOUS MAGNETIC FIELD

with:

$$\alpha_1(k) = \frac{l_0^2}{N_f} \left(1 - \delta_{k/F, N-1}\right) + l_0 \left(1 - (k/N_f)\%2\right) + \frac{1}{2} M_{k\%N_f} + \frac{1}{8}(N + N_f - 1) + \xi,$$

$$\alpha(k) = l_0(N - k/N_f - 1) + \frac{\widetilde{\mu}_{k\%N_f}}{2} + \frac{1}{2} M_{k\%N_f} (-1)^{k/N_f} + \frac{N_f}{4} \left(N - k/N_f - (k/N_f)\%2\right),$$

$$\beta'(k) = \frac{1}{2} \left(N - k/N_f - 1 + 2\xi\right),$$

$$H = -x i^{N_f-1} \sum_{f=0}^{N_f-1} \sum_{n=0}^{N-2} \Big[\sigma^+_{N_f n+f} \sigma^z_{N_f n+f+1} \cdots \sigma^z_{N_f n+N_f+f-1} \sigma^-_{N_f n+N_f+f} +$$

HOPPING TERM

$$(-1)^{N_f-1} \sigma^-_{N_f n+f} \sigma^z_{N_f n+f+1} \cdots \sigma^z_{N_f n+N_f+f-1} \sigma^+_{N_f n+N_f+f} \Big] +$$

HOPPING TERM H.c.

$$+ \sum_{k=0}^{N_f N-1} \alpha_1(k) 1 + \sum_{k=0}^{N_f N-1} \alpha(k) \sigma^z_k + \sum_{k=0}^{N_f N-1} \sum_{k'=k+1}^{N_f N-1} \beta'(k') \sigma^z_k \sigma^z_{k'},$$

INHOMOGENEOUS OFFSET — INHOMOGENEOUS MAGNETIC FIELD — GAUGE TERM

with:

$$\alpha_1(k) = \frac{l_0^2}{N_f} \left(1 - \delta_{k/F,N-1}\right) + l_0 \left(1 - (k/N_f)\%2\right) + \frac{1}{2} M_{k\%N_f} + \frac{1}{8}(N + N_f - 1) + \xi,$$

$$\alpha(k) = l_0(N - k/N_f - 1) + \frac{\widetilde{\mu}_{k\%N_f}}{2} + \frac{1}{2} M_{k\%N_f} (-1)^{k/N_f} + \frac{N_f}{4} \left(N - k/N_f - (k/N_f)\%2\right),$$

$$\beta'(k) = \frac{1}{2} \left(N - k/N_f - 1 + 2\xi\right),$$

HOPPING TERM

$$H = -xi^{N_f-1}\sum_{f=0}^{N_f-1}\sum_{n=0}^{N-2}\Big[\sigma^+_{N_f n+f}\sigma^z_{N_f n+f+1}\cdots\sigma^z_{N_f n+N_f+f-1}\sigma^-_{N_f n+N_f+f}+$$

HOPPING TERM H.c.

$$(-1)^{N_f-1}\sigma^-_{N_f n+f}\sigma^z_{N_f n+f+1}\cdots\sigma^z_{N_f n+N_f+f-1}\sigma^+_{N_f n+N_f+f}\Big]+$$

$$+\sum_{k=0}^{N_f N-1}\alpha_1(k)1+\sum_{k=0}^{N_f N-1}\alpha(k)\sigma^z_k+\sum_{k=0}^{N_f N-1}\sum_{k'=k+1}^{N_f N-1}\beta'(k')\sigma^z_k\sigma^z_{k'},$$

INHOMOGENEOUS OFFSET — INHOMOGENEOUS MAGNETIC FIELD — GAUGE TERM: long-distance interaction!

with:

$$\alpha_1(k)=\frac{l_0^2}{N_f}\left(1-\delta_{k/F,N-1}\right)+l_0\left(1-(k/N_f)\%2\right)+\frac{1}{2}M_{k\%N_f}+\frac{1}{8}(N+N_f-1)+\xi,$$

$$\alpha(k)=l_0(N-k/N_f-1)+\frac{\widetilde{\mu}_{k\%N_f}}{2}+\frac{1}{2}M_{k\%N_f}(-1)^{k/N_f}+\frac{N_f}{4}\left(N-k/N_f-(k/N_f)\%2\right),$$

$$\beta'(k)=\frac{1}{2}\left(N-k/N_f-1+2\xi\right),$$

Results

Example – spectrum

M. C. Bañuls, K.C., K. Jansen, J. I. Cirac, JHEP 1311 (2013) 158

We found the ground state energy and several lowest excitations of the $N_f = 1$ Schwinger model.

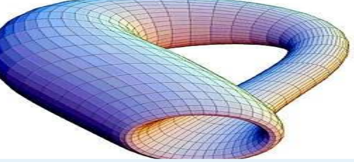

Example – spectrum

M. C. Bañuls, K.C., K. Jansen, J. I. Cirac, JHEP 1311 (2013) 158

We found the ground state energy and several lowest excitations of the $N_f = 1$ Schwinger model.

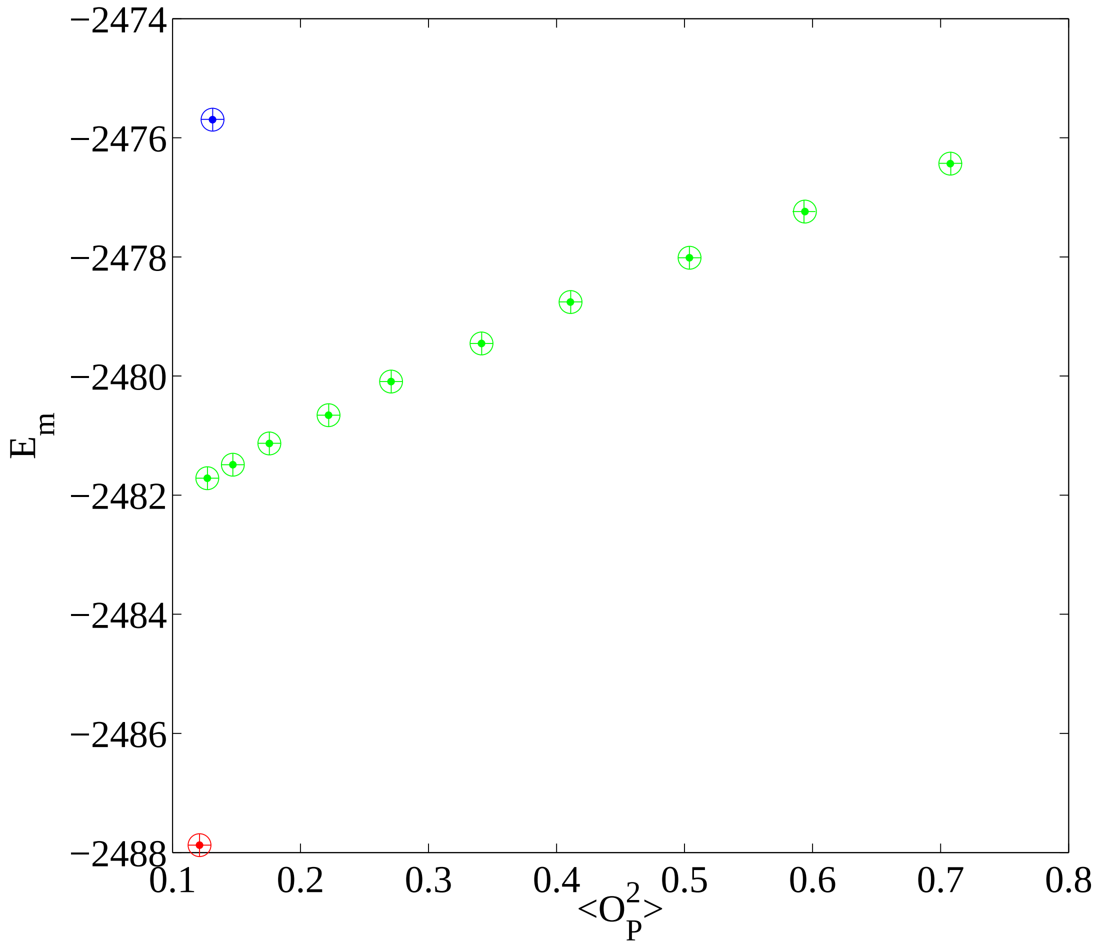

Example – spectrum

M. C. Bañuls, K.C., K. Jansen, J. I. Cirac, JHEP 1311 (2013) 158

We found the ground state energy and several lowest excitations of the $N_f = 1$ Schwinger model.

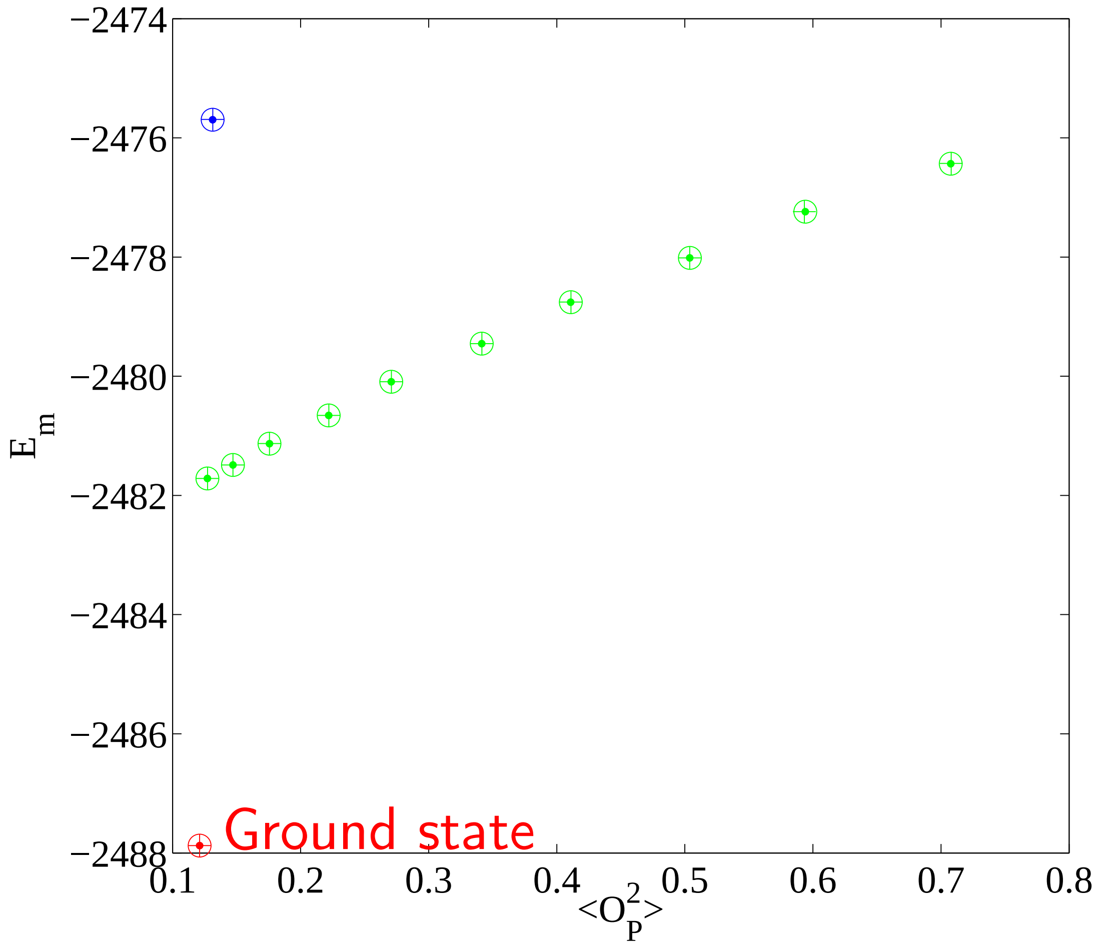

Example – spectrum

M. C. Bañuls, K.C., K. Jansen, J. I. Cirac, JHEP 1311 (2013) 158

We found the ground state energy and several lowest excitations of the $N_f = 1$ Schwinger model.

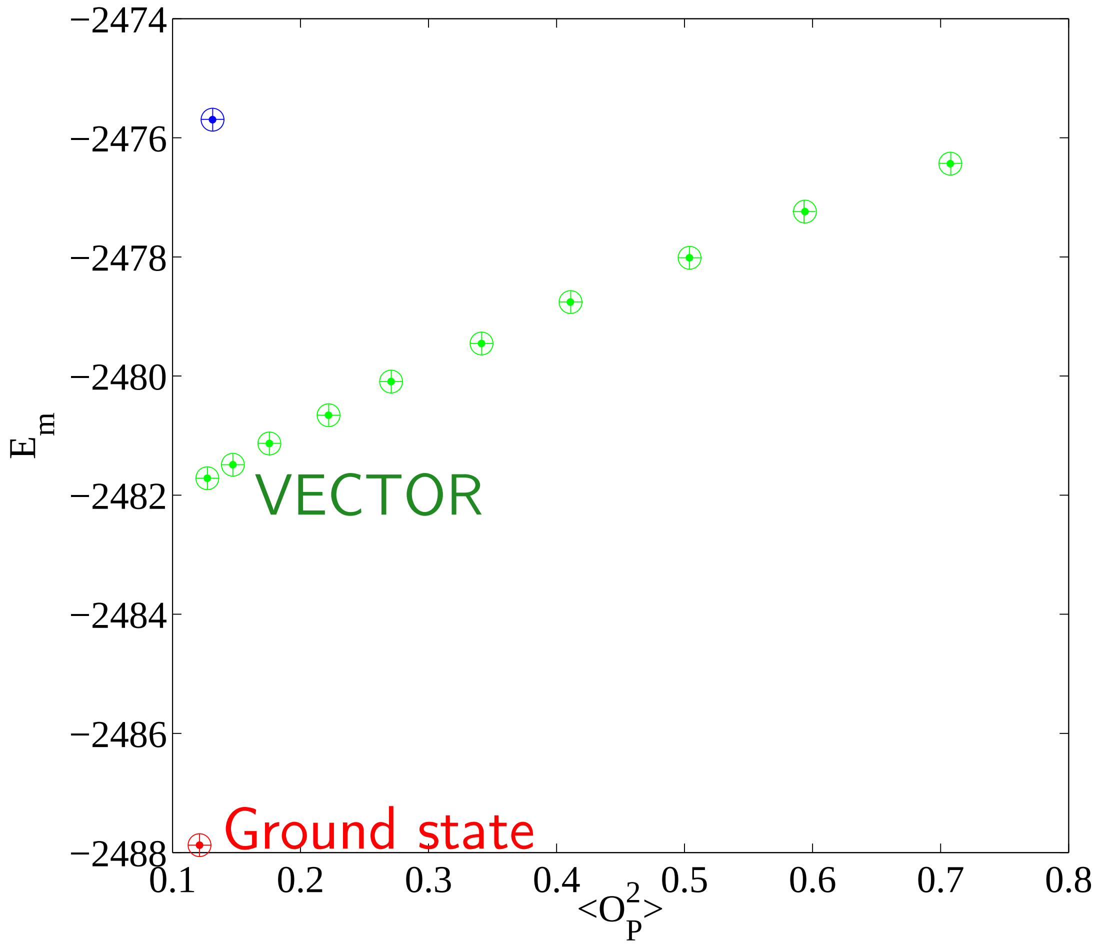

Example – spectrum

M. C. Bañuls, K.C., K. Jansen, J. I. Cirac, JHEP 1311 (2013) 158

We found the ground state energy and several lowest excitations of the $N_f = 1$ Schwinger model.

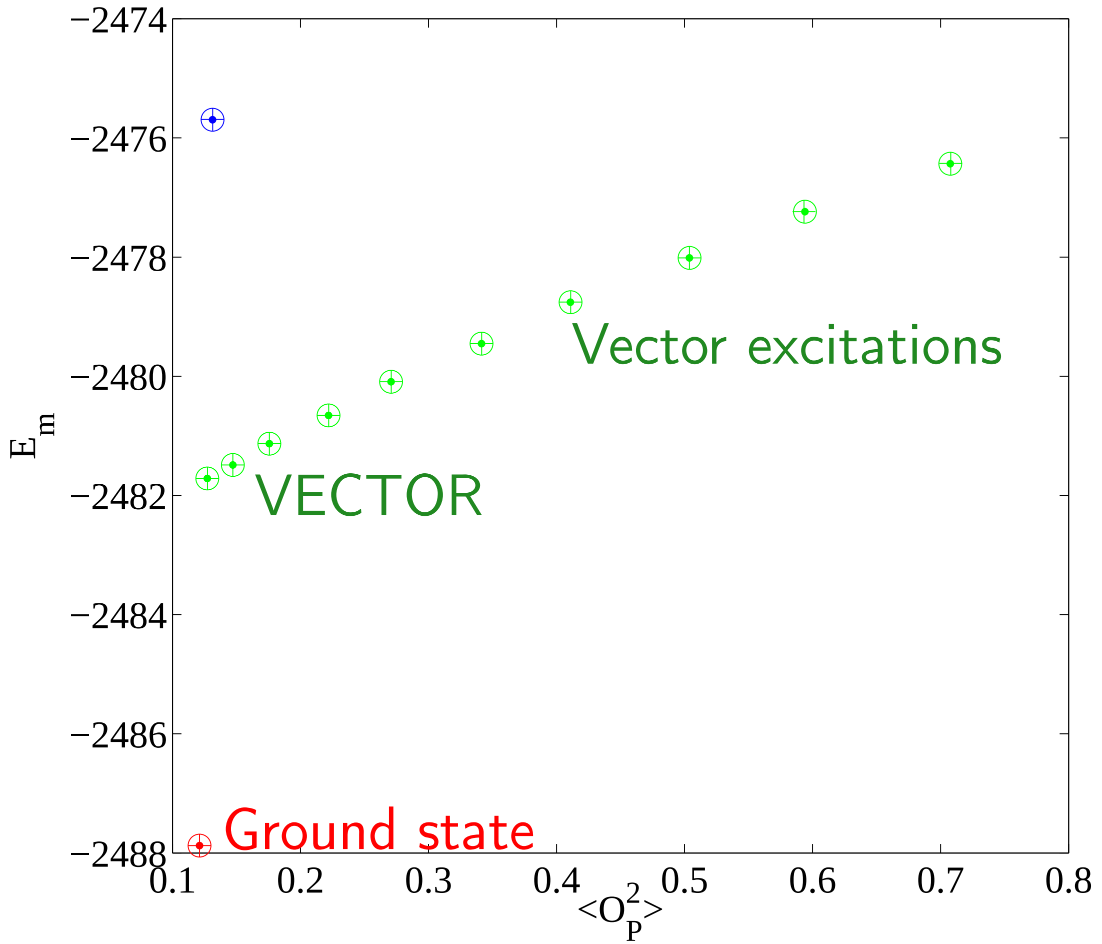

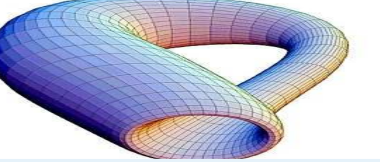

Example – spectrum

M. C. Bañuls, K.C., K. Jansen, J. I. Cirac, JHEP 1311 (2013) 158

We found the ground state energy and several lowest excitations of the $N_f = 1$ Schwinger model.

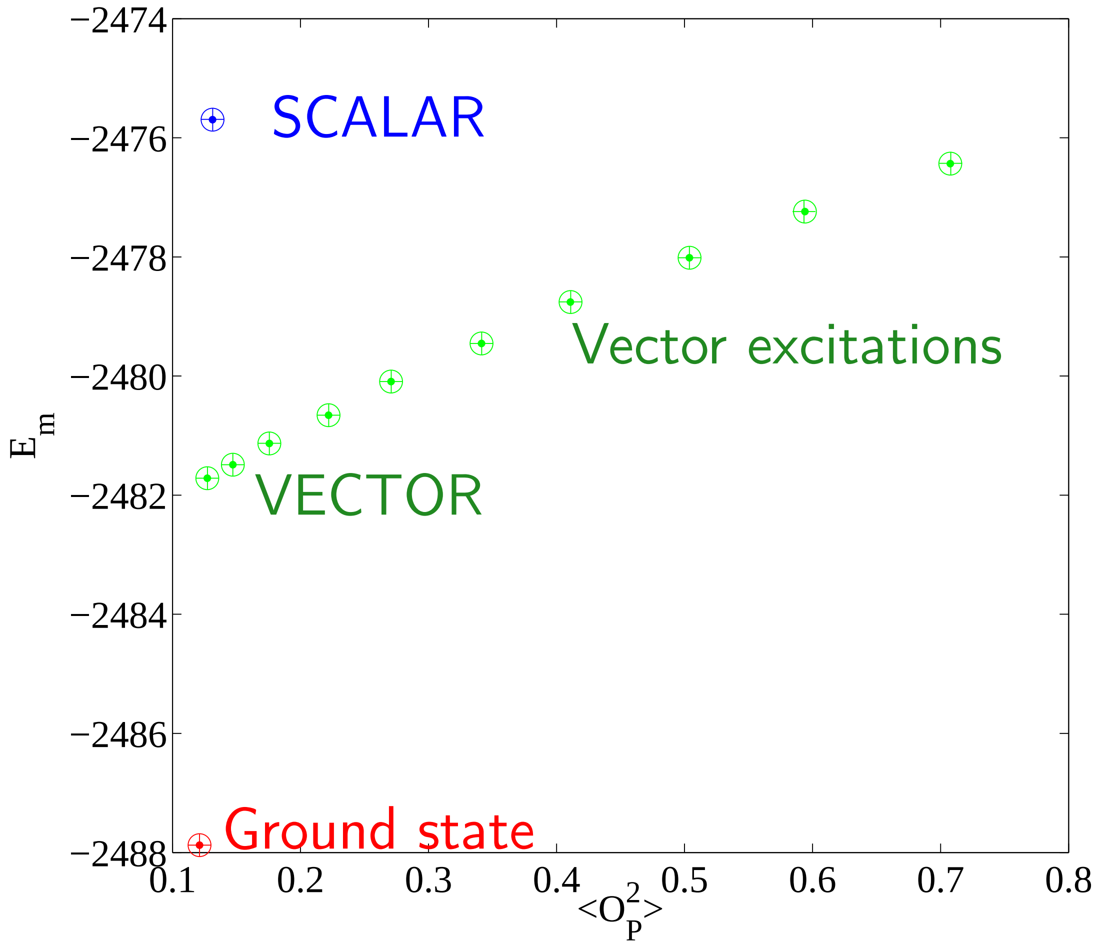

Example – spectrum

M. C. Bañuls, K.C., K. Jansen, J. I. Cirac, JHEP 1311 (2013) 158

We found the ground state energy and several lowest excitations of the $N_f = 1$ Schwinger model.

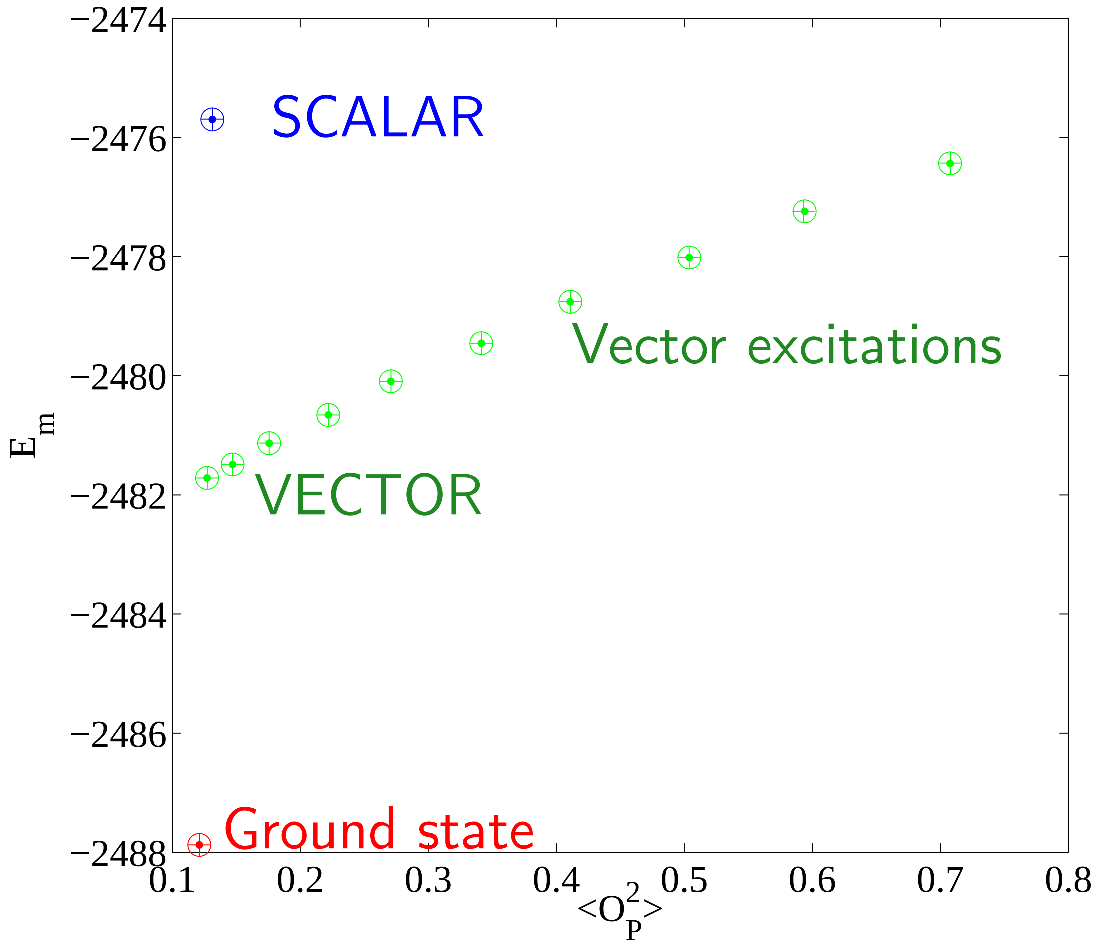

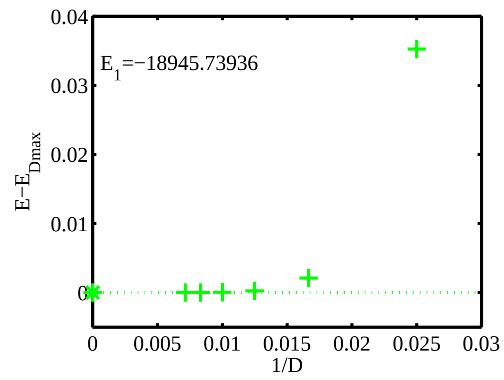

M. C. Bañuls, K.C., K. Jansen, J. I. Cirac, JHEP 1311 (2013) 158

We found the ground state energy and several lowest excitations of the $N_f = 1$ Schwinger model.

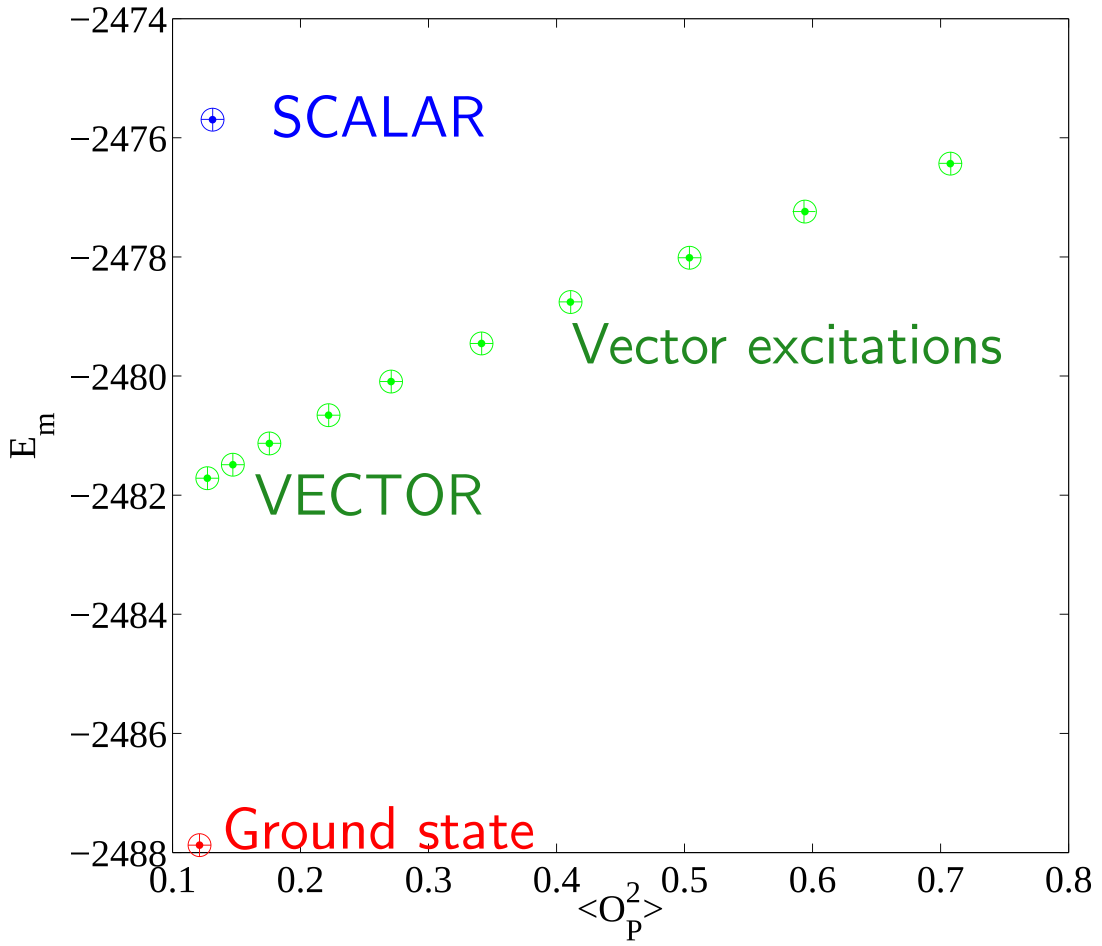

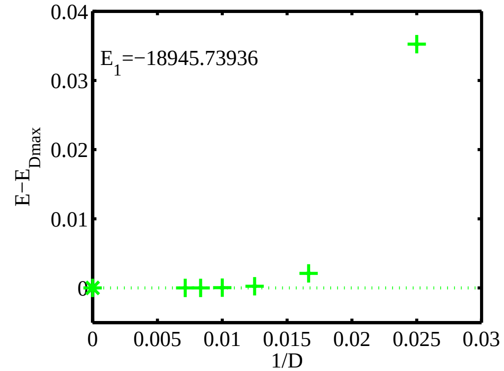

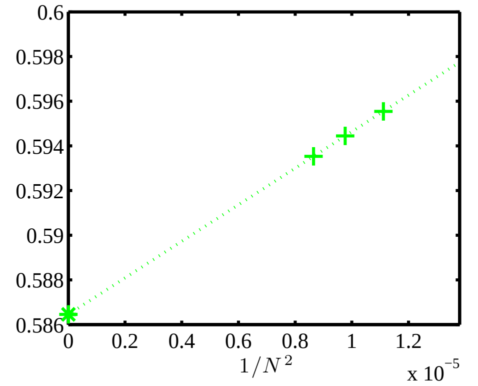

Example – spectrum

M. C. Bañuls, K.C., K. Jansen, J. I. Cirac, JHEP 1311 (2013) 158

We found the ground state energy and several lowest excitations of the $N_f = 1$ Schwinger model.

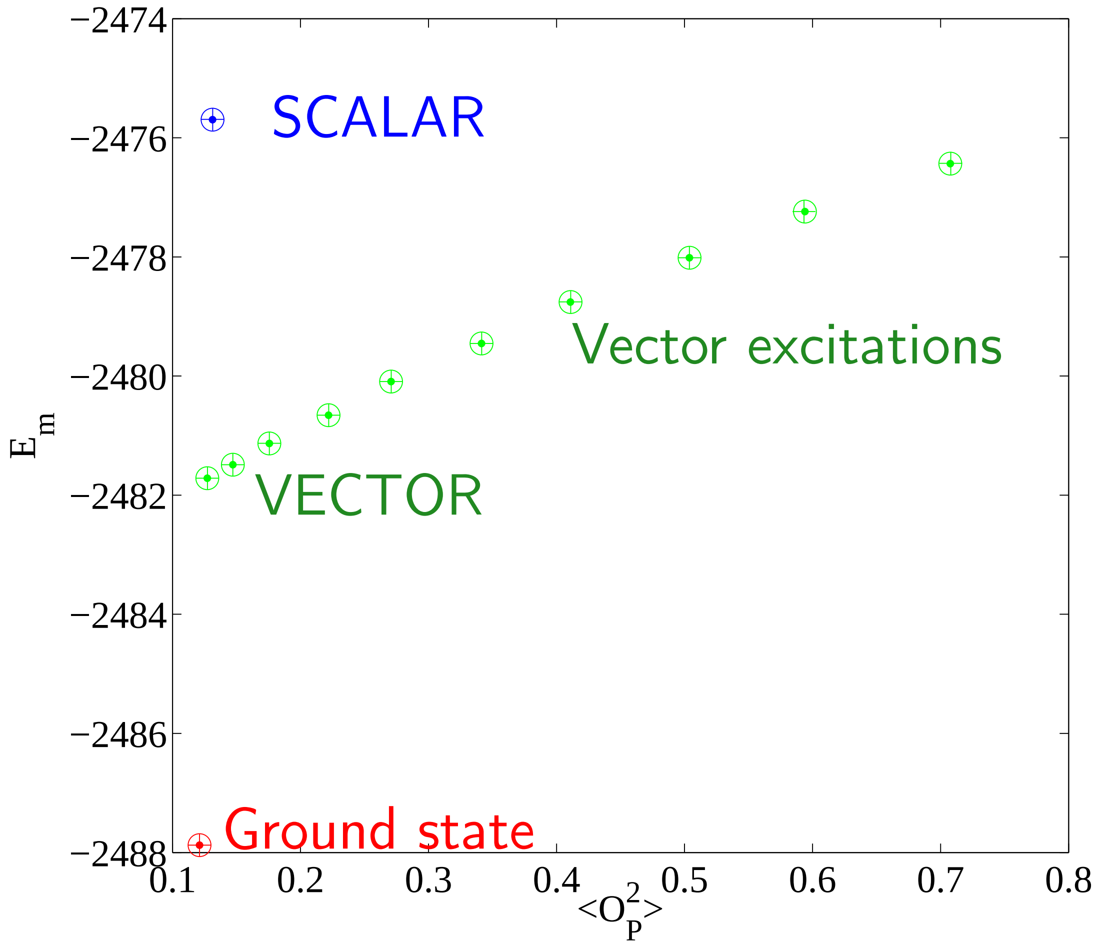

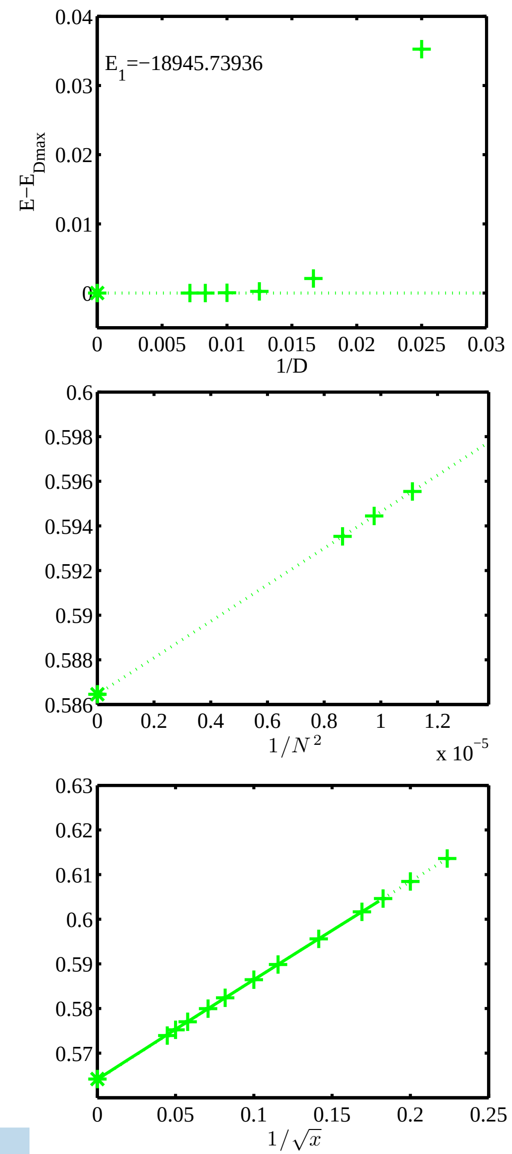

Results for the mass gaps

M. C. Bañuls, K.C., K. Jansen, J. I. Cirac, JHEP 1311 (2013) 158

	Vector binding energy exact 0.5641895	
m/g	**MPS with OBC**	DMRG result
0	**0.56421(9)**	0.56419(4)
0.125	**0.53953(5)**	0.53950(7)
0.25	**0.51922(5)**	0.51918(5)
0.5	**0.48749(3)**	0.48747(2)

	Scalar binding energy exact 1.12838	
m/g	**MPS with OBC**	SCE result
0	**1.1279(12)**	1.11(3)
0.125	**1.2155(28)**	1.22(2)
0.25	**1.2239(22)**	1.24(3)
0.5	**1.1998(17)**	1.20(3)

DMRG result:

[T. Byrnes, P. Sriganesh, R. J. Bursill and C. J. Hamer, Phys. Rev. D **66** (2002) 013002]

SCE result:

[P. Sriganesh, R. Bursill and C. J. Hamer, Phys. Rev. D **62** (2000) 034508]

Example – thermal properties

M. C. Bañuls, K.C., J. I. Cirac, K. Jansen, H. Saito, Phys. Rev. **D92** (2015) 034519

Example – thermal properties

M. C. Bañuls, K.C., J. I. Cirac, K. Jansen, H. Saito, Phys. Rev. **D92** (2015) 034519

- Thermal expectation value: $\langle \mathcal{O} \rangle_\beta = \frac{\mathrm{Tr}(\mathcal{O}\rho(\beta))}{\mathrm{Tr}(\rho(\beta))}$, where $\beta = 1/T$, $\rho(\beta) = e^{-\beta H}$ is the thermal density operator.

Example – thermal properties

M. C. Bañuls, K.C., J. I. Cirac, K. Jansen, H. Saito, Phys. Rev. **D92** (2015) 034519

- Thermal expectation value: $\langle\mathcal{O}\rangle_\beta = \frac{\mathrm{Tr}(\mathcal{O}\rho(\beta))}{\mathrm{Tr}(\rho(\beta))}$, where $\beta = 1/T$, $\rho(\beta) = e^{-\beta H}$ is the thermal density operator.
- The MPO approximation to $\rho(\beta)$ can be computed using imaginary time evolution acting on the identity matrix.

Example – thermal properties

M. C. Bañuls, K.C., J. I. Cirac, K. Jansen, H. Saito, Phys. Rev. **D92** (2015) 034519

- Thermal expectation value: $\langle \mathcal{O} \rangle_\beta = \frac{\mathrm{Tr}(\mathcal{O}\rho(\beta))}{\mathrm{Tr}(\rho(\beta))}$, where $\beta = 1/T$, $\rho(\beta) = e^{-\beta H}$ is the thermal density operator.
- The MPO approximation to $\rho(\beta)$ can be computed using imaginary time evolution acting on the identity matrix.
- $$\rho(\beta/2) = \underbrace{e^{-\frac{\delta}{2}H} \ldots e^{-\frac{\delta}{2}H}}_{N=\beta/\delta \text{ times}}$$

Example – thermal properties

M. C. Bañuls, K.C., J. I. Cirac, K. Jansen, H. Saito, Phys. Rev. **D92** (2015) 034519

- Thermal expectation value: $\langle \mathcal{O} \rangle_\beta = \frac{\mathrm{Tr}(\mathcal{O}\rho(\beta))}{\mathrm{Tr}(\rho(\beta))}$, where $\beta = 1/T$, $\rho(\beta) = e^{-\beta H}$ is the thermal density operator.
- The MPO approximation to $\rho(\beta)$ can be computed using imaginary time evolution acting on the identity matrix.
- $$\rho(\beta/2) = \underbrace{e^{-\frac{\delta}{2}H} \ldots e^{-\frac{\delta}{2}H}}_{N=\beta/\delta \text{ times}}$$
- 2nd order Trotter expansion:

$$e^{-\frac{\delta}{2}H} \approx e^{-\frac{\delta}{4}H_g} \underbrace{e^{-\frac{\delta}{2}(H_{hop}+H_{mass})}}_{\approx e^{-\frac{\delta}{4}H_e} e^{-\frac{\delta}{2}H_o} e^{-\frac{\delta}{4}H_e}} e^{-\frac{\delta}{4}H_g},$$

H_e/H_o – on even/odd sites

where:

$$H = \underbrace{x \sum_{n=0}^{N-2} \left(\sigma_n^+ e^{i\theta_n} \sigma_{n+1}^- + H.c.\right)}_{H_{hop}} + \underbrace{\mu \sum_{n=0}^{N-1} \left(1 + (-1)^n \sigma_n^3\right)}_{H_{mass}} + \underbrace{\sum_{n=0}^{N-2} \left(l + \frac{1}{2} \sum_{k=0}^{n} \left((-1)^k + \sigma_k^3\right)\right)^2}_{H_g}$$

Example – thermal properties

M. C. Bañuls, K.C., J. I. Cirac, K. Jansen, H. Saito, Phys. Rev. **D92** (2015) 034519

- Thermal expectation value: $\langle \mathcal{O} \rangle_\beta = \frac{\mathrm{Tr}(\mathcal{O}\rho(\beta))}{\mathrm{Tr}(\rho(\beta))}$, where $\beta = 1/T$, $\rho(\beta) = e^{-\beta H}$ is the thermal density operator.
- The MPO approximation to $\rho(\beta)$ can be computed using imaginary time evolution acting on the identity matrix.
- $$\rho(\beta/2) = \underbrace{e^{-\frac{\delta}{2}H} \ldots e^{-\frac{\delta}{2}H}}_{N=\beta/\delta \text{ times}}$$
- 2nd order Trotter expansion:

$$e^{-\frac{\delta}{2}H} \approx e^{-\frac{\delta}{4}H_g} \underbrace{e^{-\frac{\delta}{2}(H_{hop}+H_{mass})}}_{\approx e^{-\frac{\delta}{4}H_e} e^{-\frac{\delta}{2}H_o} e^{-\frac{\delta}{4}H_e}} e^{-\frac{\delta}{4}H_g},$$

H_e/H_o – on even/odd sites

where:

$$H = x \underbrace{\sum_{n=0}^{N-2} \left(\sigma_n^+ e^{i\theta_n} \sigma_{n+1}^- + H.c.\right)}_{H_{hop}} + \mu \underbrace{\sum_{n=0}^{N-1} \left(1 + (-1)^n \sigma_n^3\right)}_{H_{mass}} + \underbrace{\sum_{n=0}^{N-2} \left(l + \frac{1}{2} \sum_{k=0}^{n} \left((-1)^k + \sigma_k^3\right)\right)^2}_{H_g}$$

- The exponentials of H_e/H_o can be written exactly as MPO of small bond dimension ($\chi = 4$).

Example – thermal properties

M. C. Bañuls, K.C., J. I. Cirac, K. Jansen, H. Saito, Phys. Rev. **D92** (2015) 034519

- Thermal expectation value: $\langle\mathcal{O}\rangle_\beta = \frac{\mathrm{Tr}(\mathcal{O}\rho(\beta))}{\mathrm{Tr}(\rho(\beta))}$, where $\beta = 1/T$, $\rho(\beta) = e^{-\beta H}$ is the thermal density operator.
- The MPO approximation to $\rho(\beta)$ can be computed using imaginary time evolution acting on the identity matrix.
- $$\rho(\beta/2) = \underbrace{e^{-\frac{\delta}{2}H}\dots e^{-\frac{\delta}{2}H}}_{N=\beta/\delta \text{ times}}$$
- 2nd order Trotter expansion:

$$e^{-\frac{\delta}{2}H} \approx e^{-\frac{\delta}{4}H_g} \underbrace{e^{-\frac{\delta}{2}(H_{hop}+H_{mass})}}_{\approx e^{-\frac{\delta}{4}H_e}e^{-\frac{\delta}{2}H_o}e^{-\frac{\delta}{4}H_e}} e^{-\frac{\delta}{4}H_g},$$

H_e/H_o – on even/odd sites

where:

$$H = x\underbrace{\sum_{n=0}^{N-2}\left(\sigma_n^+ e^{i\theta_n}\sigma_{n+1}^- + H.c.\right)}_{H_{hop}} + \mu\underbrace{\sum_{n=0}^{N-1}\left(1+(-1)^n\sigma_n^3\right)}_{H_{mass}} + \underbrace{\sum_{n=0}^{N-2}\left(l+\frac{1}{2}\sum_{k=0}^{n}\left((-1)^k+\sigma_k^3\right)\right)^2}_{H_g}$$

- The exponentials of H_e/H_o can be written exactly as MPO of small bond dimension ($\chi = 4$).
- H_g more problematic: the long-range terms $\sigma_k^3\sigma_l^3$ lead to $\chi = N+1$

Example – thermal properties

M. C. Bañuls, K.C., J. I. Cirac, K. Jansen, H. Saito, Phys. Rev. **D92** (2015) 034519

- Thermal expectation value: $\langle \mathcal{O} \rangle_\beta = \frac{\mathrm{Tr}(\mathcal{O}\rho(\beta))}{\mathrm{Tr}(\rho(\beta))}$, where $\beta = 1/T$, $\rho(\beta) = e^{-\beta H}$ is the thermal density operator.
- The MPO approximation to $\rho(\beta)$ can be computed using imaginary time evolution acting on the identity matrix.
-
$$\rho(\beta/2) = \underbrace{e^{-\frac{\delta}{2}H} \dots e^{-\frac{\delta}{2}H}}_{N=\beta/\delta \text{ times}}$$
- 2nd order Trotter expansion:
$$e^{-\frac{\delta}{2}H} \approx e^{-\frac{\delta}{4}H_g} \underbrace{e^{-\frac{\delta}{2}(H_{hop}+H_{mass})}}_{\approx e^{-\frac{\delta}{4}H_e} e^{-\frac{\delta}{2}H_o} e^{-\frac{\delta}{4}H_e}} e^{-\frac{\delta}{4}H_g},$$

H_e/H_o – on even/odd sites

where:

$$H = \underbrace{x \sum_{n=0}^{N-2} \left(\sigma_n^+ e^{i\theta_n} \sigma_{n+1}^- + H.c.\right)}_{H_{hop}} + \underbrace{\mu \sum_{n=0}^{N-1} \left(1 + (-1)^n \sigma_n^3\right)}_{H_{mass}} + \underbrace{\sum_{n=0}^{N-2} \left(l + \frac{1}{2} \sum_{k=0}^{n} \left((-1)^k + \sigma_k^3\right)\right)^2}_{H_g}$$

- The exponentials of H_e/H_o can be written exactly as MPO of small bond dimension ($\chi = 4$).
- H_g more problematic: the long-range terms $\sigma_k^3 \sigma_l^3$ lead to $\chi = N + 1$
  - ⋆ one option: Taylor expansion

Example – thermal properties

M. C. Bañuls, K.C., J. I. Cirac, K. Jansen, H. Saito, Phys. Rev. **D92** (2015) 034519

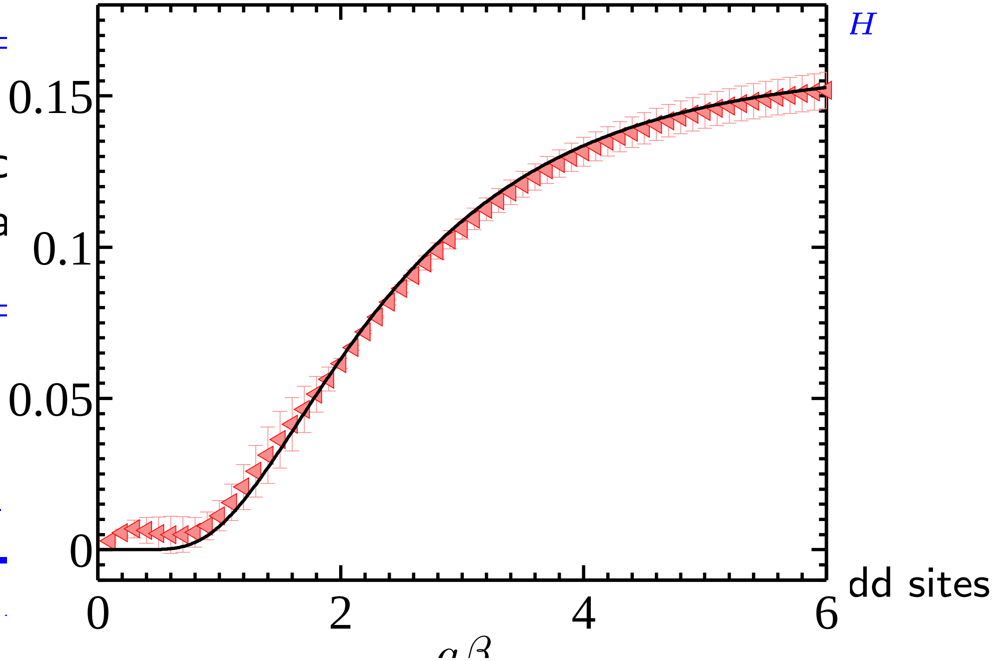

- Thermal expectation value: $\langle \mathcal{O} \rangle_\beta$ = is the thermal density operator.
- The MPO approximation to $\rho(\beta)$ c evolution acting on the identity ma
- $\rho(\beta/2)$ =
- 2nd order Trotter expansion:

$$e^{-\frac{\delta}{2}H} \approx e^{-\frac{\delta}{4}H_g} \underbrace{e^{-\frac{\delta}{2}}}_{\approx e^{-\frac{\delta}{4}}}$$

where:

$$H = \underbrace{x\sum_{n=0}^{N-2}\left(\sigma_n^+ e^{i\theta_n}\sigma_{n+1}^- + H.c.\right)}_{H_{hop}} + \underbrace{\mu\sum_{n=0}^{N-1}\left(1+(-1)^n\sigma_n^3\right)}_{H_{mass}} + \underbrace{\sum_{n=0}^{N-2}\left(l+\frac{1}{2}\sum_{k=0}^{n}\left((-1)^k+\sigma_k^3\right)\right)^2}_{H_g}$$

- The exponentials of H_e/H_o can be written exactly as MPO of small bond dimension ($\chi = 4$).
- H_g more problematic: the long-range terms $\sigma_k^3\sigma_l^3$ lead to $\chi = N+1$
  - ⋆ one option: Taylor expansion

Example – thermal properties

M. C. Bañuls, K.C., J. I. Cirac, K. Jansen, H. Saito, Phys. Rev. **D92** (2015) 034519

- Thermal expectation value: $\langle \mathcal{O} \rangle_\beta =$
  is the thermal density operator.
- The MPO approximation to $\rho(\beta)$ c
  evolution acting on the identity ma
-
  $\rho(\beta/2) =$
- 2nd order Trotter expansion:

$$e^{-\frac{\delta}{2}H} \approx e^{-\frac{\delta}{4}H_g} \underbrace{e^{-\frac{\delta}{2}}}_{\approx e^{-\frac{\delta}{4}}}$$

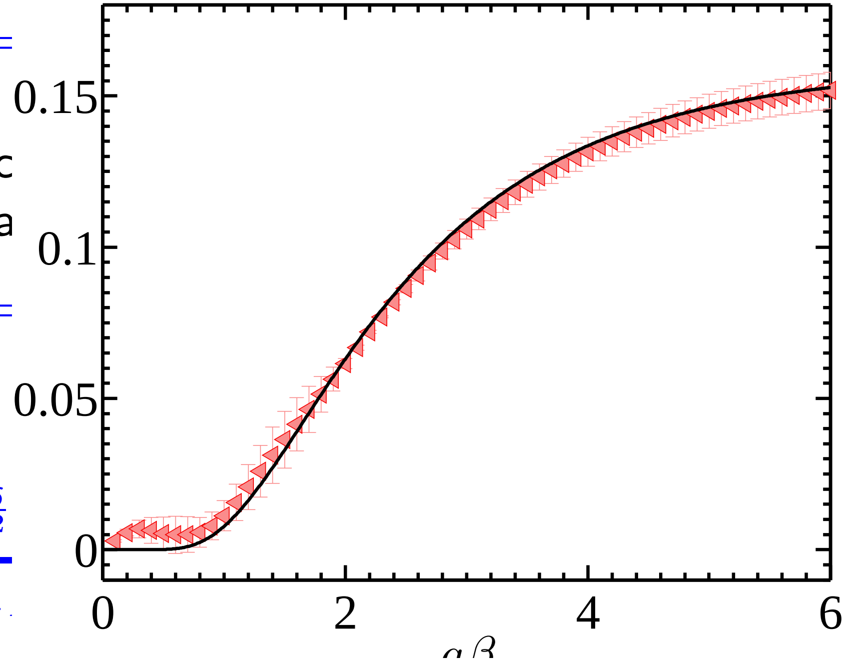

dd sites

where:

$$H = \underbrace{x \sum_{n=0}^{N-2} \left(\sigma_n^+ e^{i\theta_n} \sigma_{n+1}^- + H.c. \right)}_{H_{hop}} + \underbrace{\mu \sum_{n=0}^{N-1} \left(1 + (-1)^n \sigma_n^3 \right)}_{H_{mass}} + \underbrace{\sum_{n=0}^{N-2} \left(l + \frac{1}{2} \sum_{k=0}^{n} \left((-1)^k + \sigma_k^3 \right) \right)^2}_{H_g}$$

- The exponentials of H_e/H_o can be written exactly as MPO of small bond dimension ($\chi = 4$).
- H_g more problematic: the long-range terms $\sigma_k^3 \sigma_l^3$ lead to $\chi = N + 1$
  - ⋆ one option: Taylor expansion
  - ⋆ or: truncate the MPO by allowing $L_n \leq L_{\mathrm{cut}} \Rightarrow \chi = 2L_{\mathrm{cut}} + 1$

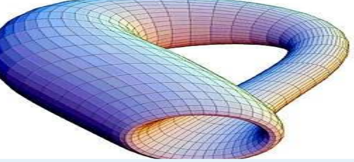

Example – thermal properties

M. C. Bañuls, K.C., J. I. Cirac, K. Jansen, H. Saito, Phys. Rev. **D92** (2015) 034519

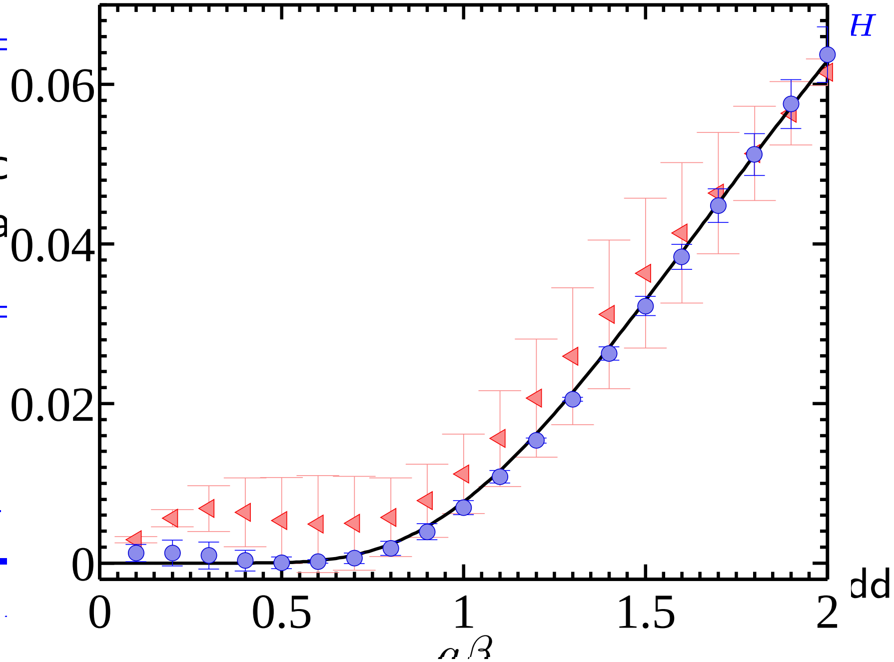

- Thermal expectation value: $\langle \mathcal{O} \rangle_\beta$ = is the thermal density operator.
- The MPO approximation to $\rho(\beta)$ c evolution acting on the identity ma
- $\rho(\beta/2)$ =
- 2nd order Trotter expansion:

$$e^{-\frac{\delta}{2}H} \approx e^{-\frac{\delta}{4}H_g} \underbrace{e^{-\frac{\delta}{2}}}_{\approx e^{-\frac{\delta}{4}}}$$

where: dd sites

$$H = \underbrace{x \sum_{n=0}^{N-2} \left(\sigma_n^+ e^{i\theta_n} \sigma_{n+1}^- + H.c.\right)}_{H_{hop}} + \underbrace{\mu \sum_{n=0}^{N-1} \left(1 + (-1)^n \sigma_n^3\right)}_{H_{mass}} + \underbrace{\sum_{n=0}^{N-2} \left(l + \frac{1}{2} \sum_{k=0}^{n} \left((-1)^k + \sigma_k^3\right)\right)^2}_{H_g}$$

- The exponentials of H_e/H_o can be written exactly as MPO of small bond dimension ($\chi = 4$).
- H_g more problematic: the long-range terms $\sigma_k^3 \sigma_l^3$ lead to $\chi = N + 1$
  - ⋆ one option: Taylor expansion
  - ⋆ or: truncate the MPO by allowing $L_n \leq L_{\text{cut}} \Rightarrow \chi = 2L_{\text{cut}} + 1$

M. C. Bañuls, K.C., J. I. Cirac, K. Jansen, H. Saito, Phys. Rev. **D92** (2015) 034519

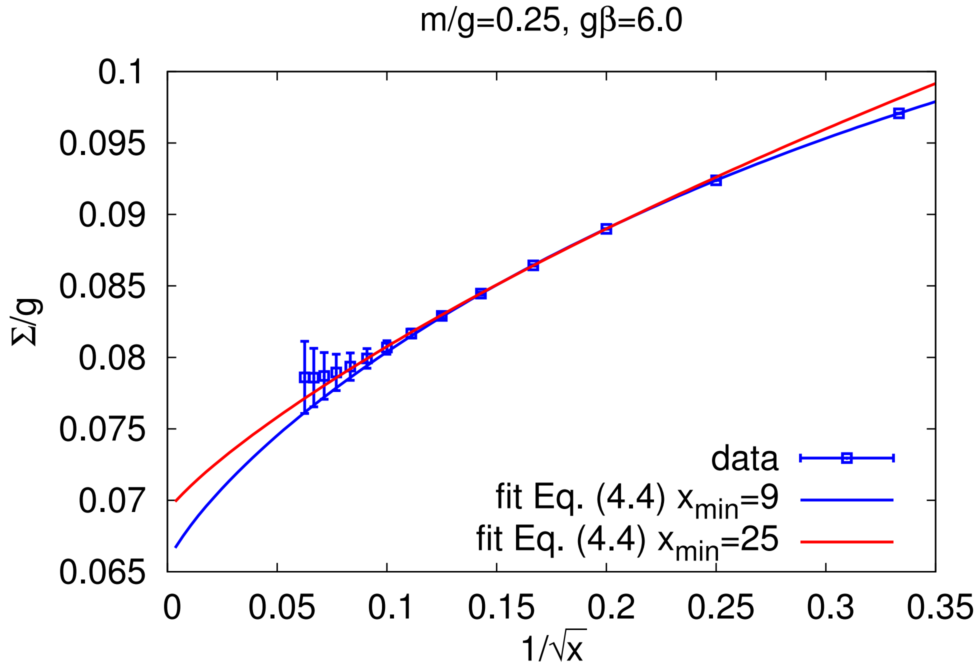

M. C. Bañuls, K.C., J. I. Cirac, K. Jansen, H. Saito, Phys. Rev. **D92** (2015) 034519

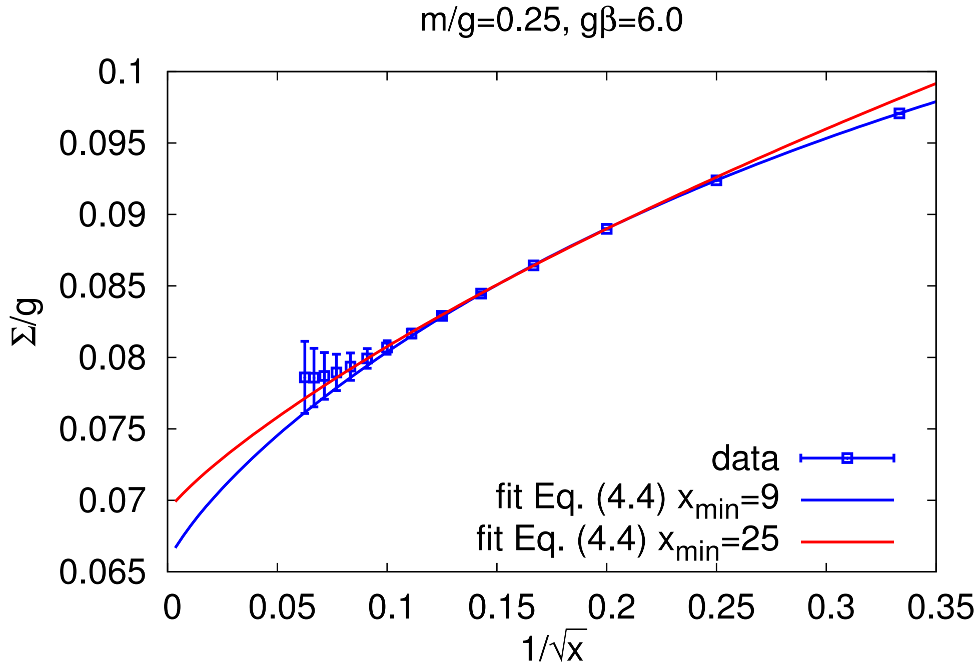

linear+log: $\Sigma_{\rm subtr}(m/g,x) = \Sigma^{(1)}_{\rm subtr}(m/g) + \frac{a^{(1)}(m/g)}{\sqrt{x}}\log(x) + \frac{b^{(1)}(m/g)}{\sqrt{x}}$

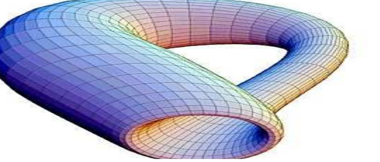

Continuum extrapolation

M. C. Bañuls, K.C., J. I. Cirac, K. Jansen, H. Saito, Phys. Rev. **D92** (2015) 034519

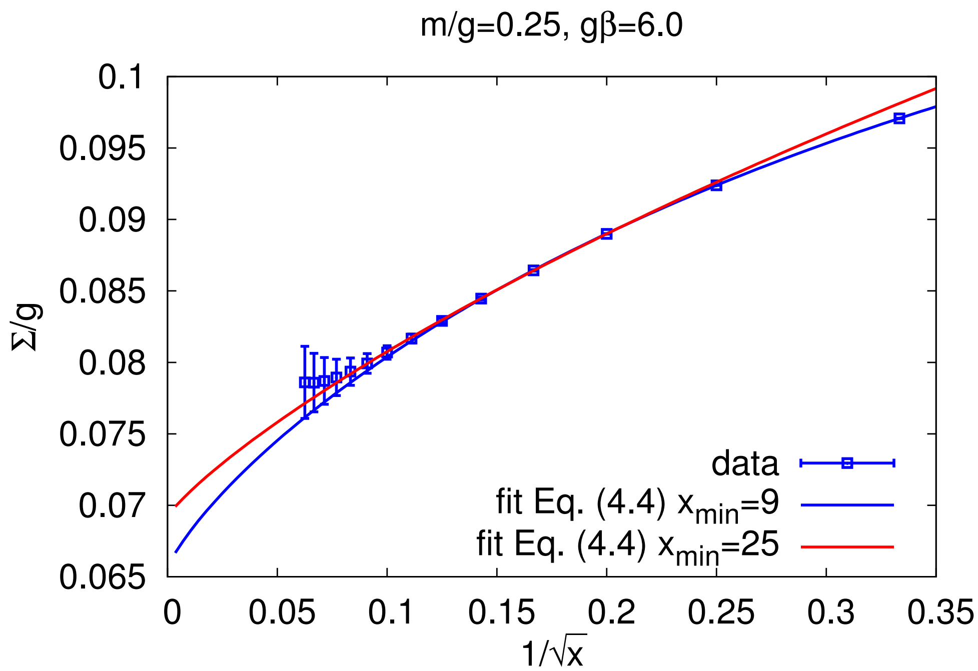

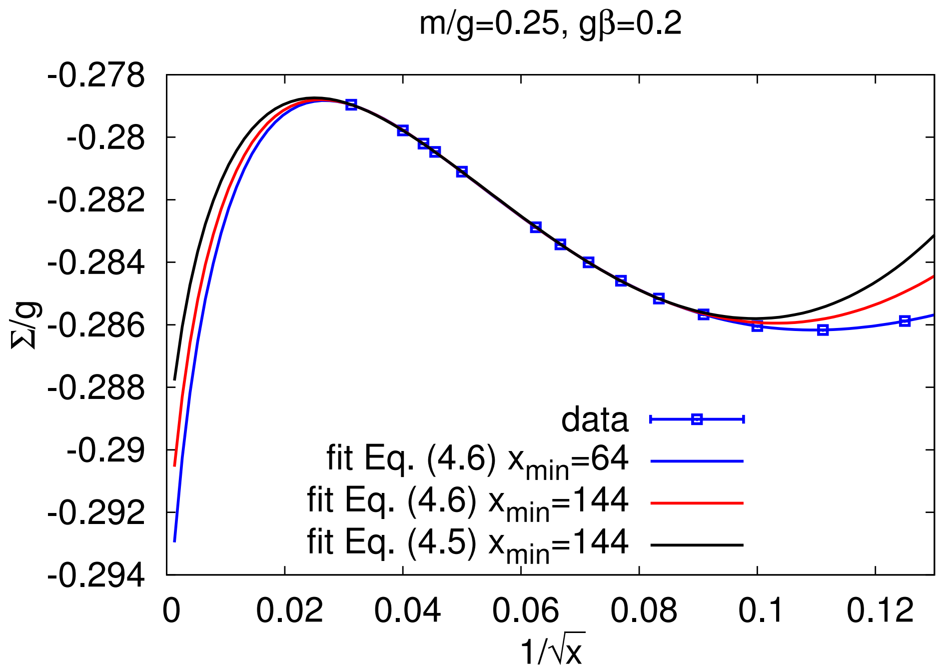

linear+log: $\Sigma_{\text{subtr}}(m/g,x) = \Sigma^{(1)}_{\text{subtr}}(m/g) + \frac{a^{(1)}(m/g)}{\sqrt{x}}\log(x) + \frac{b^{(1)}(m/g)}{\sqrt{x}}$

Continuum extrapolation

M. C. Bañuls, K.C., J. I. Cirac, K. Jansen, H. Saito, Phys. Rev. **D92** (2015) 034519

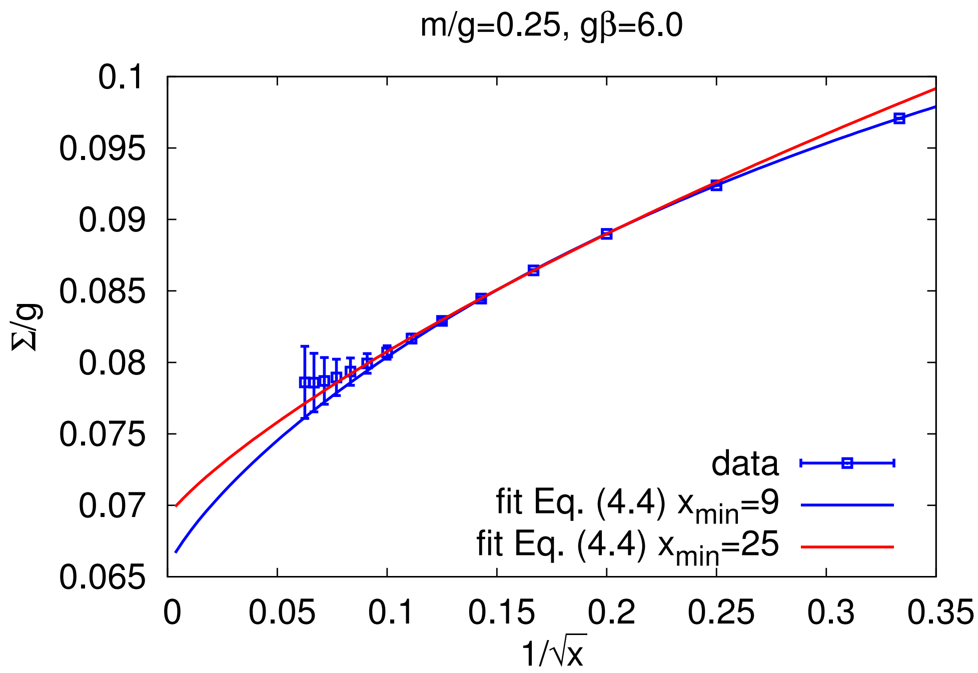

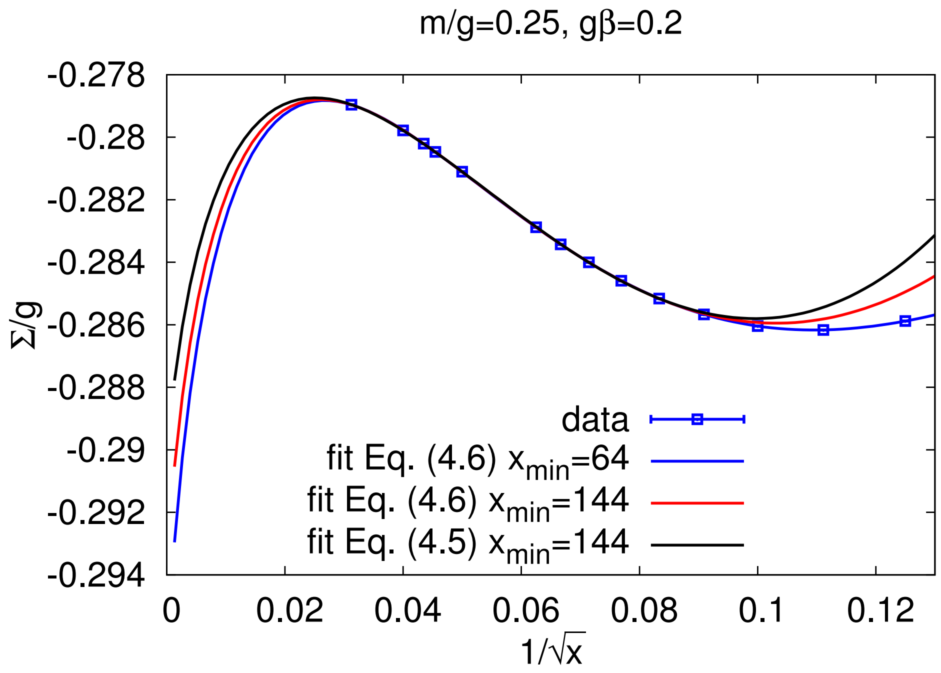

linear+log: $\Sigma_{\mathrm{subtr}}(m/g,x) = \Sigma^{(1)}_{\mathrm{subtr}}(m/g) + \frac{a^{(1)}(m/g)}{\sqrt{x}}\log(x) + \frac{b^{(1)}(m/g)}{\sqrt{x}}$

quadratic+log: $\Sigma_{\mathrm{subtr}}(m/g,x) = \Sigma^{(2)}_{\mathrm{subtr}}(m/g) + \frac{a^{(2)}(m/g)}{\sqrt{x}}\log(x) + \frac{b^{(2)}(m/g)}{\sqrt{x}} + \frac{c^{(2)}(m/g)}{x}$

Continuum extrapolation

M. C. Bañuls, K.C., J. I. Cirac, K. Jansen, H. Saito, Phys. Rev. D92 (2015) 034519

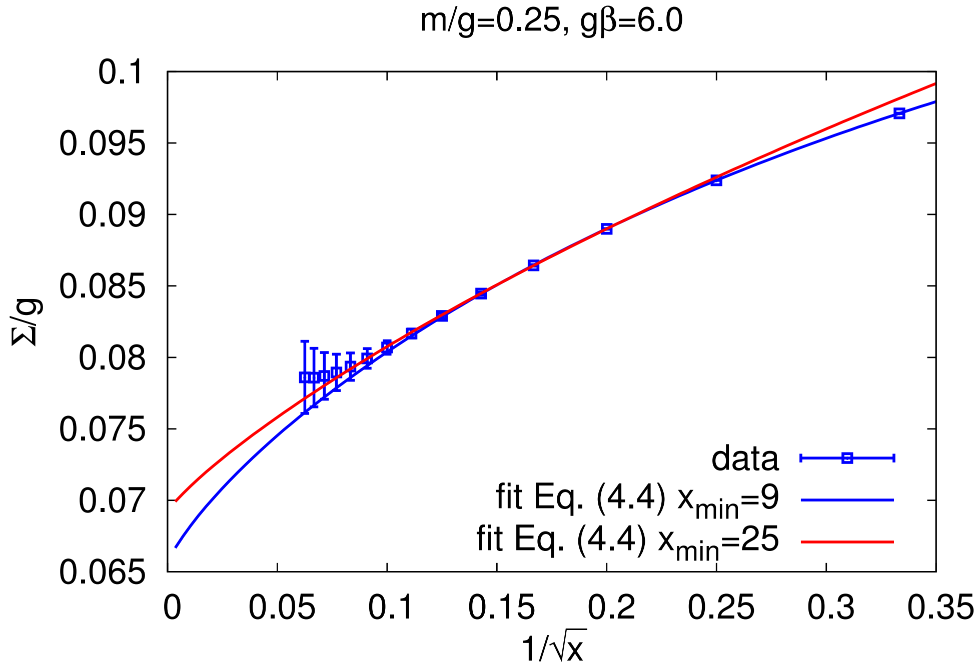

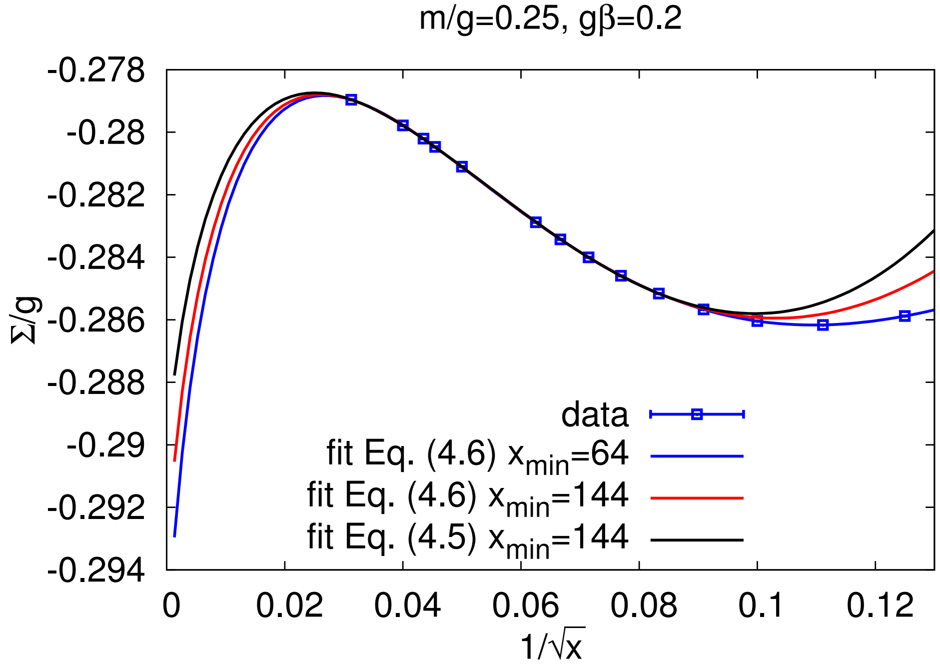

linear+log: $\Sigma_{\rm subtr}(m/g,x) = \Sigma^{(1)}_{\rm subtr}(m/g) + \frac{a^{(1)}(m/g)}{\sqrt{x}}\log(x) + \frac{b^{(1)}(m/g)}{\sqrt{x}}$

quadratic+log: $\Sigma_{\rm subtr}(m/g,x) = \Sigma^{(2)}_{\rm subtr}(m/g) + \frac{a^{(2)}(m/g)}{\sqrt{x}}\log(x) + \frac{b^{(2)}(m/g)}{\sqrt{x}} + \frac{c^{(2)}(m/g)}{x}$

cubic+log: $\Sigma_{\rm subtr}(m/g,x) = \Sigma^{(3)}_{\rm subtr}(m/g) + \frac{a^{(3)}(m/g)}{\sqrt{x}}\log(x) + \frac{b^{(3)}(m/g)}{\sqrt{x}} + \frac{c^{(3)}(m/g)}{x} + \frac{d^{(3)}(m/g)}{x^{3/2}}$

Two flavours with chemical potential

M. C. Bañuls, K.C., J. I. Cirac, K. Jansen, S. Kühn, Phys. Rev. Lett. **118** (2017) 071601

In 2017, we analyzed the first case for which a MC simulation would encounter the sign problem:

M. C. Bañuls, K.C., J. I. Cirac, K. Jansen, S. Kühn, Phys. Rev. Lett. **118** (2017) 071601

In 2017, we analyzed the first case for which a MC simulation would encounter the sign problem:

the 2-flavour Schwinger model with a chemical potential.

M. C. Bañuls, K.C., J. I. Cirac, K. Jansen, S. Kühn, Phys. Rev. Lett. **118** (2017) 071601

In 2017, we analyzed the first case for which a MC simulation would encounter the sign problem:

the 2-flavour Schwinger model with a chemical potential.

Quantity of interest:

the difference in particle numbers $N_1 - N_2$ vs. $\mu_I/2\pi \propto \mu_1 - \mu_2$.

M. C. Bañuls, K.C., J. I. Cirac, K. Jansen, S. Kühn, Phys. Rev. Lett. **118** (2017) 071601

In 2017, we analyzed the first case for which a MC simulation would encounter the sign problem:

the 2-flavour Schwinger model with a chemical potential.

Quantity of interest:

the difference in particle numbers $N_1 - N_2$ vs. $\mu_I/2\pi \propto \mu_1 - \mu_2$.

Analytical computation ($m = 0$):

[R. Narayanan, "Two flavor massless Schwinger model on a torus at a finite chemical potential," Phys. Rev. D **86** (2012) 125008]

M. C. Bañuls, K.C., J. I. Cirac, K. Jansen, S. Kühn, Phys. Rev. Lett. **118** (2017) 071601

In 2017, we analyzed the first case for which a MC simulation would encounter the sign problem:
the 2-flavour Schwinger model with a chemical potential.
Quantity of interest:
the difference in particle numbers $N_1 - N_2$ vs. $\mu_I/2\pi \propto \mu_1 - \mu_2$.

Analytical computation ($m = 0$):
[R. Narayanan, "Two flavor massless Schwinger model on a torus at a finite chemical potential," Phys. Rev. D **86** (2012) 125008]

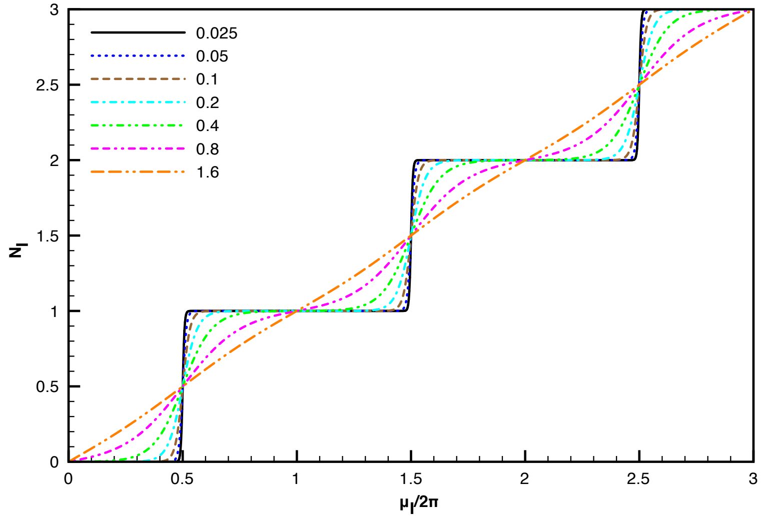

Example ($N_f = 2$)

M. C. Bañuls, K.C., J. I. Cirac, K. Jansen, S. Kühn, Phys. Rev. Lett. 118 (2017) 071601

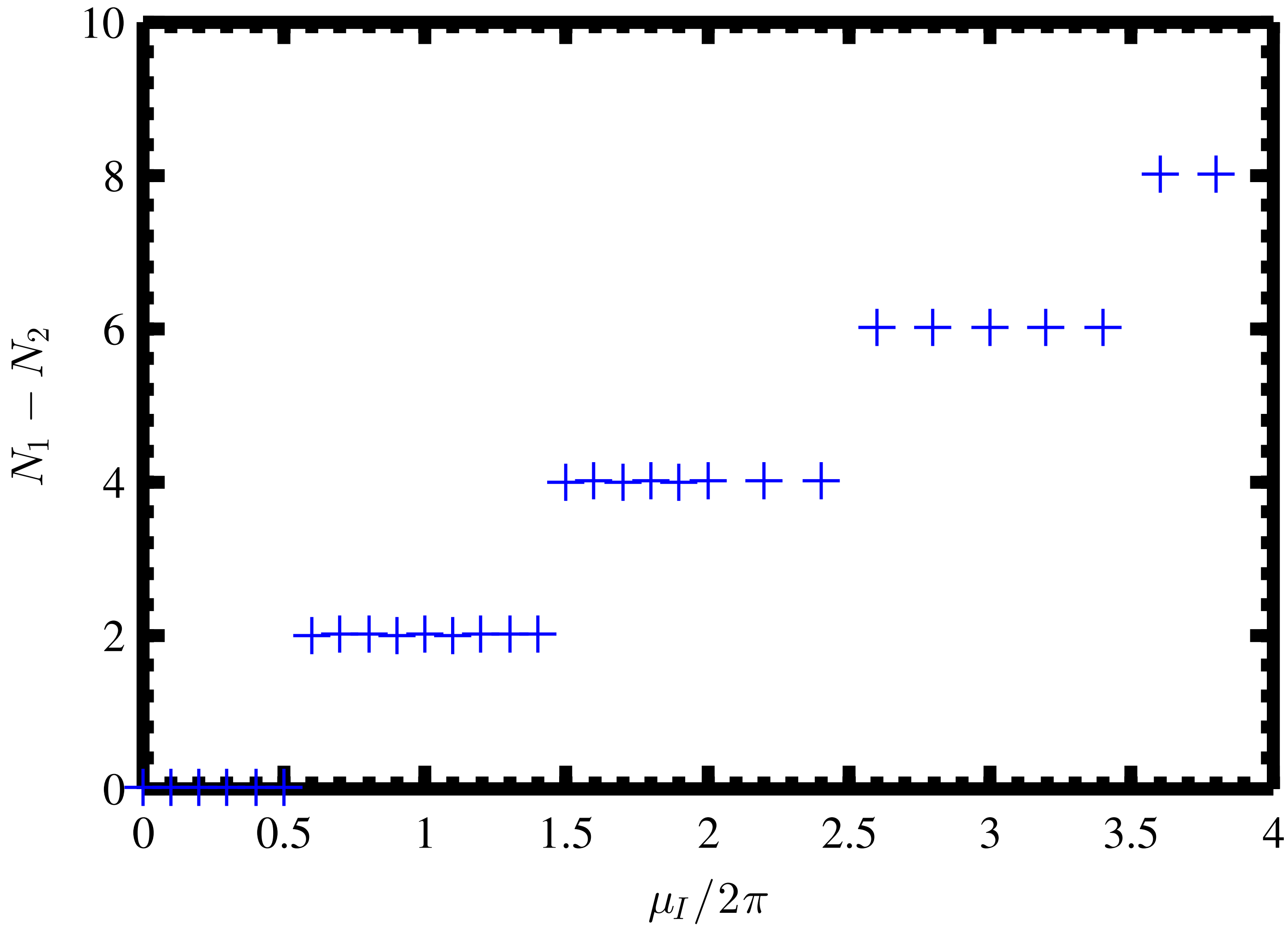

$x = 121,\ N = 88$

Extracting locations of phase transitions

M. C. Bañuls, K.C., J. I. Cirac, K. Jansen, S. Kühn, Phys. Rev. Lett. **118** (2017) 071601

Ground state energy for N sites, with isospin number ΔN:

$$E_{(N,\Delta N)}(\nu_0,\nu_1) = \nu_0 N_0 + \nu_1 N_1 + E_{\min}(W_{\text{aux}}|_{(N,\Delta N)}) = \frac{N}{2}(\nu_0+\nu_1) - \underbrace{\frac{\Delta N}{2}}_{p_{(N,\Delta N)}}(\nu_1-\nu_0) + E_{\min}(W_{\text{aux}}|_{(N,\Delta N)}).$$

$E_{\min}(W_{\text{aux}}|_{(N,\Delta N)})$ – isospin number dependent constant; having its single value inside each phase is enough to determine this constant.

Extracting locations of phase transitions

M. C. Bañuls, K.C., J. I. Cirac, K. Jansen, S. Kühn, Phys. Rev. Lett. 118 (2017) 071601

Ground state energy for N sites, with isospin number ΔN:

$$E_{(N,\Delta N)}(\nu_0,\nu_1) = \nu_0 N_0 + \nu_1 N_1 + E_{\min}(W_{\rm aux}|_{(N,\Delta N)}) = \frac{N}{2}(\nu_0+\nu_1) - \underbrace{\frac{\Delta N}{2}}_{p_{(N,\Delta N)}}(\nu_1-\nu_0) + E_{\min}(W_{\rm aux}|_{(N,\Delta N)}).$$

$E_{\min}(W_{\rm aux}|_{(N,\Delta N)})$ – isospin number dependent constant; having its single value inside each phase is enough to determine this constant.

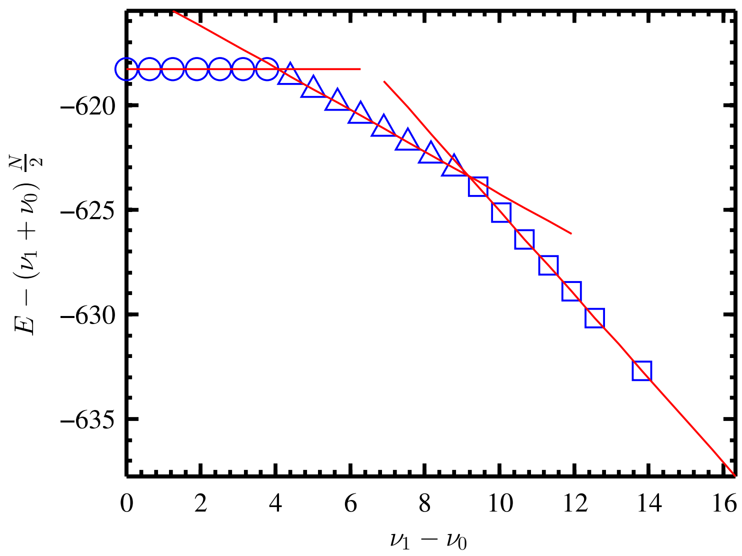

Ground state energy as a function of the chemical potential difference for $m/g = 0$, $Lg = 8$, $x = 16$, and $D = 160$. The different symbols correspond to $\Delta N = 0$ (circles), $\Delta N = 2$ (triangles) and $\Delta N = 4$ (squares). The lines represent linear fits of the slope $p_{(N,\Delta N)}$.

Continuum extrapolation of jumps

M. C. Bañuls, K.C., J. I. Cirac, K. Jansen, S. Kühn, Phys. Rev. Lett. **118** (2017) 071601

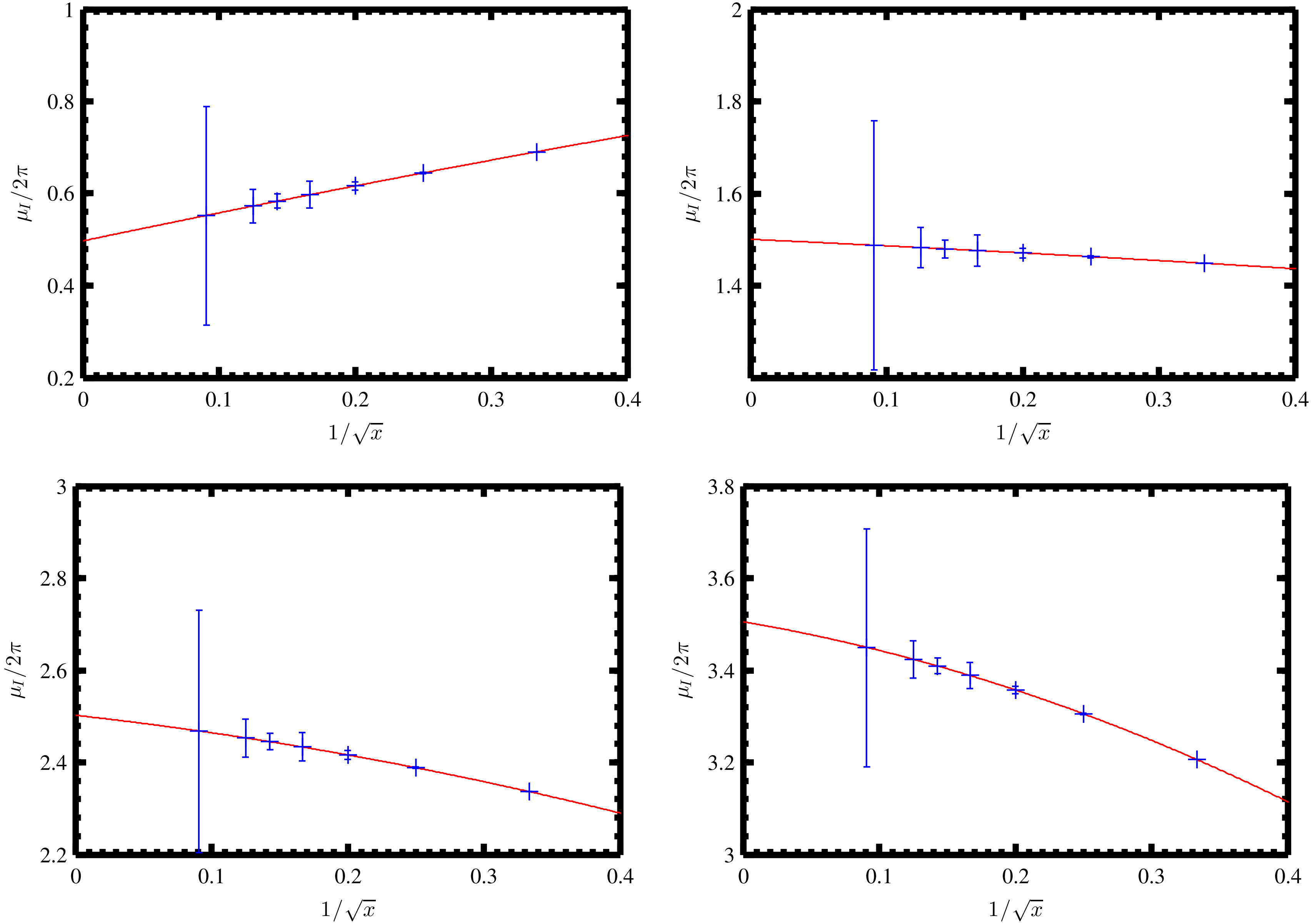

Jump locations in the continuum

M. C. Bañuls, K.C., J. I. Cirac, K. Jansen, S. Kühn, Phys. Rev. Lett. 118 (2017) 071601

$m/g = 0$

Volume	1. transition	2. transition	3. transition	4. transition
$Lg = 2$	0.499960(88)	1.513345(47)	2.617208(11)	3.716041(12)
$Lg = 6$	0.499(21)	1.501(23)	2.504(22)	3.511(20)
$Lg = 8$	0.497(49)	1.501(60)	2.502(55)	3.505(51)

$m/g = 0.125$

Volume	1. transition	2. transition	3. transition	4. transition
$Lg = 2$	0.522620(86)	1.515910(40)	2.620237(14)	3.716558(20)
$Lg = 6$	0.711(19)	1.538(26)	2.519(23)	3.520(20)
$Lg = 8$	0.831(42)	1.575(65)	2.532(57)	3.523(52)

$m/g = 0.25$

Volume	1. transition	2. transition	3. transition	4. transition
$Lg = 2$	0.554897(76)	1.522594(40)	2.624794(14)	3.720370(19)
$Lg = 6$	0.938(16)	1.617(26)	2.558(23)	3.546(20)
$Lg = 8$	1.165(39)	1.728(66)	2.606(57)	3.571(52)

$m/g = 0.5$

Volume	1. transition	2. transition	3. transition	4. transition
$Lg = 2$	0.643234(66)	1.548542(35)	2.644094(11)	3.732926(20)
$Lg = 6$	1.402(12)	1.874(23)	2.703(22)	3.647(20)
$Lg = 8$	1.816(24)	2.168(53)	2.871(55)	3.752(49)

M. C. Bañuls, K.C., J. I. Cirac, K. Jansen, S. Kühn, Phys. Rev. Lett. 118 (2017) 071601

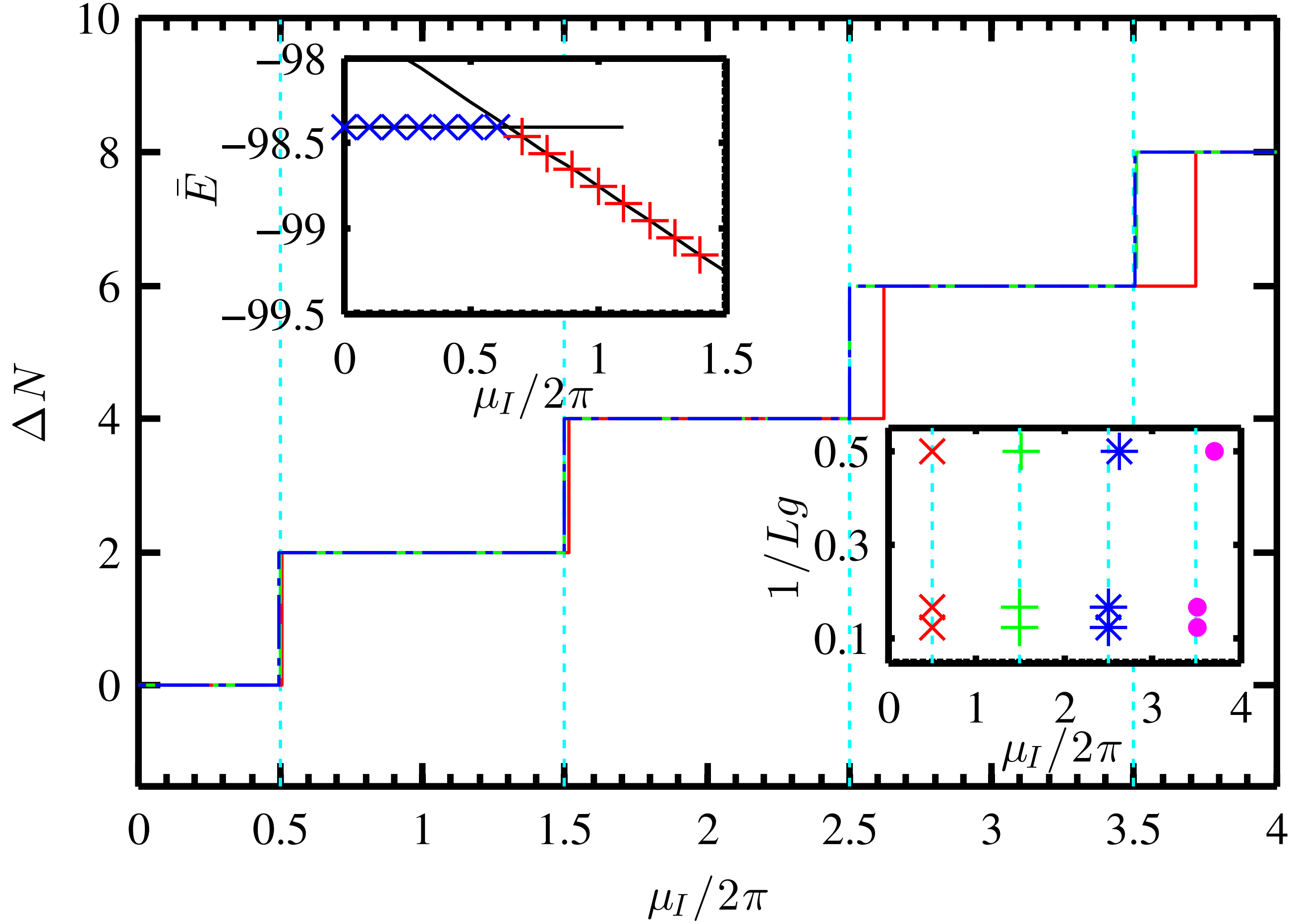

Main plot: continuum estimate for ΔN vs. $\mu_I/2\pi$, $Lg = 2$, $Lg = 6$, $Lg = 8$.

Upper inset: $Lg = 8$, $x = 16$, $m/g = 0$, $D = 160$, close-up of GS energy around the 1st transition : $\Delta N = 0$, $\Delta N = 2$.

Lower inset: volume dependence of the transitions location.

M. C. Bañuls, K.C., J. I. Cirac, K. Jansen, S. Kühn, Phys. Rev. Lett. 118 (2017) 071601

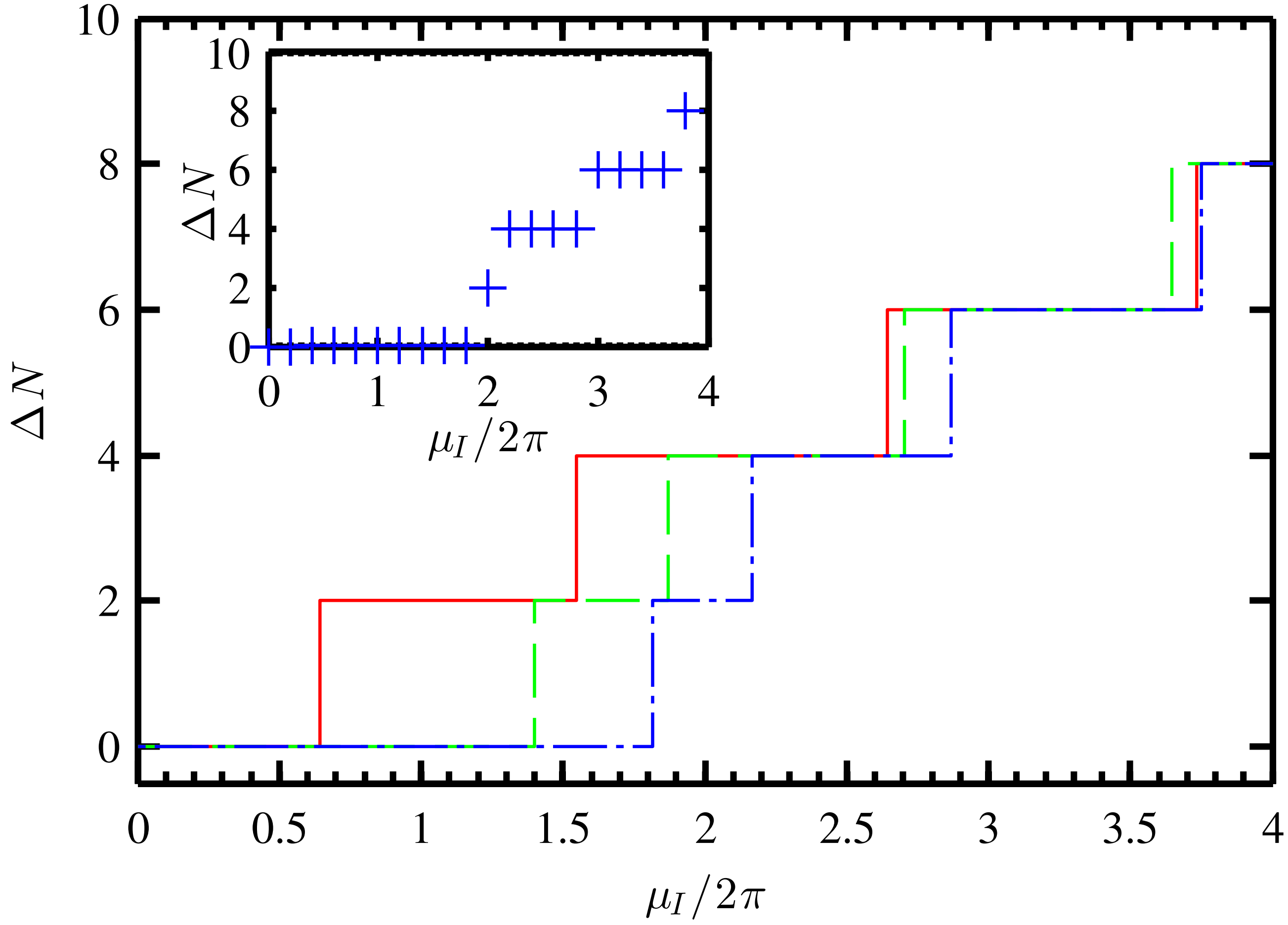

Main plot: continuum estimate for ΔN vs. $\mu_I/2\pi$, $Lg = 2$, $Lg = 6$, $Lg = 8$.

Inset: isospin number ΔN vs. $\mu_I/2\pi$ for $Lg = 8$, $x = 121$, $m/g = 0.5$, $D = 220$.

m-μ_I phase diagram ($N_f = 2$)

M. C. Bañuls, K.C., J. I. Cirac, K. Jansen, S. Kühn, Phys. Rev. Lett. 118 (2017) 071601

Phase diagram $\mu_I/2\pi$ vs. m/g, for volume $Lg = 8$

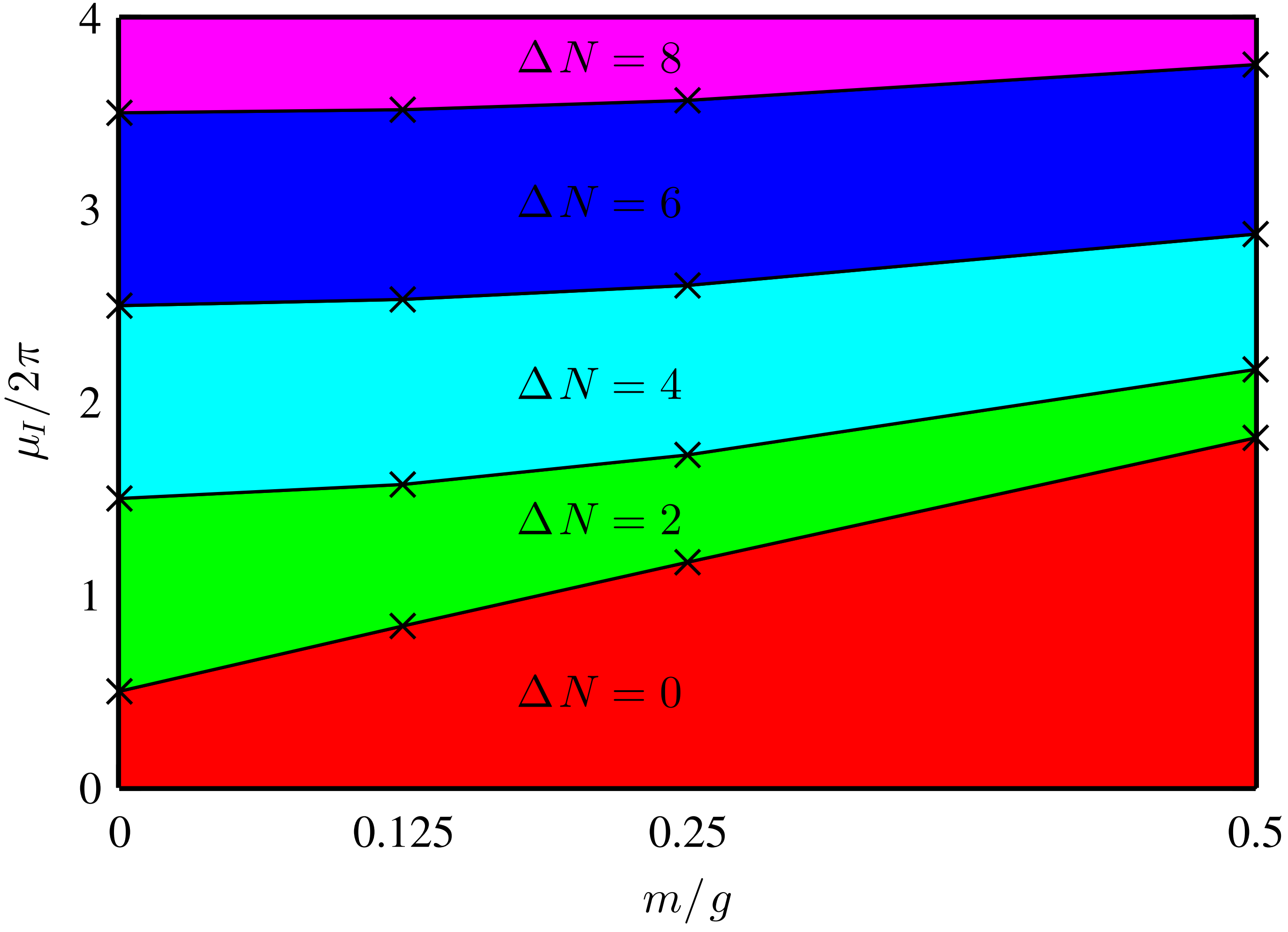

Non-Abelian SU(2) gauge theory

M. C. Bañuls, K.C., J. I. Cirac, K. Jansen, S. Kühn, Phys. Rev. **X7** (2017) 041046

Recently, we looked into the first non-Abelian case – $SU(2)$ in $1+1$d.

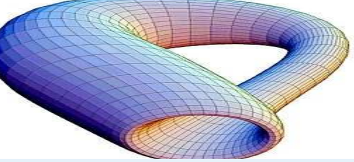

Non-Abelian SU(2) gauge theory

M. C. Bañuls, K.C., J. I. Cirac, K. Jansen, S. Kühn, Phys. Rev. **X7** (2017) 041046

Recently, we looked into the first non-Abelian case – $SU(2)$ in $1{+}1$d.

$$H = \frac{1}{2a}\sum_{k=1}^{N-1}\sum_{\ell,\ell'=1}^{2}\left(\psi_k^{\ell\,\dagger} U_k^{\ell\ell'} \psi_{k+1}^{\ell'} + \text{h.c.}\right) + m\sum_{k=1}^{N}\sum_{\ell=1}^{2}(-1)^k \psi_k^{\ell\,\dagger}\psi_k^{\ell} + \frac{ag^2}{2}\sum_{k=1}^{N-1}\mathbf{J}_k^2,$$

with:

$\psi_k^{\ell\,\dagger}$ – single component fermion field (color ℓ on site k),

$U_k^{\ell\ell'}$ – acts on the gauge link between sites k and $k+1$,

$\mathbf{J}_k^2$ – gives the color-electric energy on the link,

g – coupling constant,

a – lattice spacing,

m – bare fermion mass.

Non-Abelian SU(2) gauge theory

M. C. Bañuls, K.C., J. I. Cirac, K. Jansen, S. Kühn, Phys. Rev. **X7** (2017) 041046

- The operators $U_k^{\ell\ell'}$ are SU(2) matrices and can be interpreted as rotation matrices.

Non-Abelian SU(2) gauge theory

M. C. Bañuls, K.C., J. I. Cirac, K. Jansen, S. Kühn, Phys. Rev. **X7** (2017) 041046

- The operators $U_k^{\ell\ell'}$ are SU(2) matrices and can be interpreted as rotation matrices.
- Hence, the Hilbert space for each gauge link is analogous to a quantum rigid rotor with total angular momentum j.

Non-Abelian SU(2) gauge theory

M. C. Bañuls, K.C., J. I. Cirac, K. Jansen, S. Kühn, Phys. Rev. **X7** (2017) 041046

- The operators $U_k^{\ell\ell'}$ are SU(2) matrices and can be interpreted as rotation matrices.
- Hence, the Hilbert space for each gauge link is analogous to a quantum rigid rotor with total angular momentum j.
- It can be described in two reference frames, the body-fixed system and the space-fixed (inertial) frame of reference.

Non-Abelian SU(2) gauge theory

M. C. Bañuls, K.C., J. I. Cirac, K. Jansen, S. Kühn, Phys. Rev. **X7** (2017) 041046

- The operators $U_k^{\ell\ell'}$ are SU(2) matrices and can be interpreted as rotation matrices.
- Hence, the Hilbert space for each gauge link is analogous to a quantum rigid rotor with total angular momentum j.
- It can be described in two reference frames, the body-fixed system and the space-fixed (inertial) frame of reference.
- Thus, the links can be labeled by the angular momentum z-components of the rotor ℓ, $\ell'$and the total angular momentum j.

Non-Abelian SU(2) gauge theory

M. C. Bañuls, K.C., J. I. Cirac, K. Jansen, S. Kühn, Phys. Rev. **X7** (2017) 041046

- The operators $U_k^{\ell\ell'}$ are SU(2) matrices and can be interpreted as rotation matrices.
- Hence, the Hilbert space for each gauge link is analogous to a quantum rigid rotor with total angular momentum j.
- It can be described in two reference frames, the body-fixed system and the space-fixed (inertial) frame of reference.
- Thus, the links can be labeled by the angular momentum z-components of the rotor ℓ, $\ell'$and the total angular momentum j.
- L^τ, $\tau \in \{x, y, z\}$ (body-fixed ref. frame) and R^τ (space-fixed) can be interpreted as **left and right electric field on a link**.

Non-Abelian SU(2) gauge theory

M. C. Bañuls, K.C., J. I. Cirac, K. Jansen, S. Kühn, Phys. Rev. **X7** (2017) 041046

- The operators $U_k^{\ell\ell'}$ are SU(2) matrices and can be interpreted as rotation matrices.
- Hence, the Hilbert space for each gauge link is analogous to a quantum rigid rotor with total angular momentum j.
- It can be described in two reference frames, the body-fixed system and the space-fixed (inertial) frame of reference.
- Thus, the links can be labeled by the angular momentum z-components of the rotor ℓ, $\ell'$and the total angular momentum j.
- L^τ, $\tau \in \{x, y, z\}$ (body-fixed ref. frame) and R^τ (space-fixed) can be interpreted as **left and right electric field on a link**.
- $\mathbf{J}_k^2 = \sum_\tau L_k^\tau L_k^\tau = \sum_\tau R_k^\tau R_k^\tau$.

Non-Abelian SU(2) gauge theory

M. C. Bañuls, K.C., J. I. Cirac, K. Jansen, S. Kühn, Phys. Rev. **X7** (2017) 041046

- The operators $U_k^{\ell\ell'}$ are SU(2) matrices and can be interpreted as rotation matrices.
- Hence, the Hilbert space for each gauge link is analogous to a quantum rigid rotor with total angular momentum j.
- It can be described in two reference frames, the body-fixed system and the space-fixed (inertial) frame of reference.
- Thus, the links can be labeled by the angular momentum z-components of the rotor ℓ, $\ell'$and the total angular momentum j.
- L^τ, $\tau \in \{x, y, z\}$ (body-fixed ref. frame) and R^τ (space-fixed) can be interpreted as **left and right electric field on a link**.
- $\mathbf{J}_k^2 = \sum_\tau L_k^\tau L_k^\tau = \sum_\tau R_k^\tau R_k^\tau$.
- Suitable basis: $|n^1, n^2\rangle \otimes |j\ell\ell'\rangle \otimes |n^1, n^2\rangle \otimes \ldots$, where n^ℓ – fermionic occupation number for color ℓ.

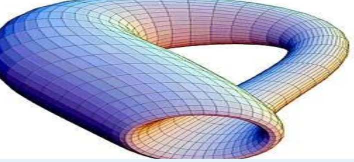

SU(2) Gauss law

M. C. Bañuls, K.C., J. I. Cirac, K. Jansen, S. Kühn, Phys. Rev. **X7** (2017) 041046

The physical states, $|\phi\rangle$, of the system have to satisfy the Gauss law:

$$G_k^\tau|\phi\rangle = 0, \forall k, \tau,$$

SU(2) Gauge law

M. C. Bañuls, K.C., J. I. Cirac, K. Jansen, S. Kühn, Phys. Rev. **X7** (2017) 041046

The physical states, $|\phi\rangle$, of the system have to satisfy the Gauss law:

$$G_k^\tau |\phi\rangle = 0, \forall k, \tau,$$

where:

$$G_k^\tau = L_k^\tau - R_{k-1}^\tau - Q_k^\tau,$$

are the generators for gauge transformations.

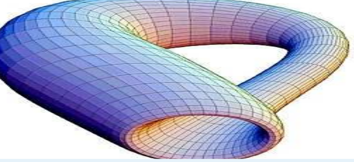

SU(2) Gauss law

M. C. Bañuls, K.C., J. I. Cirac, K. Jansen, S. Kühn, Phys. Rev. **X7** (2017) 041046

The physical states, $|\phi\rangle$, of the system have to satisfy the Gauss law:

$$G_k^\tau|\phi\rangle = 0, \forall k, \tau,$$

where:

$$G_k^\tau = L_k^\tau - R_{k-1}^\tau - Q_k^\tau,$$

are the generators for gauge transformations.
In the formula above $Q_k^\tau = \sum_{\ell=1}^{2} \frac{1}{2} {\psi_k^\ell}^\dagger \sigma_{\ell\ell'}^\tau \psi_k^{\ell''}$ are the components of the non-Abelian charge at site k and σ^τ are the usual Pauli matrices.
.

Integrating out the gauge field

M. C. Bañuls, K.C., J. I. Cirac, K. Jansen, S. Kühn, Phys. Rev. **X7** (2017) 041046

- For the non-Abelian case, it is **not** possible to fully integrate out the gauge field.

Integrating out the gauge field

M. C. Bañuls, K.C., J. I. Cirac, K. Jansen, S. Kühn, Phys. Rev. **X7** (2017) 041046

- For the non-Abelian case, it is **not** possible to fully integrate out the gauge field.
- Nevertheless, it is possible to drastically reduce the link Hilbert space size.

Integrating out the gauge field

M. C. Bañuls, K.C., J. I. Cirac, K. Jansen, S. Kühn, Phys. Rev. **X7** (2017) 041046

- For the non-Abelian case, it is **not** possible to fully integrate out the gauge field.
- Nevertheless, it is possible to drastically reduce the link Hilbert space size.
- Instead of working in the basis containing the full color information, we can restrict ourselves to a basis formed by color-singlet states.

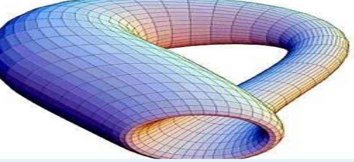

Integrating out the gauge field

M. C. Bañuls, K.C., J. I. Cirac, K. Jansen, S. Kühn, Phys. Rev. **X7** (2017) 041046

- For the non-Abelian case, it is **not** possible to fully integrate out the gauge field.
- Nevertheless, it is possible to drastically reduce the link Hilbert space size.
- Instead of working in the basis containing the full color information, we can restrict ourselves to a basis formed by color-singlet states.
- Gauss law in the color-singlet basis reduces to the fact that the electric flux j_{k+1} can only differ from the one on the previous link by one quantum, if the site is occupied by a single fermion:

$$j_{k+1} = \begin{cases} j_k & \text{if } n_{k+1} = 0, 2 \\ j_k \pm \frac{1}{2} & \text{if } n_{k+1} = 1. \end{cases}$$

Integrating out the gauge field

M. C. Bañuls, K.C., J. I. Cirac, K. Jansen, S. Kühn, Phys. Rev. **X7** (2017) 041046

- In addition to reducing the degrees of freedom significantly compared to the full basis, the color-singlet basis also offers the possibility to trivially truncate the color-electric flux at a certain value of $j_{\rm max}$ in a gauge invariant manner.

Integrating out the gauge field

M. C. Bañuls, K.C., J. I. Cirac, K. Jansen, S. Kühn, Phys. Rev. **X7** (2017) 041046

- In addition to reducing the degrees of freedom significantly compared to the full basis, the color-singlet basis also offers the possibility to trivially truncate the color-electric flux at a certain value of $j_{\max}$ in a gauge invariant manner.
- Taking into account only states with $j \leq j_{\max}$ results in a truncated model with Hilbert spaces of dimension $d_{\text{link}} = 2j_{\max} + 1$ for the gauge links.

Integrating out the gauge field

M. C. Bañuls, K.C., J. I. Cirac, K. Jansen, S. Kühn, Phys. Rev. **X7** (2017) 041046

- In addition to reducing the degrees of freedom significantly compared to the full basis, the color-singlet basis also offers the possibility to trivially truncate the color-electric flux at a certain value of j_{max} in a gauge invariant manner.
- Taking into account only states with $j \le j_{\mathrm{max}}$ results in a truncated model with Hilbert spaces of dimension $d_{\mathrm{link}} = 2j_{\mathrm{max}} + 1$ for the gauge links.
- Compared to the full basis, where for $j_{\mathrm{max}} = 1/2,\ 1,\ 3/2,\ 2$ one would have link Hilbert spaces of dimension $5,\ 14,\ 30,\ 55$, one only has to deal with spaces of dimension $d_{\mathrm{link}} = 2,\ 3,\ 4,\ 5$.

Integrating out the gauge field

M. C. Bañuls, K.C., J. I. Cirac, K. Jansen, S. Kühn, Phys. Rev. **X7** (2017) 041046

- In addition to reducing the degrees of freedom significantly compared to the full basis, the color-singlet basis also offers the possibility to trivially truncate the color-electric flux at a certain value of j_{max} in a gauge invariant manner.
- Taking into account only states with $j \leq j_{\mathrm{max}}$ results in a truncated model with Hilbert spaces of dimension $d_{\mathrm{link}} = 2j_{\mathrm{max}} + 1$ for the gauge links.
- Compared to the full basis, where for $j_{\mathrm{max}} = 1/2,\ 1,\ 3/2,\ 2$ one would have link Hilbert spaces of dimension $5,\ 14,\ 30,\ 55$, one only has to deal with spaces of dimension $d_{\mathrm{link}} = 2,\ 3,\ 4,\ 5$.
- Note that this reduction is **essential** from the point of view of potential experimental realization!

Integrating out the gauge field

M. C. Bañuls, K.C., J. I. Cirac, K. Jansen, S. Kühn, Phys. Rev. **X7** (2017) 041046

- Hence, a suitable basis for a system with N sites is given by

$$|\phi\rangle = |\alpha_1\rangle \otimes |\alpha_2\rangle \otimes \cdots \otimes |\alpha_N\rangle$$

with $|\alpha_k\rangle \in \{|0\rangle, |1_-\rangle, |1_+\rangle, |2\rangle\}$.

Integrating out the gauge field

M. C. Bañuls, K.C., J. I. Cirac, K. Jansen, S. Kühn, Phys. Rev. **X7** (2017) 041046

- Hence, a suitable basis for a system with N sites is given by

$$|\phi\rangle = |\alpha_1\rangle \otimes |\alpha_2\rangle \otimes \cdots \otimes |\alpha_N\rangle$$

with $|\alpha_k\rangle \in \{|0\rangle, |1_-\rangle, |1_+\rangle, |2\rangle\}$.

- Similar to the (Abelian) Schwinger model, in this basis the configuration of the sites uniquely determines the content of the gauge links, thus, effectively *abelianizing* the model.

Integrating out the gauge field

M. C. Bañuls, K.C., J. I. Cirac, K. Jansen, S. Kühn, Phys. Rev. **X7** (2017) 041046

- Hence, a suitable basis for a system with N sites is given by

$$|\phi\rangle = |\alpha_1\rangle \otimes |\alpha_2\rangle \otimes \cdots \otimes |\alpha_N\rangle$$

  with $|\alpha_k\rangle \in \{|0\rangle, |1_-\rangle, |1_+\rangle, |2\rangle\}$.
- Similar to the (Abelian) Schwinger model, in this basis the configuration of the sites uniquely determines the content of the gauge links, thus, effectively *abelianizing* the model.
- Analogous construction possible for a generic gauge group $SU(N)$.

Extrapolation in D and N

M. C. Bañuls, K.C., J. I. Cirac, K. Jansen, S. Kühn, Phys. Rev. **X7** (2017) 041046

$N = 150$

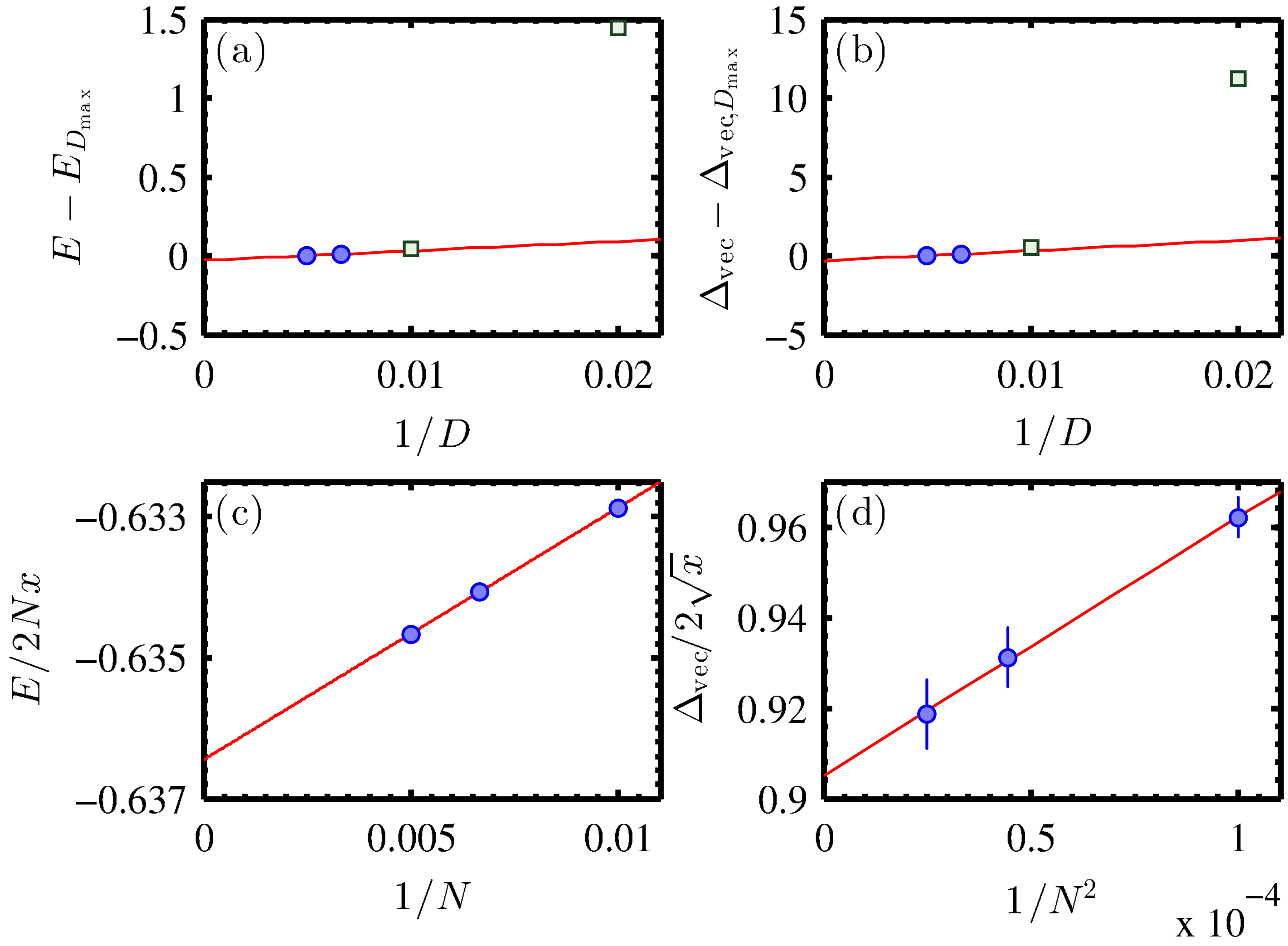

$m/g = 0.3,\ j_{\max} = 2,\ x = 150$

GS energy continuum extrapolation

M. C. Bañuls, K.C., J. I. Cirac, K. Jansen, S. Kühn, Phys. Rev. **X7** (2017) 041046

$m/g = 0.3$

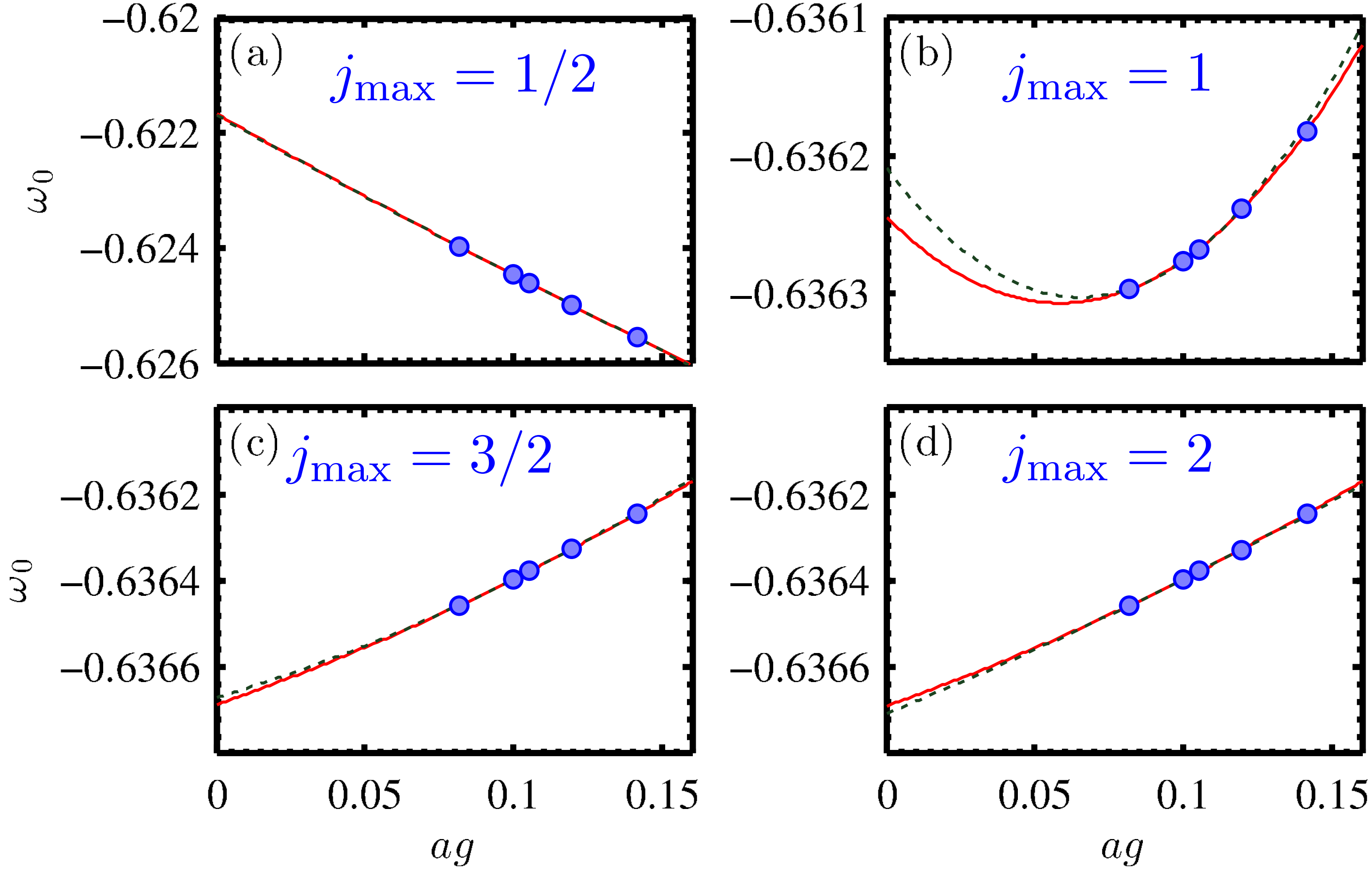

GS energy

M. C. Bañuls, K.C., J. I. Cirac, K. Jansen, S. Kühn, Phys. Rev. **X7** (2017) 041046

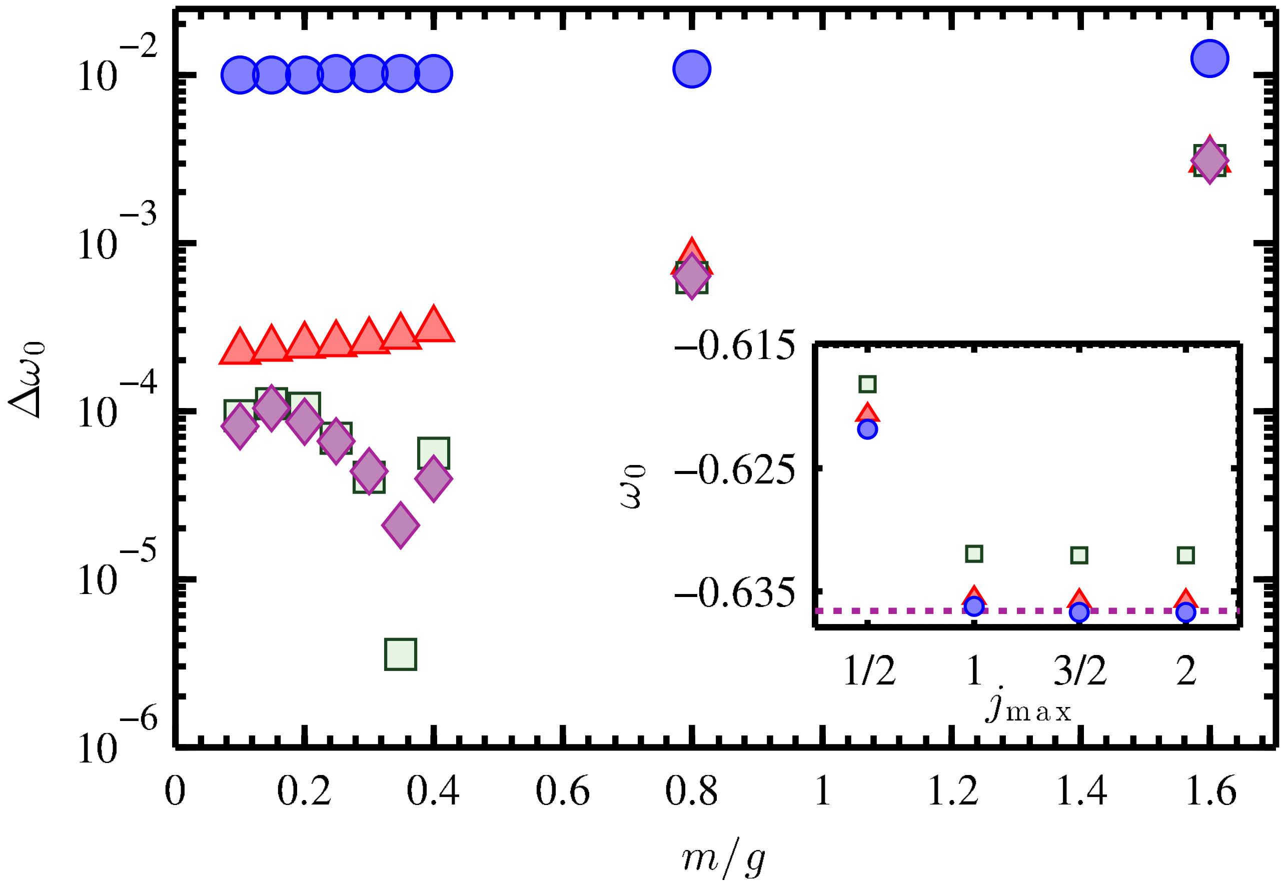

Main plot: blue circles – $j_{\max} = 1/2$, red triangles – $j_{\max} = 1$, green squares – $j_{\max} = 3/2$, magenta diamonds – $j_{\max} = 2$.
Inset: blue circles – $m/g = 0.1$, red triangles – $m/g = 0.8$, green squares – $m/g = 1.6$.

Analytic solution: $-2/\pi$ in the massless and continuum limit.

Vector mass continuum extrapolation

M. C. Bañuls, K.C., J. I. Cirac, K. Jansen, S. Kühn, Phys. Rev. **X7** (2017) 041046

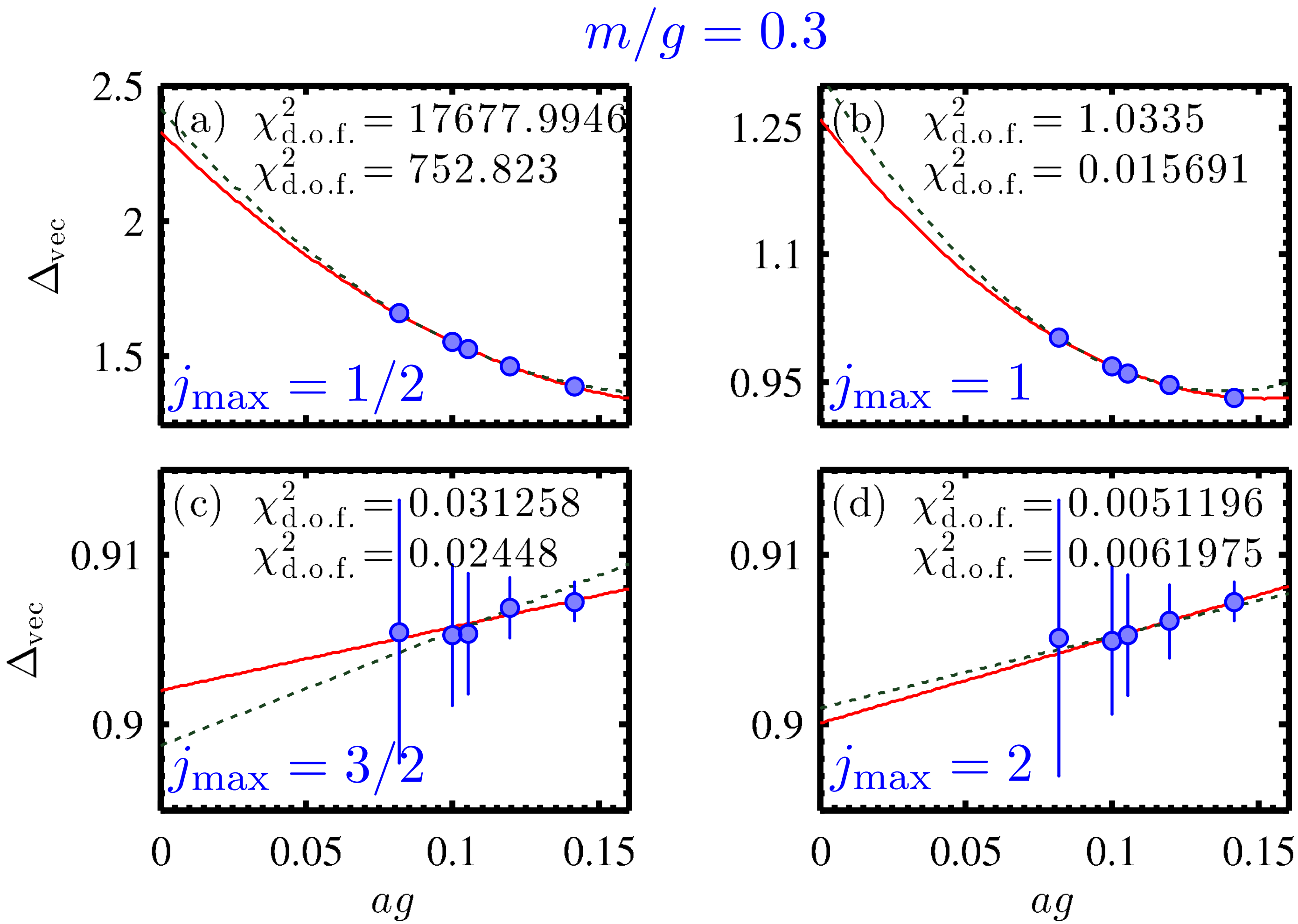

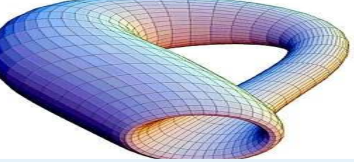

Vector mass scaling

M. C. Bañuls, K.C., J. I. Cirac, K. Jansen, S. Kühn, Phys. Rev. **X7** (2017) 041046

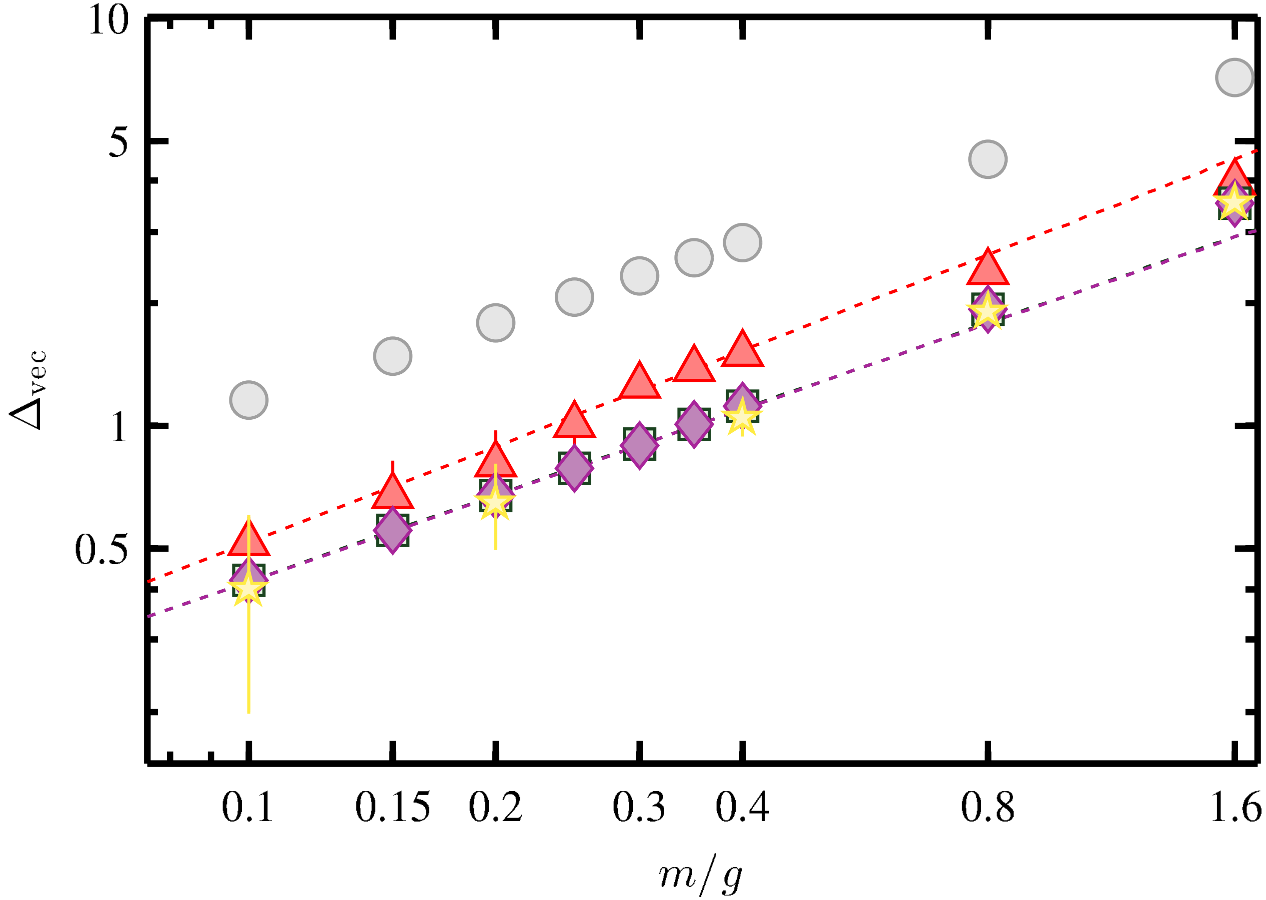

gray circles – $j_{\max} = 1/2$, red triangles – $j_{\max} = 1$, green squares – $j_{\max} = 3/2$, magenta diamonds – $j_{\max} = 2$,
yellow stars – strong coupling expansion [C. Hamer, Nucl. Phys. B195, 503 (1982)]

Dotted lines: best fit of the form $\gamma(m/g)^{\nu}$ in the interval $[0.1; (m/g)_{\max}]$ with $0.25 \leq (m/g)_{\max} \leq 0.4$.

Vector mass scaling

M. C. Bañuls, K.C., J. I. Cirac, K. Jansen, S. Kühn, Phys. Rev. **X7** (2017) 041046

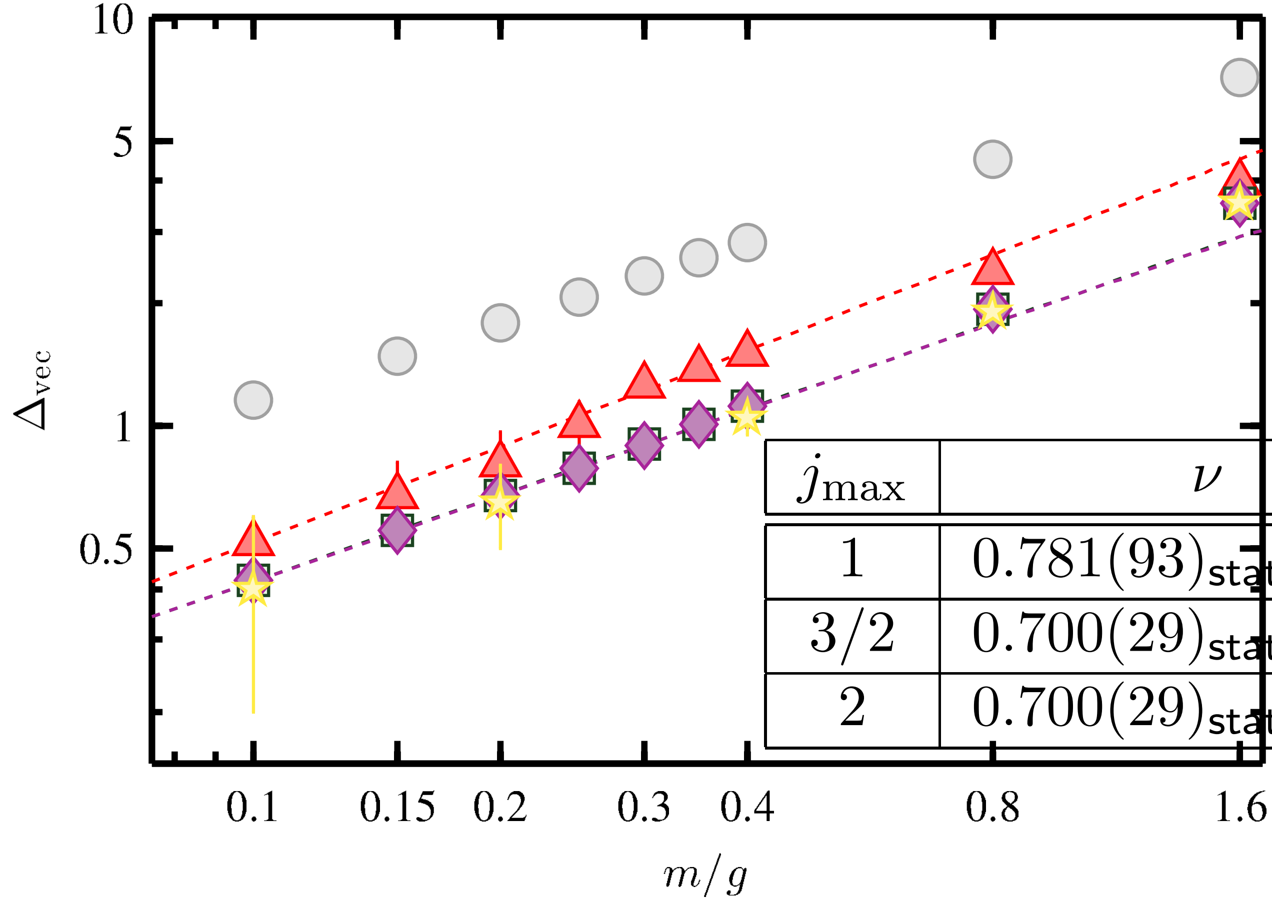

$j_{\max}$	ν
1	$0.781(93)_{\text{stat}}(65)_{\text{sys}}$
3/2	$0.700(29)_{\text{stat}}(11)_{\text{sys}}$
2	$0.700(29)_{\text{stat}}(12)_{\text{sys}}$

gray circles – $j_{\max} = 1/2$, red triangles – $j_{\max} = 1$, green squares – $j_{\max} = 3/2$, magenta diamonds – $j_{\max} = 2$,
yellow stars – strong coupling expansion [C. Hamer, Nucl. Phys. B195, 503 (1982)]

Dotted lines: best fit of the form $\gamma(m/g)^{\nu}$ in the interval $[0.1; (m/g)_{\max}]$ with $0.25 \leq (m/g)_{\max} \leq 0.4$.

Entanglement entropy

M. C. Bañuls, K.C., J. I. Cirac, K. Jansen, S. Kühn, Phys. Rev. **X7** (2017) 041046

There is a renewed interest in understanding the structure of entanglement in the gauge invariant scenario, motivated in part by a deep connection between entanglement and space-time geometry suggested in the context of the gauge/gravity duality.

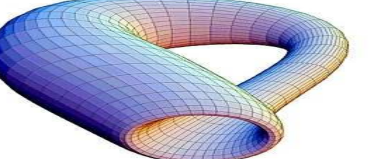

Entanglement entropy

M. C. Bañuls, K.C., J. I. Cirac, K. Jansen, S. Kühn, Phys. Rev. **X7** (2017) 041046

There is a renewed interest in understanding the structure of entanglement in the gauge invariant scenario, motivated in part by a deep connection between entanglement and space-time geometry suggested in the context of the gauge/gravity duality.

For the $SU(2)$ theory, one can write:

$$S(\rho) = -\sum_j p_j \log_2(p_j) + \sum_j p_j \log_2(2j+1) + \sum_j p_j S(\bar{\rho}_j),$$

Entanglement entropy

M. C. Bañuls, K.C., J. I. Cirac, K. Jansen, S. Kühn, Phys. Rev. **X7** (2017) 041046

There is a renewed interest in understanding the structure of entanglement in the gauge invariant scenario, motivated in part by a deep connection between entanglement and space-time geometry suggested in the context of the gauge/gravity duality.

For the $SU(2)$ theory, one can write:

$$S(\rho) = -\sum_j p_j \log_2(p_j) + \sum_j p_j \log_2(2j+1) + \sum_j p_j S(\bar{\rho}_j),$$

- 3rd term – distillable (physical) entropy – can be distilled from the system by means of local operations and classical communication (LOCC)

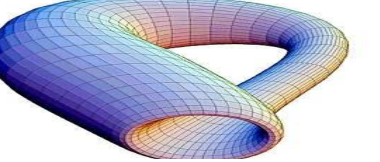

Entanglement entropy

M. C. Bañuls, K.C., J. I. Cirac, K. Jansen, S. Kühn, Phys. Rev. **X7** (2017) 041046

There is a renewed interest in understanding the structure of entanglement in the gauge invariant scenario, motivated in part by a deep connection between entanglement and space-time geometry suggested in the context of the gauge/gravity duality.

For the $SU(2)$ theory, one can write:

$$S(\rho) = -\sum_j p_j \log_2(p_j) + \sum_j p_j \log_2(2j+1) + \sum_j p_j S(\bar{\rho}_j),$$

- 3rd term – distillable (physical) entropy – can be distilled from the system by means of local operations and classical communication (LOCC)
- 1st term – classical entropy

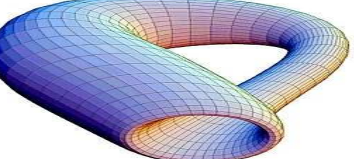

Entanglement entropy

M. C. Bañuls, K.C., J. I. Cirac, K. Jansen, S. Kühn, Phys. Rev. **X7** (2017) 041046

There is a renewed interest in understanding the structure of entanglement in the gauge invariant scenario, motivated in part by a deep connection between entanglement and space-time geometry suggested in the context of the gauge/gravity duality.

For the $SU(2)$ theory, one can write:

$$S(\rho) = -\sum_j p_j \log_2(p_j) + \sum_j p_j \log_2(2j+1) + \sum_j p_j S(\bar{\rho}_j),$$

- 3rd term – distillable (physical) entropy – can be distilled from the system by means of local operations and classical communication (LOCC)
- 1st term – classical entropy
- 2nd term – representation entropy – both result from the Gauss law, implying that the physical subspace is not a direct product of the Hilbert spaces for the links and the sites; cannot be extracted by LOCC.

Entanglement entropy

M. C. Bañuls, K.C., J. I. Cirac, K. Jansen, S. Kühn, Phys. Rev. **X7** (2017) 041046

- In 1+1 dimensions, a massive relativistic quantum field theory corresponds to a spin model off criticality in the scaling limit, for which the correlation length in lattice units, $\hat{\xi}$, is large.

M. C. Bañuls, K.C., J. I. Cirac, K. Jansen, S. Kühn, Phys. Rev. **X7** (2017) 041046

- In 1+1 dimensions, a massive relativistic quantum field theory corresponds to a spin model off criticality in the scaling limit, for which the correlation length in lattice units, $\hat{\xi}$, is large.
- For such a system the entanglement entropy for the reduced density matrix describing half of the system is given by $S \propto (c/6)\log_2(\hat{\xi})$ [P. Calabrese, J. Cardy, J. Stat. Mech. 2004, P06002 (2004)].

Entanglement entropy

M. C. Bañuls, K.C., J. I. Cirac, K. Jansen, S. Kühn, Phys. Rev. **X7** (2017) 041046

- In 1+1 dimensions, a massive relativistic quantum field theory corresponds to a spin model off criticality in the scaling limit, for which the correlation length in lattice units, $\hat{\xi}$, is large.
- For such a system the entanglement entropy for the reduced density matrix describing half of the system is given by $S \propto (c/6) \log_2(\hat{\xi})$ [P. Calabrese, J. Cardy, J. Stat. Mech. 2004, P06002 (2004)].
- The parameter c is the central charge of the underlying conformal field theory describing the system at the critical point.

Entanglement entropy

M. C. Bañuls, K.C., J. I. Cirac, K. Jansen, S. Kühn, Phys. Rev. **X7** (2017) 041046

- In 1+1 dimensions, a massive relativistic quantum field theory corresponds to a spin model off criticality in the scaling limit, for which the correlation length in lattice units, $\hat{\xi}$, is large.
- For such a system the entanglement entropy for the reduced density matrix describing half of the system is given by $S \propto (c/6)\log_2(\hat{\xi})$ [P. Calabrese, J. Cardy, J. Stat. Mech. 2004, P06002 (2004)].
- The parameter c is the central charge of the underlying conformal field theory describing the system at the critical point.
- Taking the continuum limit of the lattice formulation, $ag = 1/\sqrt{x} \to 0$, corresponds to approaching the limit of diverging correlation length in lattice units.

Entanglement entropy

M. C. Bañuls, K.C., J. I. Cirac, K. Jansen, S. Kühn, Phys. Rev. **X7** (2017) 041046

- In 1+1 dimensions, a massive relativistic quantum field theory corresponds to a spin model off criticality in the scaling limit, for which the correlation length in lattice units, $\hat{\xi}$, is large.
- For such a system the entanglement entropy for the reduced density matrix describing half of the system is given by $S \propto (c/6)\log_2(\hat{\xi})$ [P. Calabrese, J. Cardy, J. Stat. Mech. 2004, P06002 (2004)].
- The parameter c is the central charge of the underlying conformal field theory describing the system at the critical point.
- Taking the continuum limit of the lattice formulation, $ag = 1/\sqrt{x} \to 0$, corresponds to approaching the limit of diverging correlation length in lattice units.
- Thus, we expect the entropy to be logarithmically UV divergent as:

$$S = -\frac{c}{6}\log_2(ag) + c_2 \times ag + c_3 + \mathcal{O}\left((ag)^2\right),$$

where c, c_2, c_3 are fitting coefficients.

Entanglement entropy

M. C. Bañuls, K.C., J. I. Cirac, K. Jansen, S. Kühn, Phys. Rev. **X7** (2017) 041046

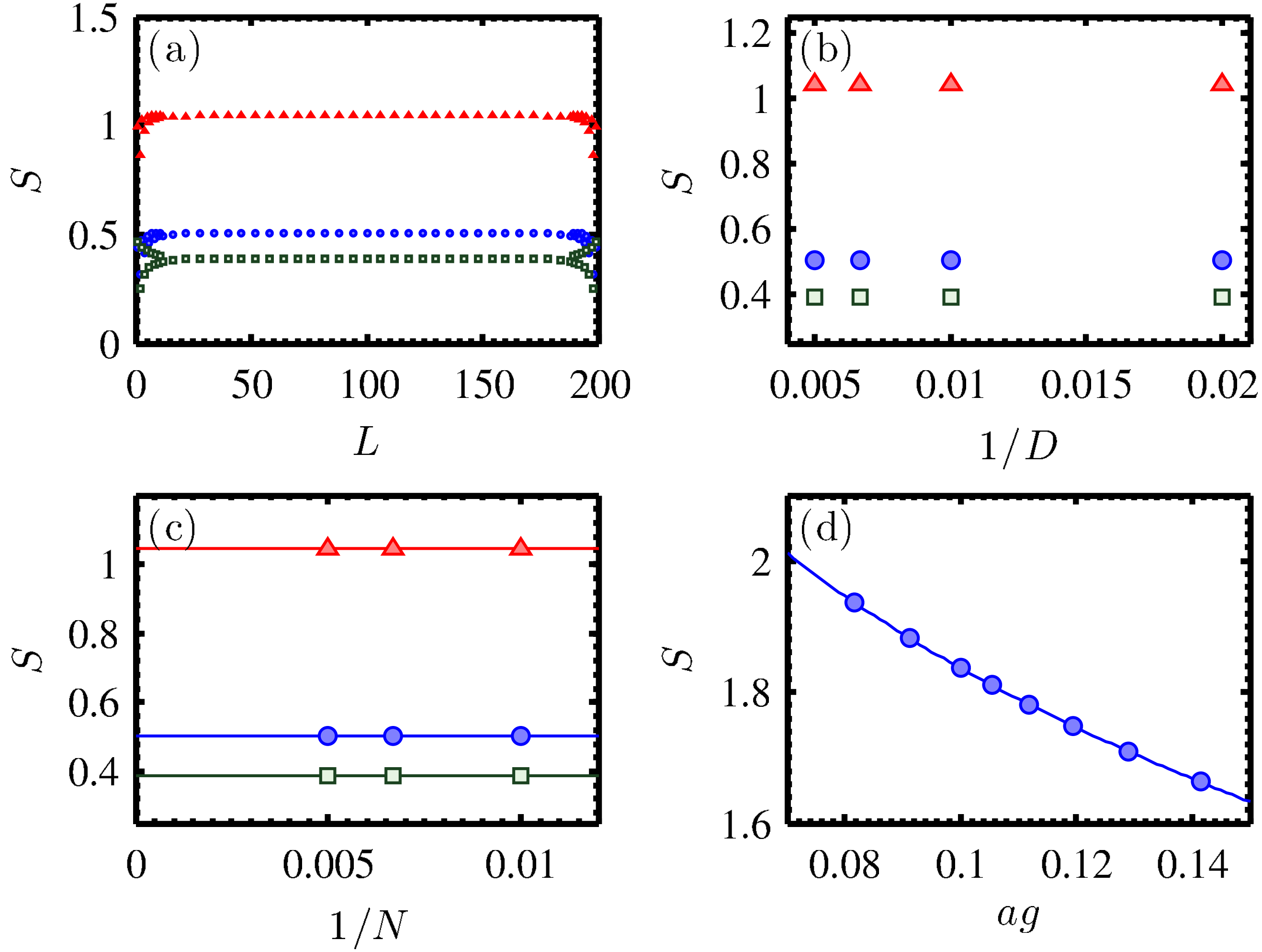

blue circles – distillable, red triangles – classical, green squares – representation

Entanglement entropy

M. C. Bañuls, K.C., J. I. Cirac, K. Jansen, S. Kühn, Phys. Rev. **X7** (2017) 041046

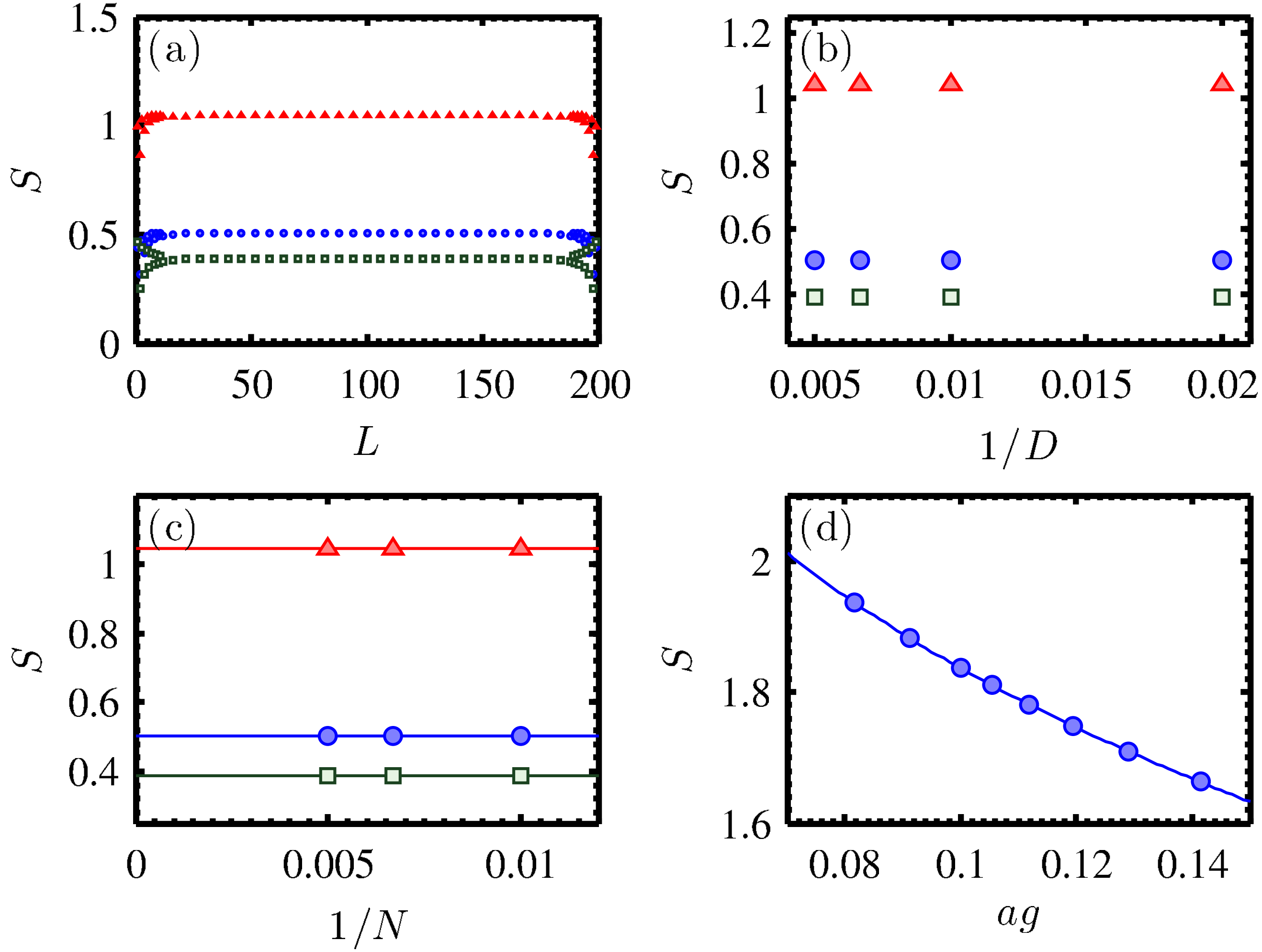

blue circles – distillable, red triangles – classical, green squares – representation**Fit in panel d (total entropy):**

$S = -\frac{c}{6}\log_2(ag) + c_2 \times ag + c_3 + \mathcal{O}\left((ag)^2\right)$

Entanglement entropy

M. C. Bañuls, K.C., J. I. Cirac, K. Jansen, S. Kühn, Phys. Rev. **X7** (2017) 041046

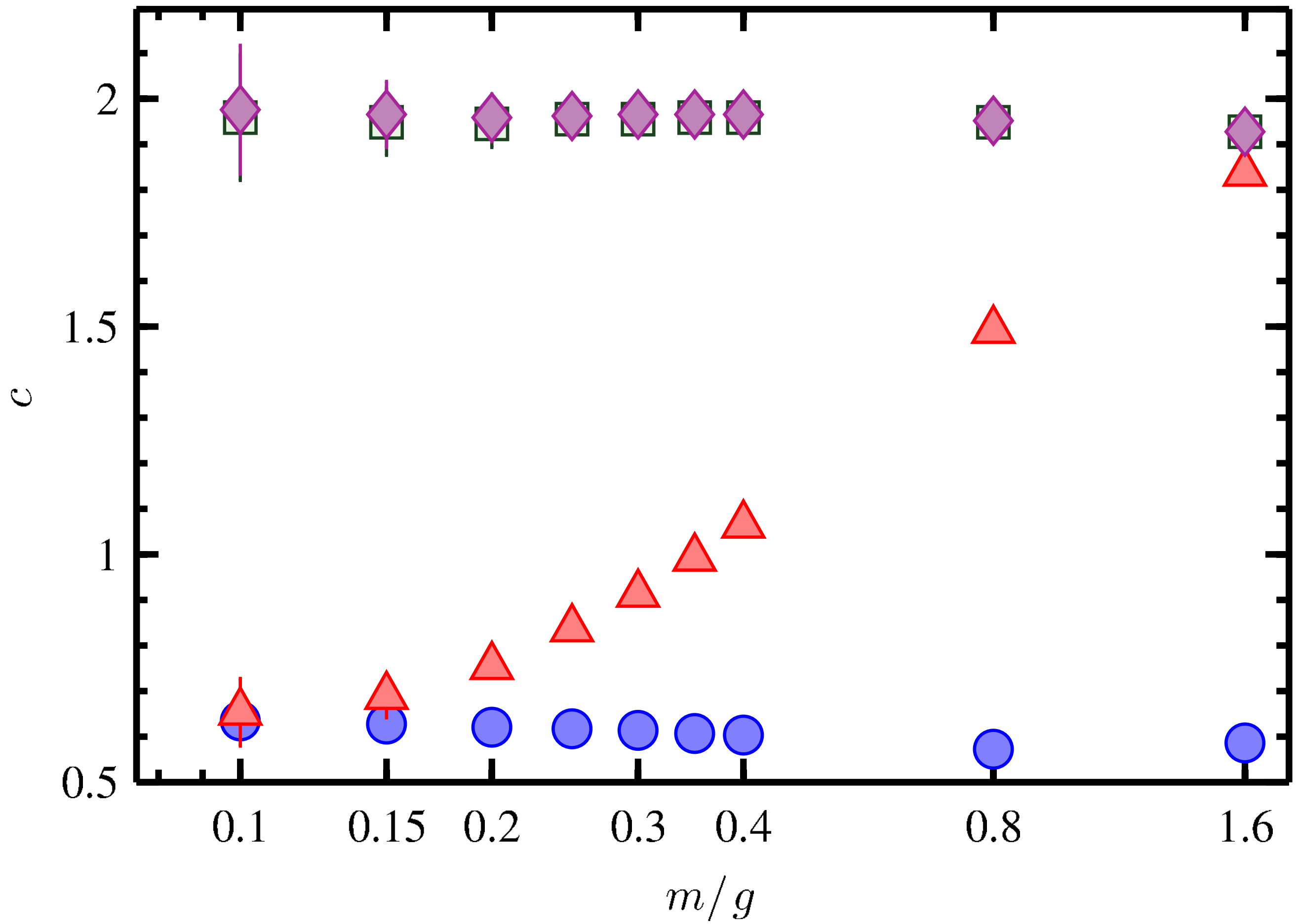

blue circles – $j_{\max} = 1/2$, red triangles – $j_{\max} = 1$,
green squares – $j_{\max} = 3/2$, magenta diamonds – $j_{\max} = 2$.

Entanglement entropy

M. C. Bañuls, K.C., J. I. Cirac, K. Jansen, S. Kühn, Phys. Rev. **X7** (2017) 041046

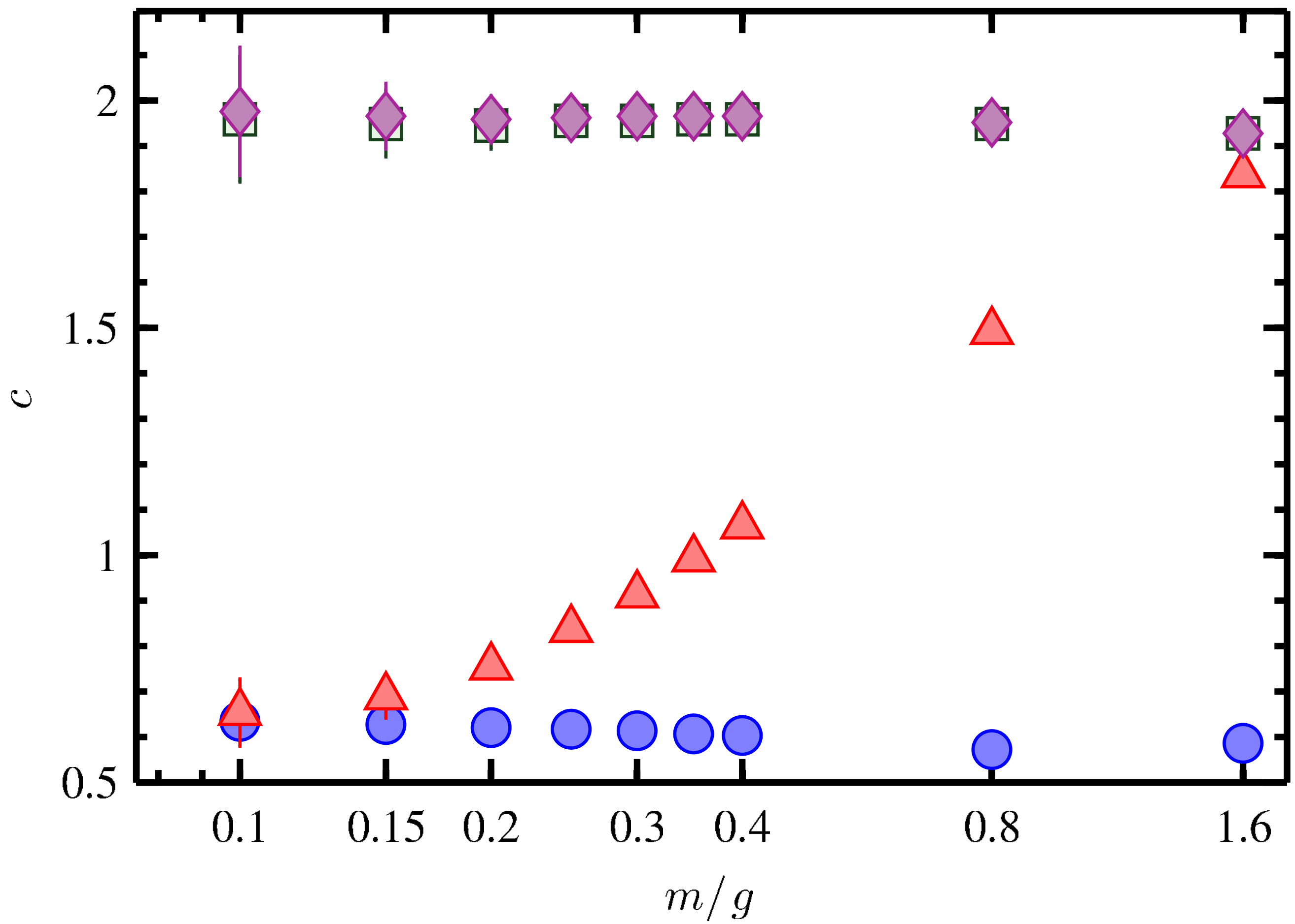

blue circles – $j_{\max} = 1/2$, red triangles – $j_{\max} = 1$,
green squares – $j_{\max} = 3/2$, magenta diamonds – $j_{\max} = 2$.

$c = 2$ – expected for 2 flavours of Dirac fermions!

The way to apply TNS to QCD is a long one.

The way to apply TNS to QCD is a long one.

- STARTING POINT: Schwinger model, i.e. an Abelian gauge theory with U(1) gauge group, 1+1 dimensions

$$\mathcal{L} = -\frac{1}{4}F_{\mu\nu}F^{\mu\nu} + \bar{\psi}(i\,\partial\!\!\!/ - g\,A\!\!\!/ - m)\psi$$

Road map to QCD with Tensor Networks

The way to apply TNS to QCD is a long one.

- STARTING POINT: Schwinger model, i.e. an Abelian gauge theory with U(1) gauge group, 1+1 dimensions

$$\mathcal{L} = -\frac{1}{4} F_{\mu\nu} F^{\mu\nu} + \bar{\psi}(i \not{\partial} - g \not{A} - m)\psi$$

- NATURAL NEXT STEP: non-Abelian gauge theories (SU(2), SU(3)) in 1+1 dimensions

Road map to QCD with Tensor Networks

The way to apply TNS to QCD is a long one.

- STARTING POINT: Schwinger model, i.e. an Abelian gauge theory with U(1) gauge group, 1+1 dimensions

$$\mathcal{L} = -\frac{1}{4}F_{\mu\nu}F^{\mu\nu} + \bar{\psi}(i\,\partial\!\!\!/ - g\,A\!\!\!/ - m)\psi$$

- NATURAL NEXT STEP: non-Abelian gauge theories (SU(2), SU(3)) in 1+1 dimensions
- AND ALSO: go to 2+1 dimensions

The way to apply TNS to QCD is a long one.

- STARTING POINT: Schwinger model, i.e. an Abelian gauge theory with U(1) gauge group, 1+1 dimensions

$$\mathcal{L} = -\frac{1}{4} F_{\mu\nu} F^{\mu\nu} + \bar{\psi}(i \not{\partial} - g \not{A} - m)\psi$$

- NATURAL NEXT STEP: non-Abelian gauge theories (SU(2), SU(3)) in 1+1 dimensions
- AND ALSO: go to 2+1 dimensions CRUCIAL!

Road map to QCD with Tensor Networks

The way to apply TNS to QCD is a long one.

- STARTING POINT: Schwinger model, i.e. an Abelian gauge theory with U(1) gauge group, 1+1 dimensions

$$\mathcal{L} = -\frac{1}{4}F_{\mu\nu}F^{\mu\nu} + \bar{\psi}(i\,\partial\!\!\!/ - g\,A\!\!\!/ - m)\psi$$

- NATURAL NEXT STEP: non-Abelian gauge theories (SU(2), SU(3)) in 1+1 dimensions
- AND ALSO: go to 2+1 dimensions CRUCIAL!
- FINALLY: go to 3+1 dimensions, non-Abelian gauge group SU(3) for QCD

The way to apply TNS to QCD is a long one.

- STARTING POINT: Schwinger model, i.e. an Abelian gauge theory with U(1) gauge group, 1+1 dimensions

$$\mathcal{L} = -\frac{1}{4} F_{\mu\nu} F^{\mu\nu} + \bar{\psi}(i \not{\partial} - g \not{A} - m)\psi$$

- NATURAL NEXT STEP: non-Abelian gauge theories (SU(2), SU(3)) in 1+1 dimensions
- AND ALSO: go to 2+1 dimensions CRUCIAL!
- FINALLY: go to 3+1 dimensions, non-Abelian gauge group SU(3) for QCD

All these next steps non-trivial and challenging.

Summary

- The tensor network approach can offer an alternative and very robust way of analyzing lattice gauge theories.

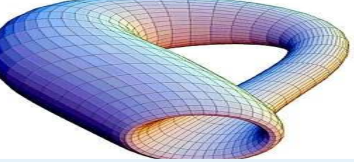

Summary

- The tensor network approach can offer an alternative and very robust way of analyzing lattice gauge theories.
- Its biggest advantage over Monte Carlo methods is that there is **no sign problem in any physical situation**.

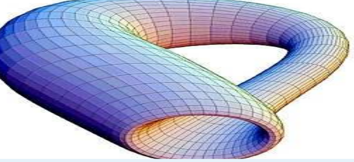

Summary

- The tensor network approach can offer an alternative and very robust way of analyzing lattice gauge theories.
- Its biggest advantage over Monte Carlo methods is that there is **no sign problem in any physical situation**.
- It has proven to be successful for various physical systems in 1+1-dimensions, including Abelian and non-Abelian lattice gauge theories.

Summary

- The tensor network approach can offer an alternative and very robust way of analyzing lattice gauge theories.
- Its biggest advantage over Monte Carlo methods is that there is **no sign problem in any physical situation**.
- It has proven to be successful for various physical systems in 1+1-dimensions, including Abelian and non-Abelian lattice gauge theories.
- **The biggest challenge – to go to higher dimensions**.

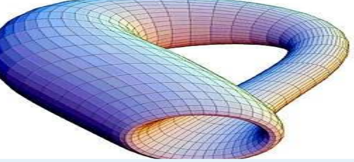

Summary

- The tensor network approach can offer an alternative and very robust way of analyzing lattice gauge theories.
- Its biggest advantage over Monte Carlo methods is that there is **no sign problem in any physical situation**.
- It has proven to be successful for various physical systems in 1+1-dimensions, including Abelian and non-Abelian lattice gauge theories.
- **The biggest challenge – to go to higher dimensions**.
- Next step: perhaps $(2+1)d$ QED?

Summary

- The tensor network approach can offer an alternative and very robust way of analyzing lattice gauge theories.
- Its biggest advantage over Monte Carlo methods is that there is **no sign problem in any physical situation**.
- It has proven to be successful for various physical systems in 1+1-dimensions, including Abelian and non-Abelian lattice gauge theories.
- **The biggest challenge – to go to higher dimensions**.
- Next step: perhaps $(2+1)d$ QED?
  For sure one of the most complicated TN calculations in history!

Summary

- The tensor network approach can offer an alternative and very robust way of analyzing lattice gauge theories.
- Its biggest advantage over Monte Carlo methods is that there is **no sign problem in any physical situation**.
- It has proven to be successful for various physical systems in 1+1-dimensions, including Abelian and non-Abelian lattice gauge theories.
- **The biggest challenge – to go to higher dimensions**.
- Next step: perhaps $(2+1)d$ QED?
  For sure one of the most complicated TN calculations in history!

Thank you for your attention!

Backup slides

$\mathcal{L} \to \mathcal{H}$

The Hamiltonian $\mathcal{H}$ is the Legendre transform of the Lagrangian $\mathcal{L}$:

$$\mathcal{H} = \pi^\mu \dot{A}_\mu - \mathcal{L},$$

where:

$$\pi^\mu = \frac{\partial \mathcal{L}}{\partial \dot{A}_\mu} = -F^{0\mu}.$$

We choose the time like axial gauge $A_0 = 0$:

$$H = \int dx \left(-i\bar{\psi}\gamma^1(\partial_1 + igA_1)\psi + m\bar{\psi}\psi + \frac{1}{2}E^2 \right).$$

The γ matrices:

$$\gamma^0 = \begin{pmatrix} 1 & 0 \\ 0 & -1 \end{pmatrix}, \qquad \gamma^1 = \begin{pmatrix} 0 & 1 \\ -1 & 0 \end{pmatrix}.$$

Going to the lattice:

$$U(n, n+1) = e^{i\theta(n)} = e^{-iagA^1(n)}$$

fermionic fields are associated with lattice sites and gauge fields with lattice links

Staggered discretization

The Hamiltonian becomes:

$$H = -\frac{i}{2a}\sum_{n=0}^{M-1}\left(\phi^\dagger(n)e^{i\theta(n)}\phi(n+1) - \phi^\dagger(n+1)e^{-i\theta(n)}\phi(n)\right) + \\ + m\sum_{n=0}^{M-1}(-1)^n\phi^\dagger(n)\phi(n) + \frac{ag^2}{2}\sum_{n=0}^{M-1}L^2(n),$$

in the Kogut-Susskind discretization:

[T. Banks, L. Susskind and J. B. Kogut, Phys. Rev. D **13** (1976) 1043]

[J. B. Kogut and L. Susskind, Phys. Rev. D **11** (1975) 395.]

$$\phi(n)/\sqrt{a} \to \begin{cases} \psi_{\text{upper}}(x) & n \text{ even} \\ \psi_{\text{lower}}(x) & n \text{ odd} \end{cases}$$

The correspondence between lattice and continuum fields is:

$$\begin{aligned} \frac{1}{ag}\theta(n) &\to -A^1(x) \\ gL(n) &\to E(x). \end{aligned}$$

Basic ingredients

- $\phi(n)$ is a single-component fermion field, defined on each site of a M-site lattice with periodic b.c. and obeying the anticomm. relations: $\{\phi^\dagger(n), \phi(m)\} = \delta_{nm}$, $\{\phi(n), \phi(m)\} = 0$, $\{\phi^\dagger(n), \phi^\dagger(m)\} = 0$
- The gauge field variable $\theta(n)$ is defined on the link between sites n and $n+1$ and is related to the spatial component of the Abelian vector potential by $\theta(n) = agA(n)$
- The angular momentum variable $L(n)$ is related to the electric field $E(n)$ by the relation $L(n) = E(n)/g$ and to the gauge field by the commutation relations: $[\theta(n), L(m)] = i\delta_{nm}$. The possible values of $L(n)$ are quantized: $L(n)|l\rangle = l|l\rangle$, $l = 0, \pm 1, \pm 2, \ldots$. This implies: $e^{\pm i\theta(n)}|l\rangle = |l \pm 1\rangle$
- m – fermion mass
- g – gauge coupling
- a – lattice spacing
- M – lattice size

Jordan-Wigner transformation

$$H = -\frac{i}{2a}\sum_{n=0}^{M-1}\Big(\phi^\dagger(n)e^{i\theta(n)}\phi(n+1) - \phi^\dagger(n+1)e^{-i\theta(n)}\phi(n)\Big)+$$
$$+m\sum_{n=0}^{M-1}(-1)^n\phi^\dagger(n)\phi(n) + \frac{ag^2}{2}\sum_{n=0}^{M-1}L^2(n),$$

For numerics, it is convenient to perform the Jordan-Wigner transformation: [P. Jordan, E. Wigner, Z. Phys. **47** (1928) 631.]

$$\phi(n) = \prod_{p<n}(i\sigma^3(p))\sigma^-(n),$$

where $\sigma^i(n)$ are Pauli matrices ($\sigma^\pm = \sigma^1 \pm i\sigma^2$). This gives:

$$H = -\frac{1}{2a}\sum_{n=0}^{M-1}\Big(\sigma^+(n)e^{i\theta(n)}\sigma^-(n+1) + \sigma^+(n+1)e^{-i\theta(n)}\sigma^-(n)\Big)+$$
$$+\frac{m}{2}\sum_{n=0}^{M-1}\Big(1+(-1)^n\sigma^3(n)\Big) + \frac{ag^2}{2}\sum_{n=0}^{M-1}L^2(n).$$

Choice of basis

Rewrite Hamiltonian in a dimensionless form: $W = \frac{2}{ag^2} H_{\mathrm{JW}} = W_0 - xV$, with:

$$W_0 = \frac{m}{ag^2} \sum_{n=0}^{M-1} \left(1 + (-1)^n \sigma^3(n)\right) + \sum_{n=0}^{M-1} L^2(n),$$

$$V = \sum_{n=0}^{M-1} \left(\sigma^+(n) e^{i\theta(n)} \sigma^-(n+1) + \sigma^+(n+1) e^{-i\theta(n)} \sigma^-(n)\right)$$

$$x \equiv \beta = 1/a^2 g^2.$$

- Natural choice of basis: direct product of Ising basis $\{|i\rangle\}$, acted upon by Pauli spin operators, and the ladder space of states $\{|l\rangle\}$:

  $$|i_0 i_1 \ldots i_{M-2} i_{M-1}\rangle \otimes |l_{0,1} l_{1,2} \ldots l_{M-2,M-1} (l_{M-1,0})\rangle,$$

  where $(l_{M-1,0})$ is present if PBC are considered and absent for OBC.
- Formally, the operator W_0 can be treated as an unperturbed part and V as a perturbation. Ground state of W_0: $|0\rangle = |\downarrow\uparrow\downarrow\uparrow \ldots \downarrow\uparrow\rangle \otimes |0000\ldots00\rangle$,
- The perturbation operator V flips two neighbouring spins and couples them via a gauge field excitation (flux line): $V\,|\bullet \quad \bullet\rangle = |\uparrow \rightsquigarrow \downarrow\rangle$

Choice of basis

- The gauge degrees of freedom $l_{i,i+1}$ can be eliminated using the Gauss law:

$$L_n - L_{n-1} = \frac{1}{2}\left(\sigma_n^z + (-1)^n\right),$$

leaving the basis states as: $|i_0 i_1 \ldots i_{M-2} i_{M-1}\rangle \otimes |l\rangle$,
with:
  - ⋆ $l = 0, \pm 1, \pm 2, \ldots$ for PBC,
  - ⋆ $l = 0$ (or other constant) for OBC.
- With M-site lattice, dim(spin part)=2^M, while for the gauge part the basis is
  - ⋆ infinite-dimensional for PBC ⇒ truncation needed,
  - ⋆ one-dimensional for OBC.
- Truncation for PBC:
  - ⋆ at some finite $\pm l_{\max}$, thus reducing the basis to dimension $(2l_{\max} + 1)2^M$,
  - ⋆ or use strong coupling expansion (SCE):

    [T. Banks, L. Susskind and J. B. Kogut, Phys. Rev. D **13** (1976) 1043]

    [J. B. Kogut and L. Susskind, Phys. Rev. D **11** (1975) 395.]

SCE+ED, infinite volume extrapolation

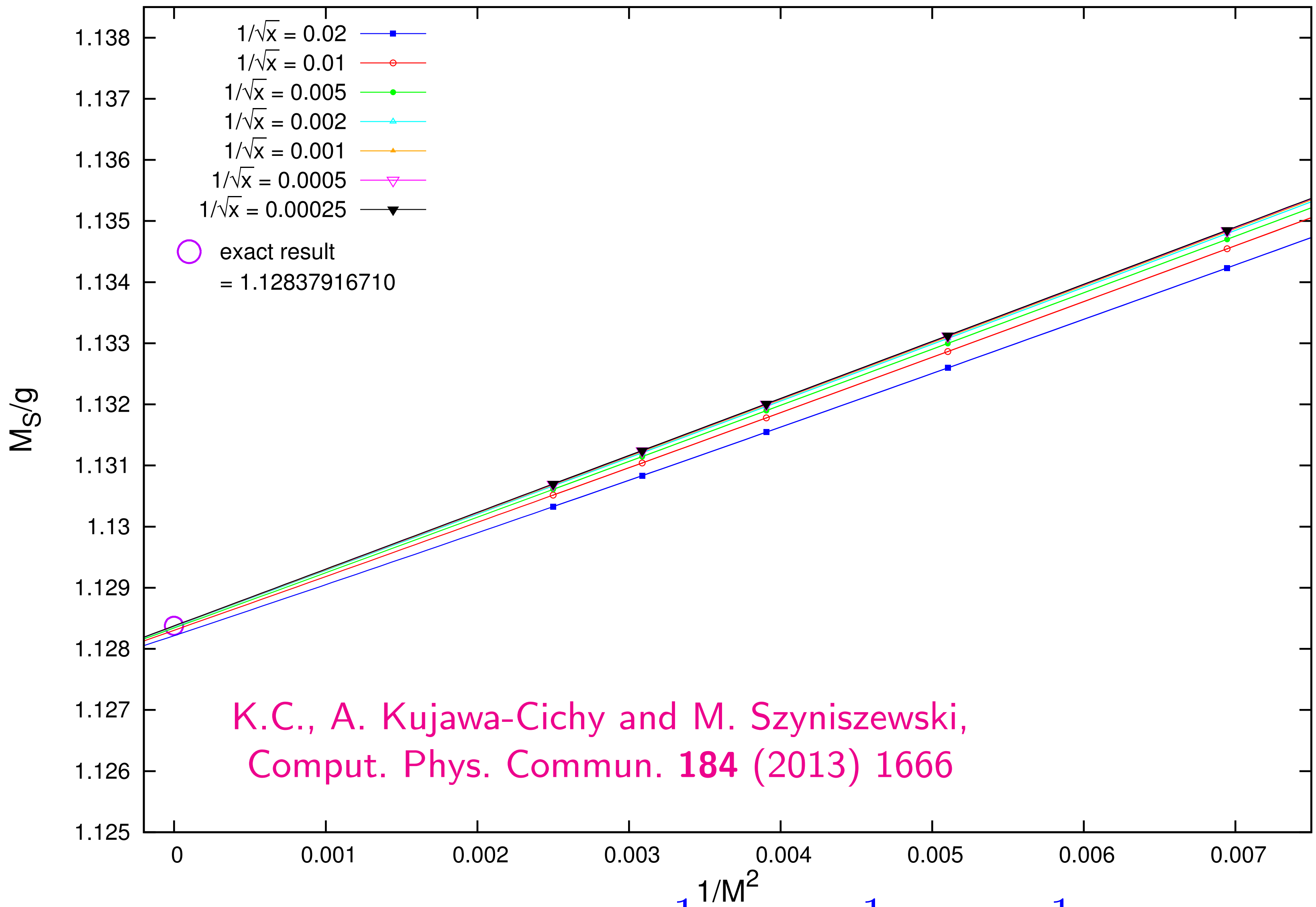

$$F(1/M^2) = F_0 + F_2 \frac{1}{M^2} + F_4 \frac{1}{M^4} + F_6 \frac{1}{M^6}$$

SCE+ED, infinite volume extrapolation

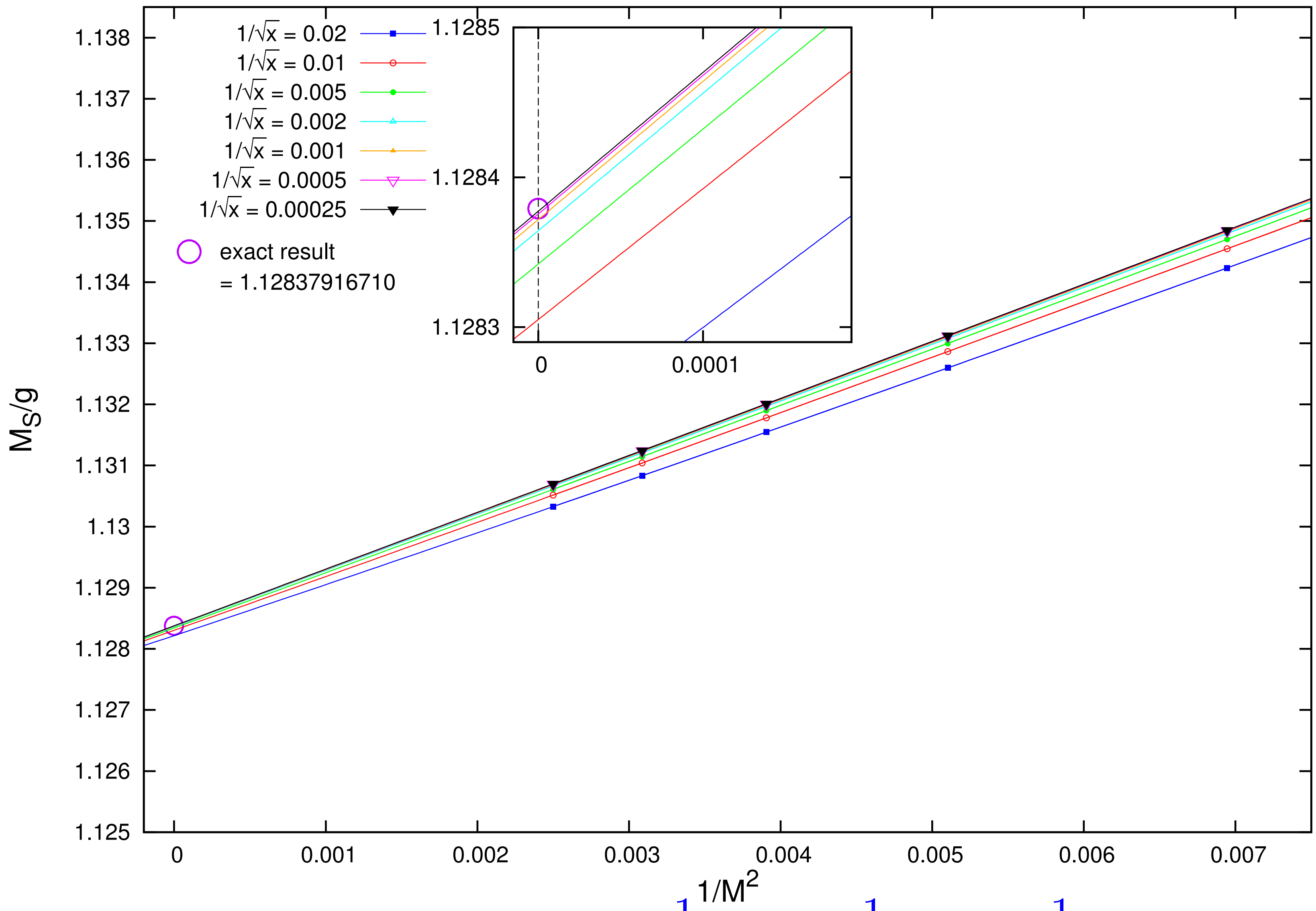

$$F(1/M^2) = F_0 + F_2 \frac{1}{M^2} + F_4 \frac{1}{M^4} + F_6 \frac{1}{M^6}$$

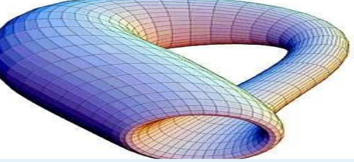

SCE+ED, continuum extrapolation

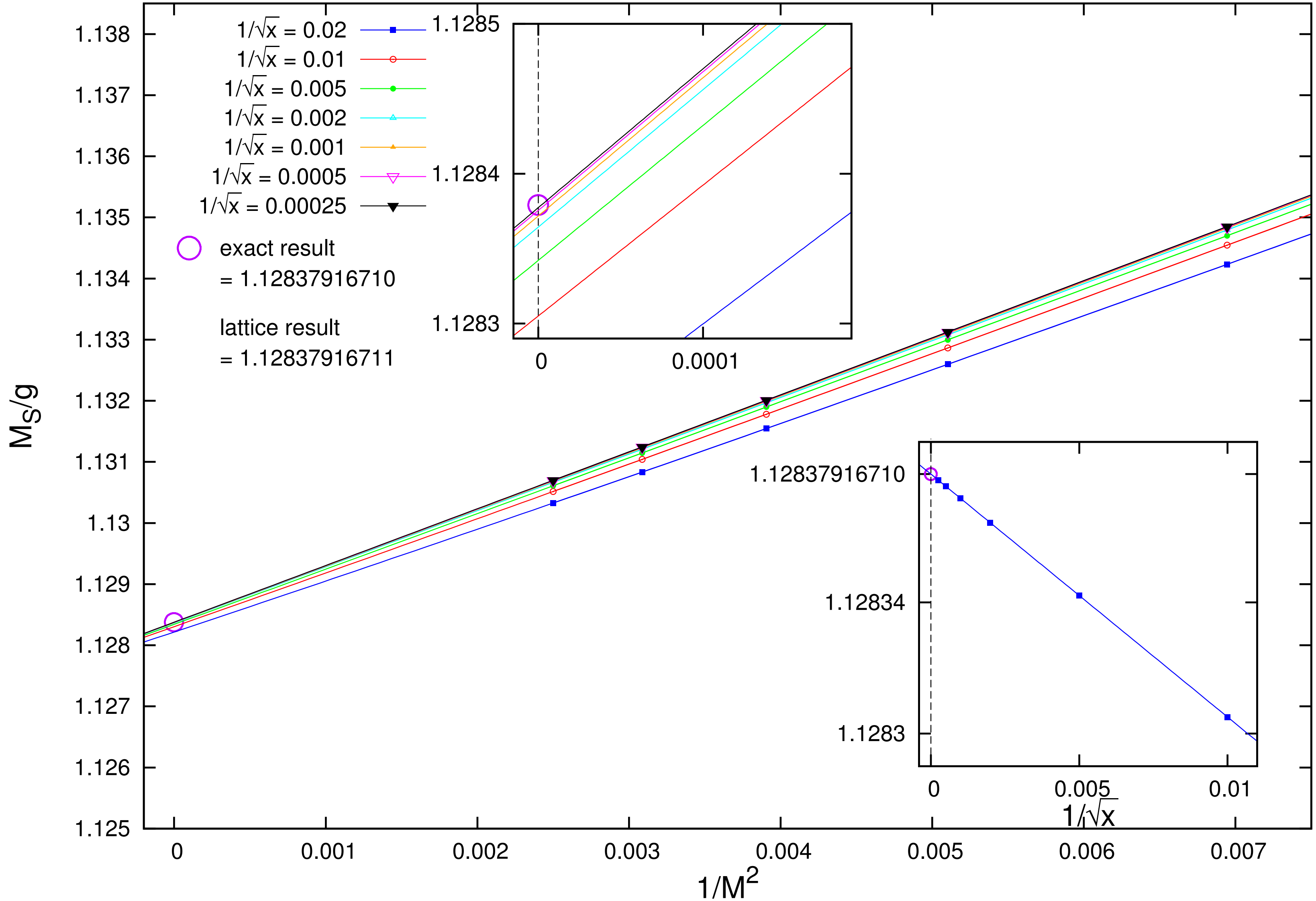

$$F_0(ag) = F_{00} + F_{01} \cdot ag + F_{02} \cdot (ag)^2$$

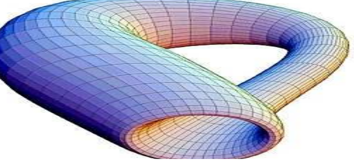

SCE+ED, comparison with literature

	M_S/g		M_V/g	
	result	error	result	error
exact	1.12837916710	–	0.5641895836	–
this work	1.12837916711	$1.3 \cdot 10^{-9}\%$	0.5641895845	$1.8 \cdot 10^{-7}\%$
[Crewther, Hamer 1980]	1.120	0.7%	0.560	0.7%
[Irving, Thomas 1982]	1.128	0.03%	0.565	0.1%
[Hamer et al. 1997] (I)	1.25	11%	0.56	0.7%
[Hamer et al. 1997] (II)	1.14	1%	0.57	1%
[Sriganesh et al. 1999] (I)	1.11	1.6%	0.563	0.2%
[Sriganesh et al. 1999] (II)	1.1284	0.002%	0.56417	0.003%
[Byrnes et al. 2002]	–	–	0.56419	$7 \cdot 10^{-5}\%$

Matrix Product States

We want to find:

- ground state energy
- vector mass gap
- scalar mass gap

for selected values of the fermion mass $m/g = 0,\ 0.125,\ 0.25,\ 0.5$.

Simulate with finite D (bond dimension), N (system size), x (inverse lattice spacing). We want:

- large enough D – check $D \in [20, 140]$,
- $N \to \infty$ – choose $N \in [100, 850]$ (note that $N \propto \sqrt{x}$),
- $x \to \infty$ – choose $x \in [5, 600]$.

GS energy. Bond dimension

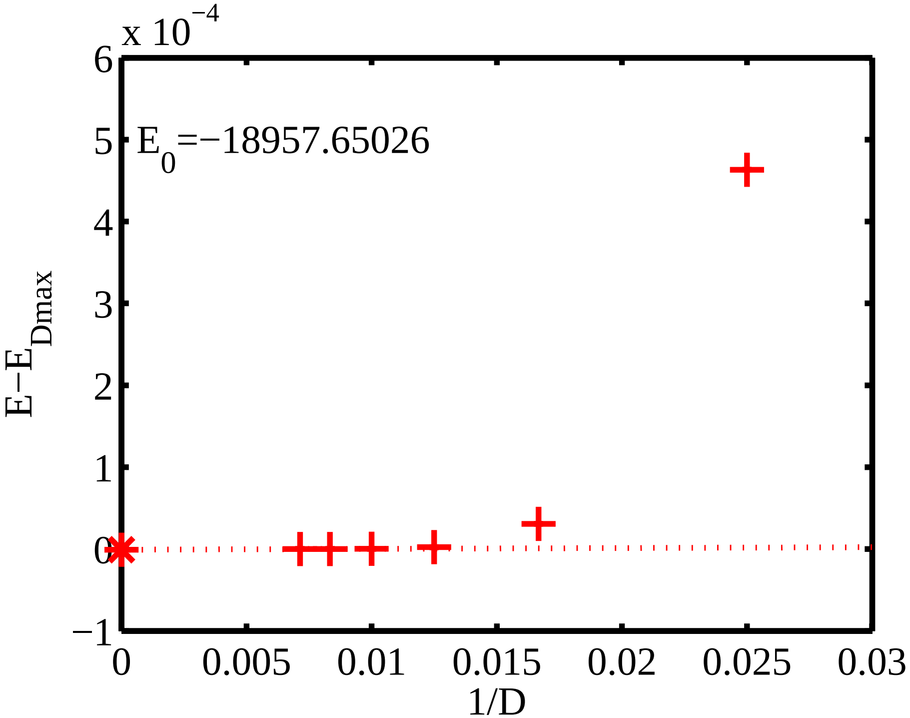

$m/g = 0,\ x = 100,\ N = 300$

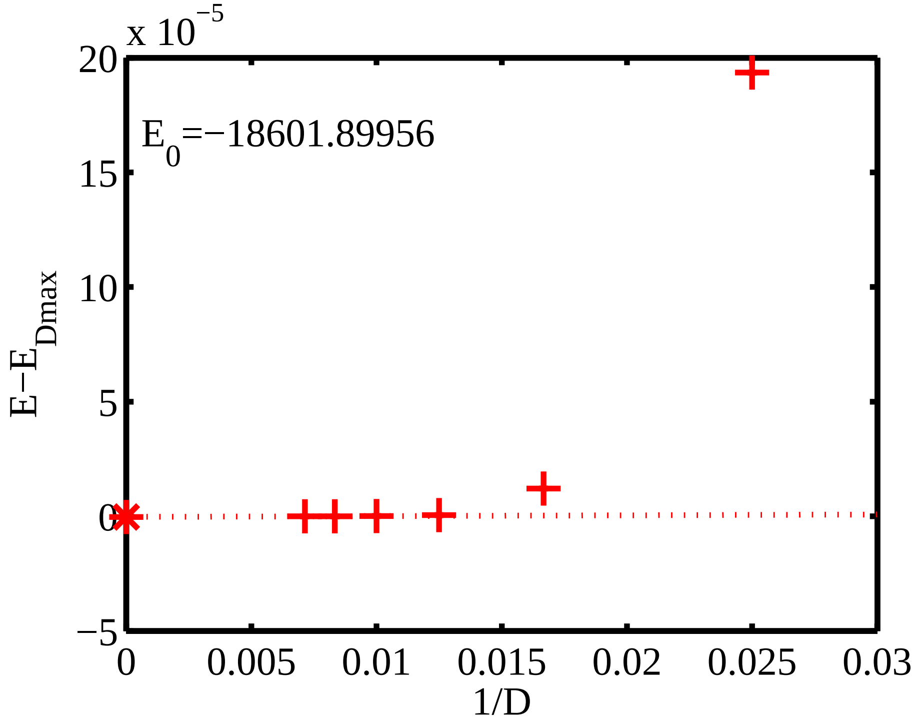

$m/g = 0.125,\ x = 100,\ N = 300$

GS energy. Finite size scaling

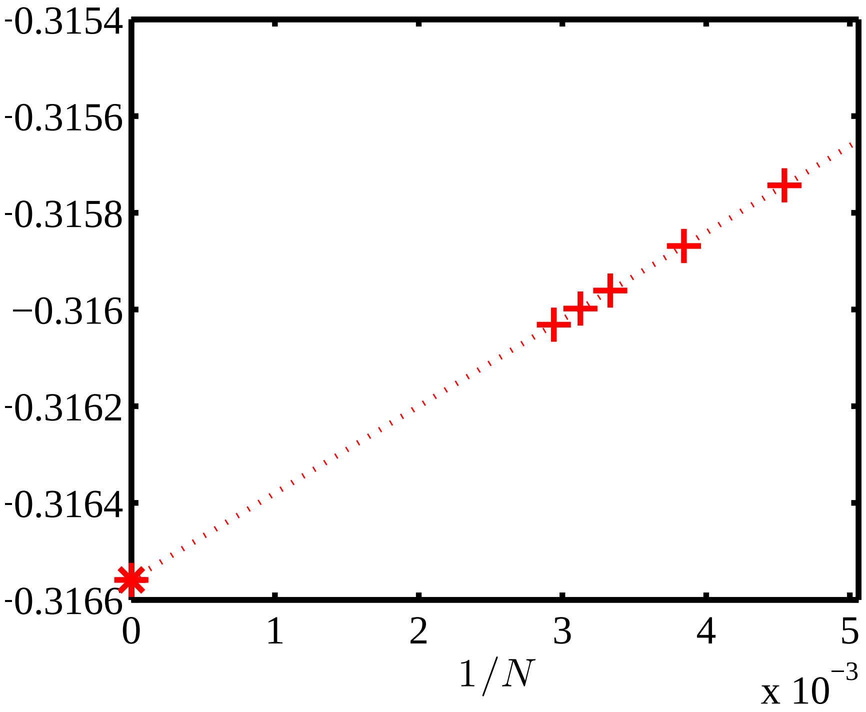

$m/g = 0,\ x = 100$

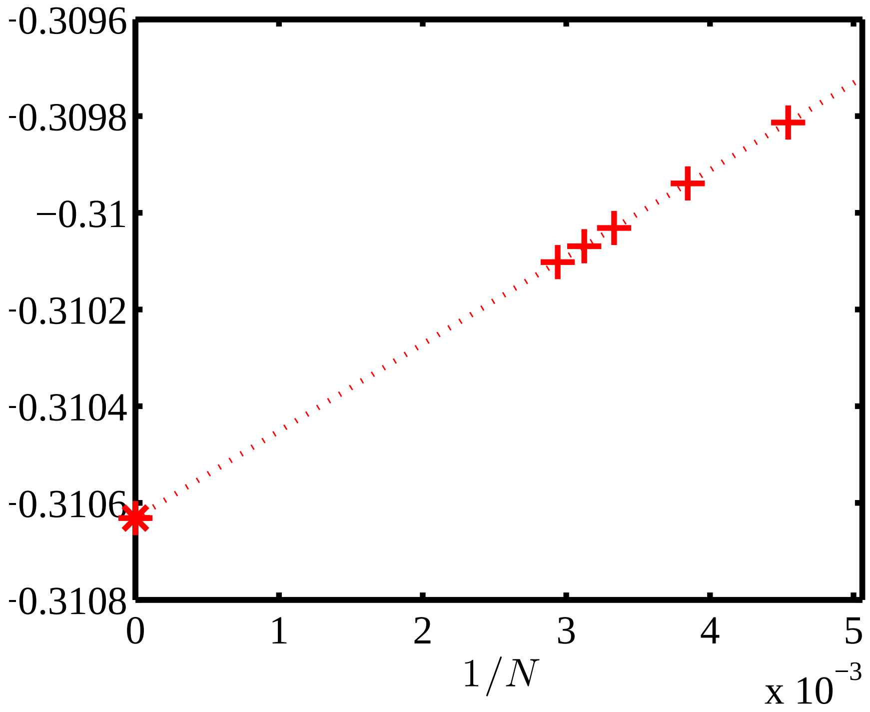

$m/g = 0.125,\ x = 100$

GS energy. Continuum extrapolation

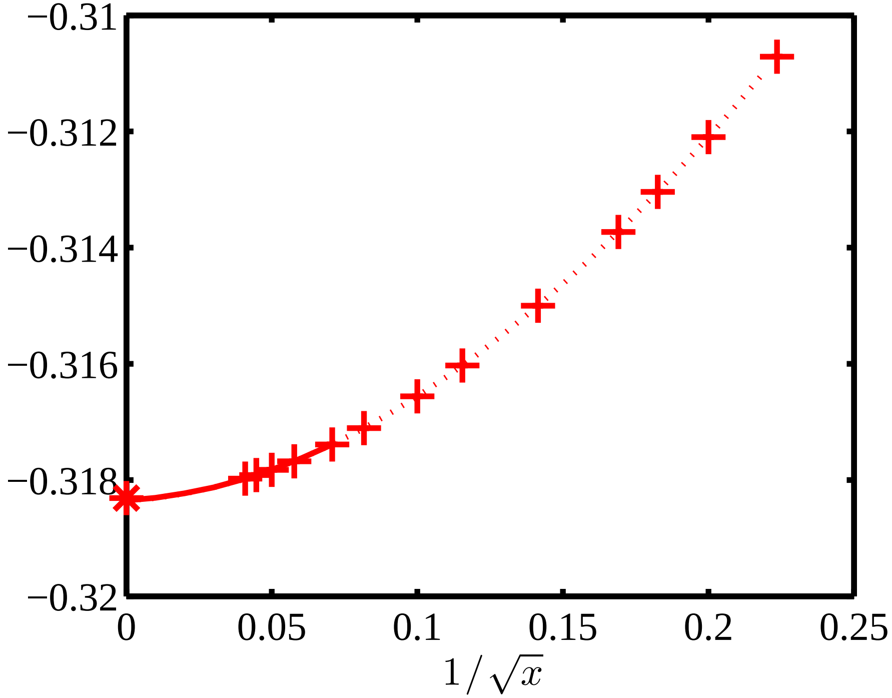

$m/g = 0$

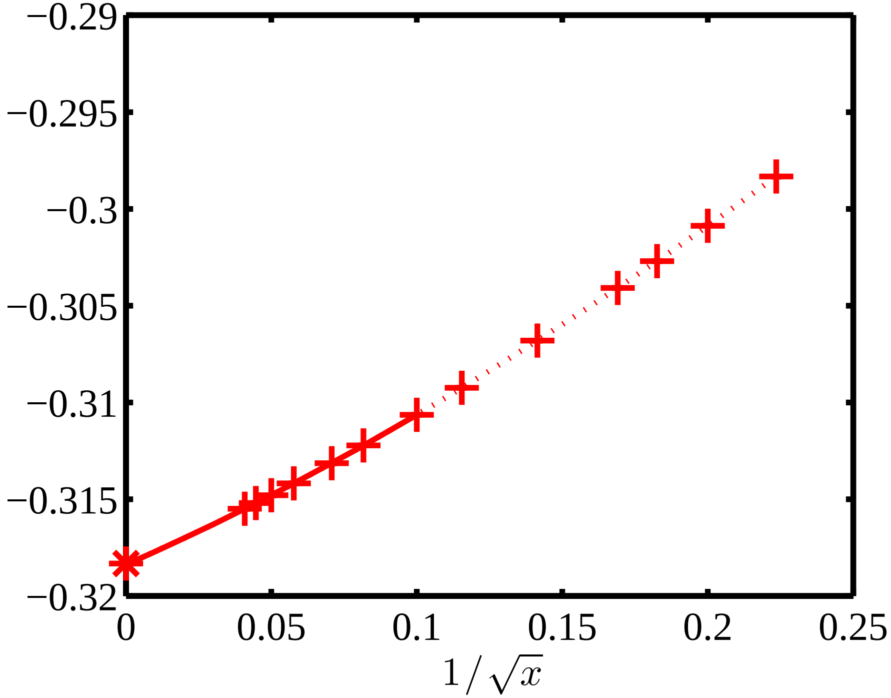

$m/g = 0.125$

continuum result:

$-0.318338(22)_{D,N,x\,\text{extrapol.}}(24)_{\text{fitansatz}}$ $-0.318343(96)_{D,N,x\,\text{extrapol.}}(25)_{\text{fit ansatz}}$

exact result: $1/\pi \approx -0.318310$

Computing the mass gap

- After having computed the GS energy, we want to compute the masses of the two lightest bound states ("mesons") of the theory:
  - ⋆ vector meson,
  - ⋆ scalar meson.
- Important: we have to recognize the vector and scalar states – use the charge conjugation transformation:
  - ⋆ PBC – $C = -1 \Rightarrow$ vector state, $C = +1 \Rightarrow$ scalar state,
  - ⋆ OBC – C no longer an exact symmetry, but "enough" to differentiate vector vs. scalar.
- Note: with OBC translational symmetry is lost – hence we also have momentum excitations of the vector meson *before* we reach the scalar.

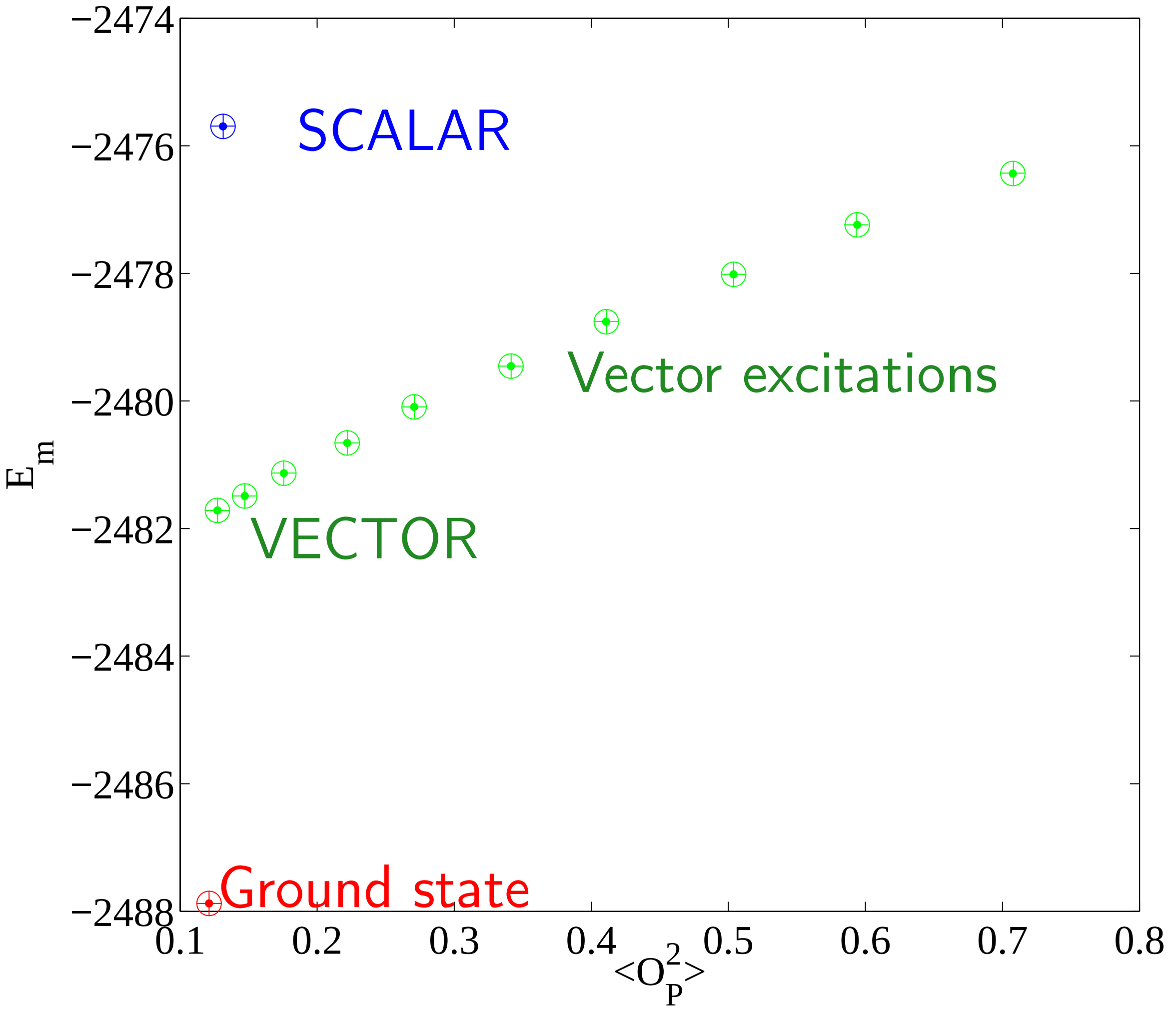

Continuum momentum operator

$$\hat{P} = \int dx \Psi^\dagger(x) i\partial_x \Psi(x)$$

Lattice spin representation

$$\hat{O}_P = -ix \sum_n \left(\sigma_n^- \sigma_{n+1}^z \sigma_{n+2}^+ - H.c.\right)$$

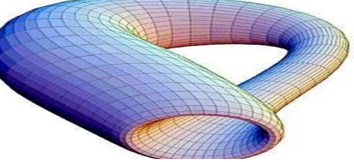

Results for the mass gaps, $m/g = 0$

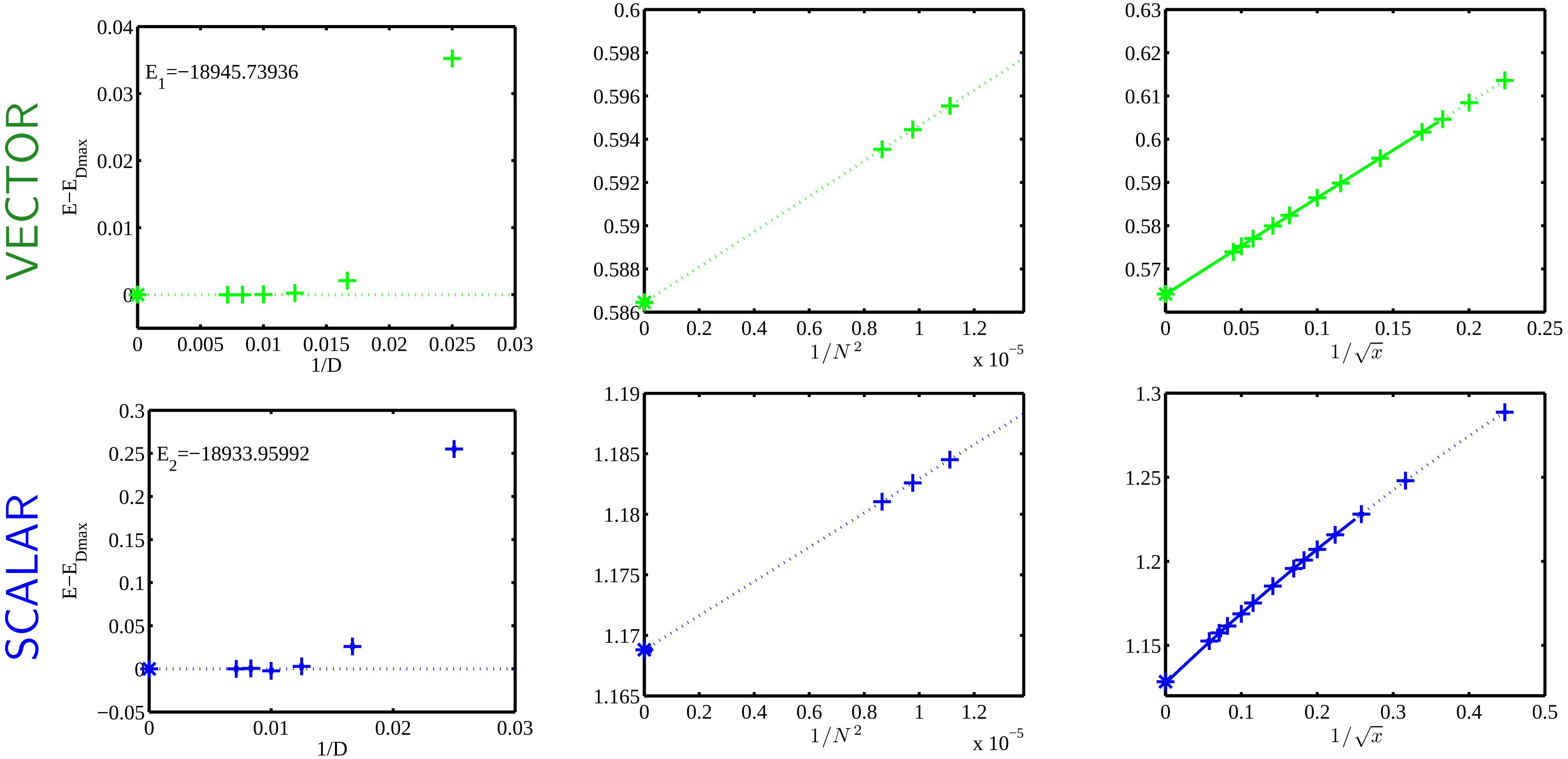

Truncation
$x = 100,\ N = 300$

Finite size scaling
$x = 100$

Continuum extrapolation

Results for the mass gaps, $m/g = 0.125$

VECTOR

SCALAR

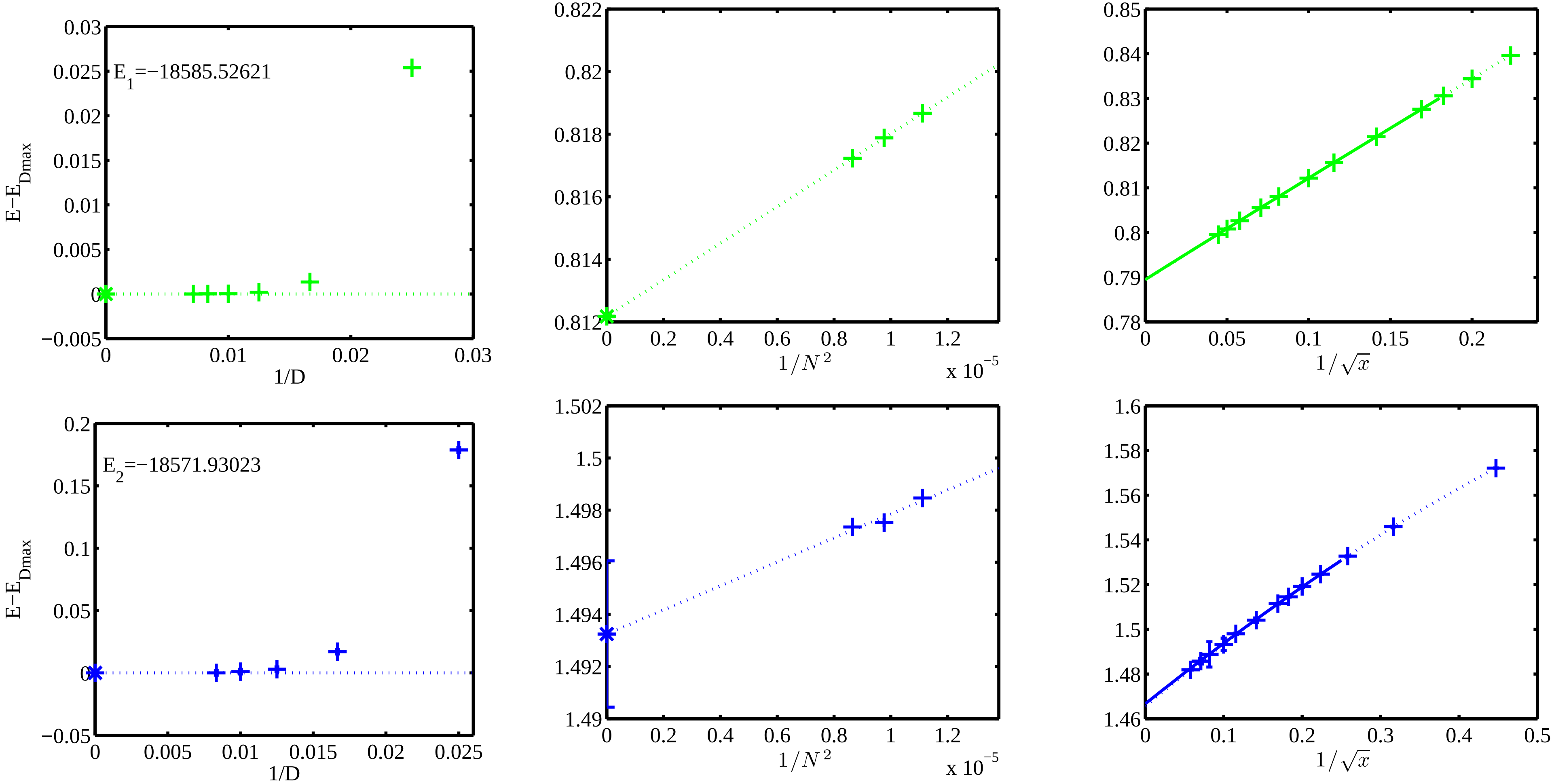

Truncation

$x = 100,\ N = 300$

Finite size scaling

$x = 100$

Continuum extrapolation

Results for the mass gaps

	Vector binding energy exact 0.5641895	
m/g	**MPS with OBC**	DMRG result
0	**0.56421(9)**	0.56419(4)
0.125	**0.53953(5)**	0.53950(7)
0.25	**0.51922(5)**	0.51918(5)
0.5	**0.48749(3)**	0.48747(2)

	Scalar binding energy exact 1.12838	
m/g	**MPS with OBC**	SCE result
0	**1.1279(12)**	1.11(3)
0.125	**1.2155(28)**	1.22(2)
0.25	**1.2239(22)**	1.24(3)
0.5	**1.1998(17)**	1.20(3)

DMRG result:

[T. Byrnes, P. Sriganesh, R. J. Bursill and C. J. Hamer, Phys. Rev. D **66** (2002) 013002]

SCE result:

[P. Sriganesh, R. Bursill and C. J. Hamer, Phys. Rev. D **62** (2000) 034508]

- The Schwinger model posesses a $U(1)_A$ chiral symmetry, which is broken by the chiral anomaly.
- This symmetry breaking is signaled by a non-zero value of the chiral condensate:

$$\Sigma = \frac{\sqrt{x}}{N} \sum_n (-1)^n \frac{1+\sigma_n^z}{2}$$

$\longrightarrow$ compute GS expectation value of Σ.

- The naively computed condensate has a logarithmic divergence $\propto \frac{m}{g} \log ag$. This divergence can be subtracted off by subtracting the free theory contribution (in the infinite volume limit):

$$\Sigma_{\text{free}}^{(\text{bulk})}(m/g, x) = \frac{m}{\pi g} \frac{1}{\sqrt{1+\frac{m^2}{g^2 x}}} \mathrm{K}\left(\frac{1}{1+\frac{m^2}{g^2 x}}\right),$$

where $\mathrm{K}(u)$ is the complete elliptic integral of the first kind.

Results for the chiral condensate $T = 0$ ($N_f = 1$)

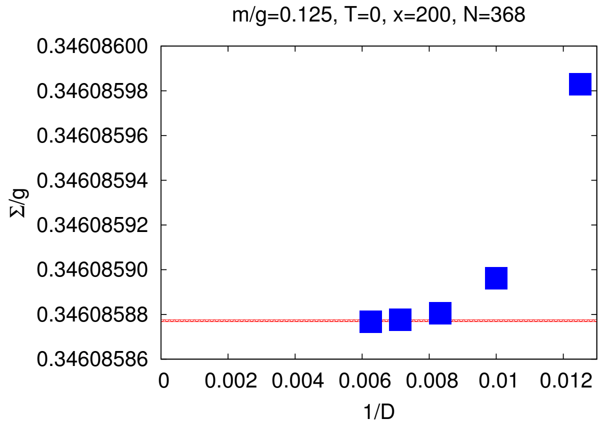

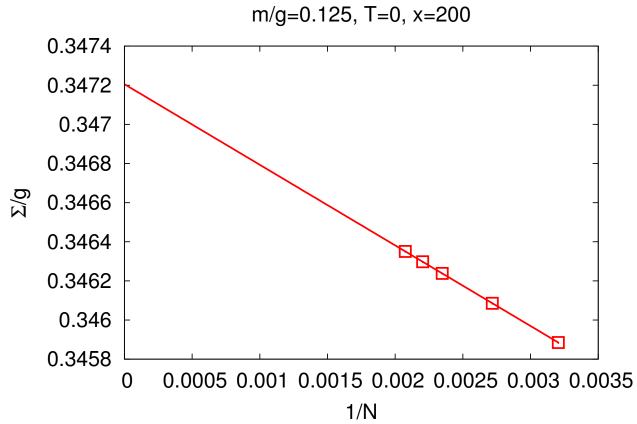

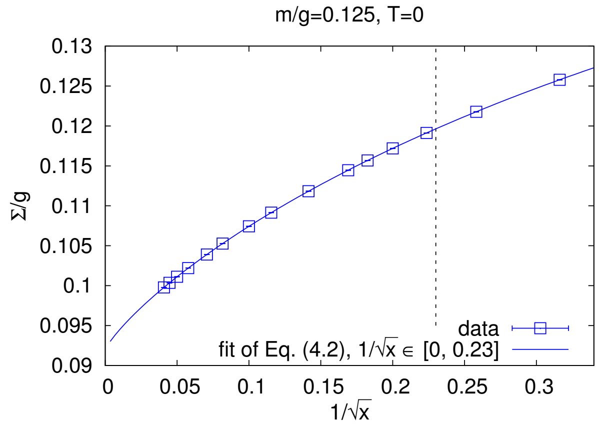

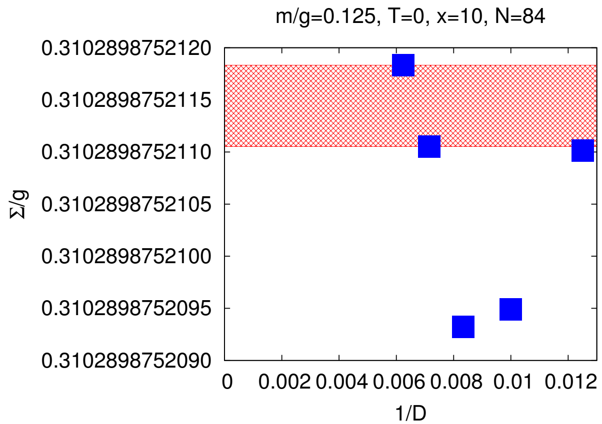

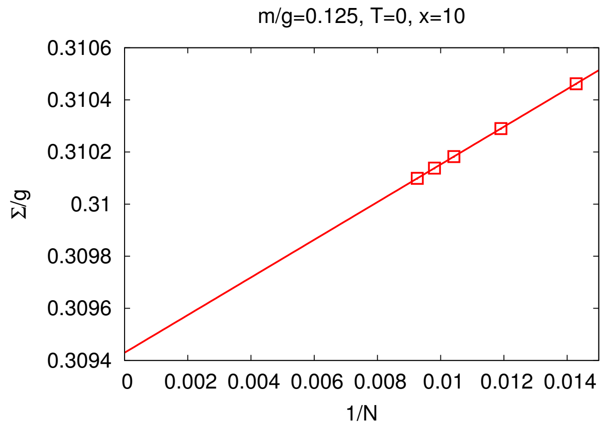

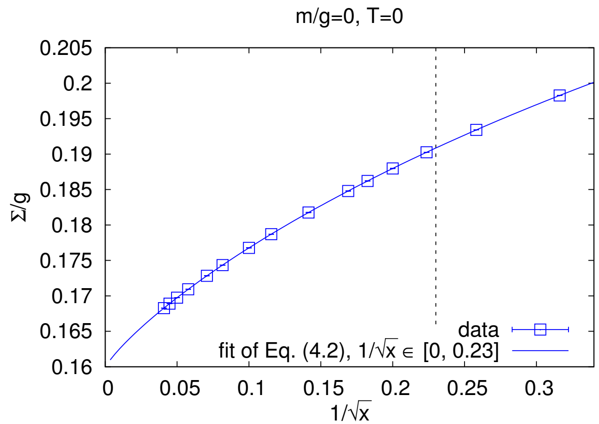

Truncation

Finite size scaling (linear in $1/N$)

Continuum extrapolation (quadratic in lat.spac., + log.-corrections)

	Subtracted condensate		
m/g	Our result MPS	Buyens et al. MPS	Exact ($m = 0$) or Hosotani ($m > 0$)
0	0.159929(7)	0.159929(1)	0.159929
0.0625	0.1139657(8)	–	0.1314
0.125	0.0920205(5)	0.092019(2)	0.1088
0.25	0.0666457(3)	0.066647(4)	0.0775
0.5	0.0423492(20)	0.042349(2)	0.0464
1.0	0.0238535(28)	0.023851(8)	0.0247

Exact result (massless case): $\frac{\Sigma}{g} = \frac{1}{2\pi^{3/2}} e^{\gamma_E} \approx 0.1599288$.

[K. Van Acoleyen, B. Buyens, J. Haegeman and F. Verstraete, "Matrix product states for Hamiltonian lattice gauge theories," PoS LATTICE **2014** (2014) 308]

[Y. Hosotani, "Chiral dynamics in weak, intermediate, and strong coupling QED in two-dimensions," In: Nagoya 1996, Perspectives of strong coupling gauge theories, 390-397 [hep-th/9703153].]

Computation of thermal states

Given some operator $\mathcal{O}$, we want to calculate its thermal expectation value:

$$\langle \mathcal{O} \rangle_\beta = \frac{\mathrm{Tr}\left(\mathcal{O}\rho(\beta)\right)}{\mathrm{Tr}\left(\rho(\beta)\right)},$$

where $\beta = 1/T$, $\rho(\beta) = e^{-\beta H}$ is the thermal density operator.

The MPO representation of $\rho(\beta)$:

$$\rho(\beta) = \sum_{\{i_k, j_k\}} \mathrm{Tr}\left(M[0]^{i_0 j_0} \cdots M[N-1]^{i_{N-1} j_{N-1}}\right) |i_0 \ldots i_{N-1}\rangle\langle j_0 \ldots j_{N-1}|$$

The resulting MPO will in general not be positive, as the truncation procedure does not guarantee positivity.
Therefore, we take: $\rho(\beta) = \rho(\beta/2)^\dagger \rho(\beta/2)$ to ensure positivity.

The MPO approximation to $\rho(\beta)$ can be computed using imaginary time evolution acting on the identity matrix, which corresponds (up to normalization) to the exact thermal state at $\beta = 0$, and is an MPO of bond dimension 1.

The MPO is vectorized and the procedure is illustrated as:

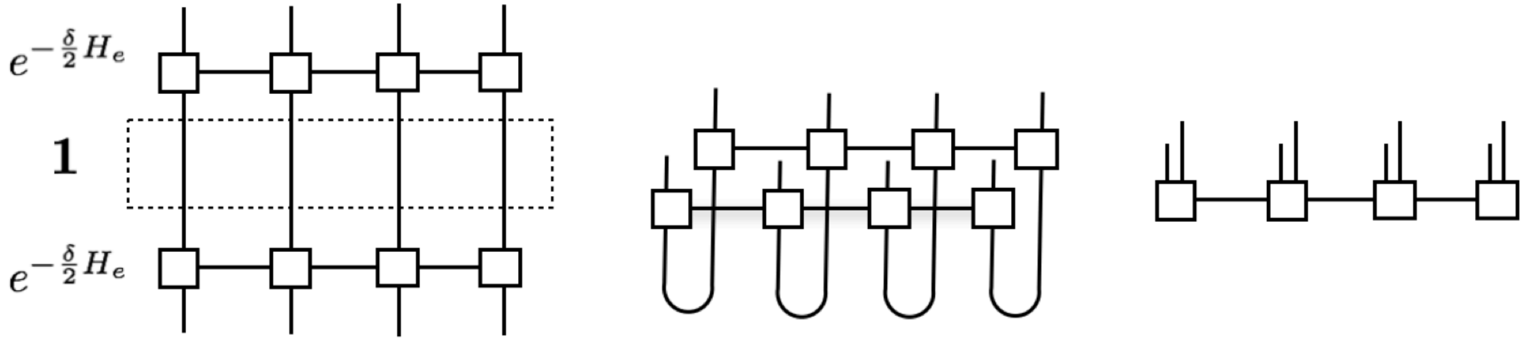

Computation of thermal states

- To apply the imaginary time evolution, we divide the interval $\beta/2$ into $N = \beta/\delta$ steps of length $\delta/2$:

$$\rho(\beta/2) = \underbrace{e^{-\frac{\delta}{2}H} \dots e^{-\frac{\delta}{2}H}}_{N=\beta/\delta \text{ times}}$$

- We apply 2nd order Trotter expansion:

$$e^{-\frac{\delta}{2}H} \approx e^{-\frac{\delta}{4}H_g} \underbrace{e^{-\frac{\delta}{2}(H_{hop}+H_{mass})}}_{\approx e^{-\frac{\delta}{4}H_e} e^{-\frac{\delta}{2}H_o} e^{-\frac{\delta}{4}H_e}} e^{-\frac{\delta}{4}H_g},$$

H_e/H_o – on even/odd sites

where:

$$H = \underbrace{x \sum_{n=0}^{N-2} \left(\sigma_n^+ e^{i\theta_n} \sigma_{n+1}^- + H.c.\right)}_{H_{hop}} + \underbrace{\mu \sum_{n=0}^{N-1} \left(1 + (-1)^n \sigma_n^3\right)}_{H_{mass}} + \underbrace{\sum_{n=0}^{N-2} \left(l + \frac{1}{2} \sum_{k=0}^{n} \left((-1)^k + \sigma_k^3\right)\right)^2}_{H_g}$$

- The exponentials of H_e/H_o can be written exactly as MPO of small bond dimension ($\chi = 4$).

Computation of thermal states

- The remaining term:

$$H_g = \sum_{n=0}^{N-2} \left(l + \frac{1}{2} \sum_{k=0}^{n} \left((-1)^k + \sigma_k^3 \right) \right)^2$$

  is more problematic: the long-range terms $\sigma_k^3 \sigma_l^3$ yields a bond dimension $N+1$.

- One can proceed in three ways:
  - ⋆ agree to $\chi = N+1$,
  - ⋆ Taylor expand H_g,
  - ⋆ truncate the MPO by allowing $L_n \leq L_{\text{cut}}$, so that the maximum bond dimension is $\chi = 2L_{\text{cut}} + 1$. This corresponds to a truncation of the physical space to only those spin configurations for which all links have small enough electric flux, since the rest will be projected out when multiplying by the truncated exponential.

- Starting from an initial MPS $|\psi\rangle_{\text{init}}$, the best MPS approximation $|\psi\rangle_{\text{MPS}}$ to the product $\mathcal{O}\,|\psi\rangle_{\text{init}}$ can be found by minimizing the distance

$$\Delta \equiv \left\| \mathcal{O}\,|\psi\rangle_{\text{init}} - |\psi\rangle_{\text{MPS}} \right\|^2 .$$

- In our case, we consider operators with an MPO description and the minimization is performed by varying one tensor at a time and sweeping back and forth over the chain until convergence.

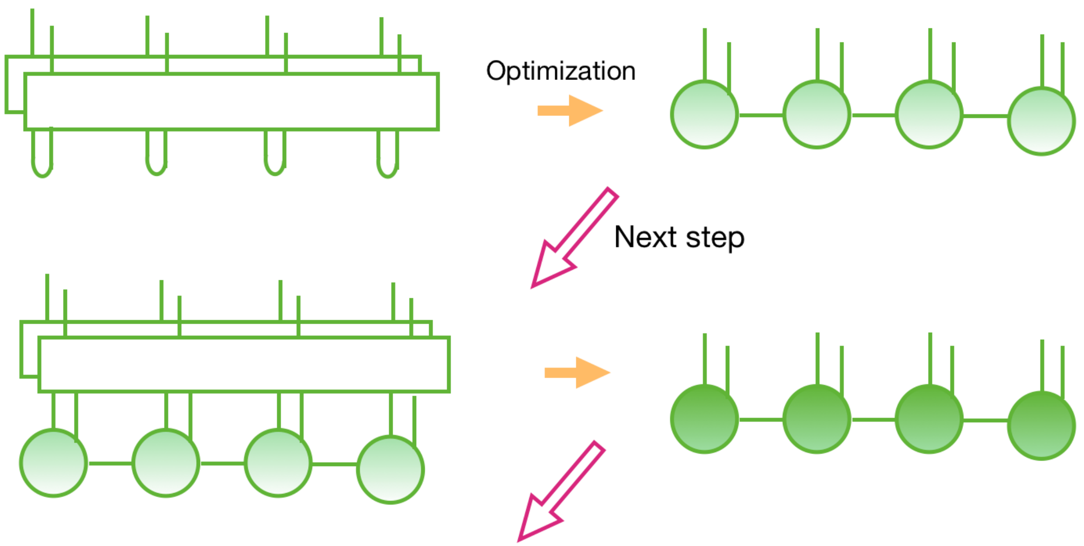

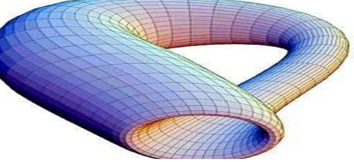

Thermal case – D and δ extrapolations

$$m/g = 0.25,\ g\beta = 0.5,\ L_{\text{cut}} = 10,\ x = 9,\ N = 60$$

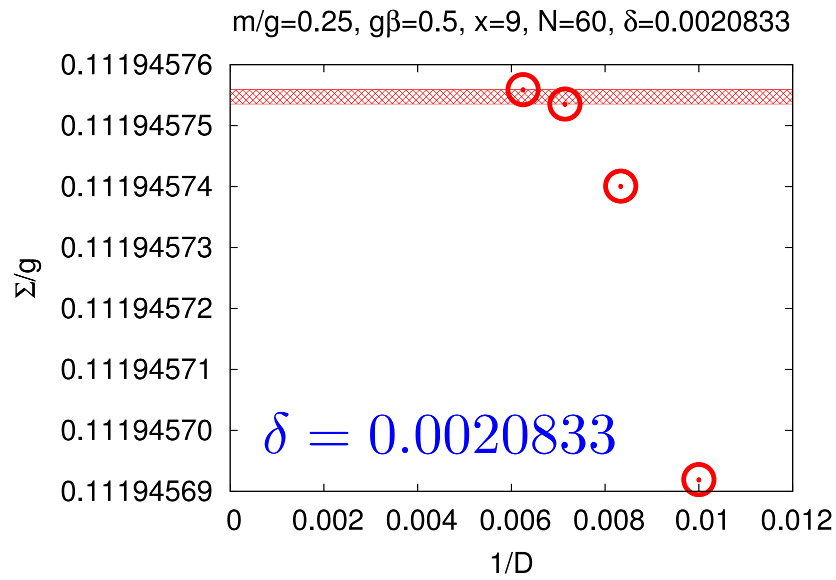

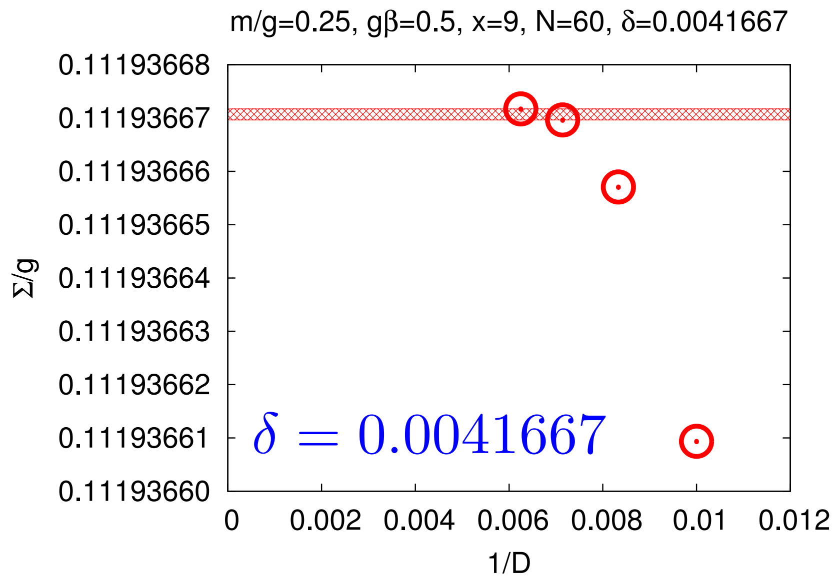

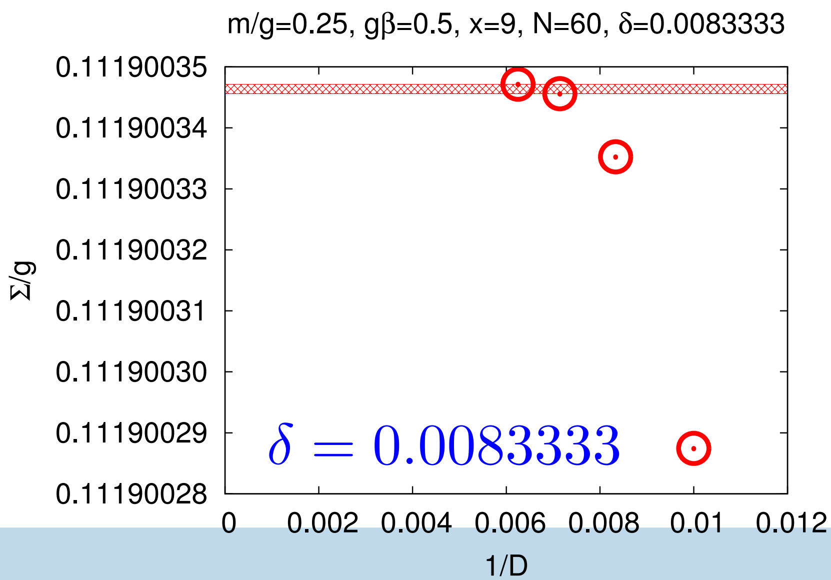

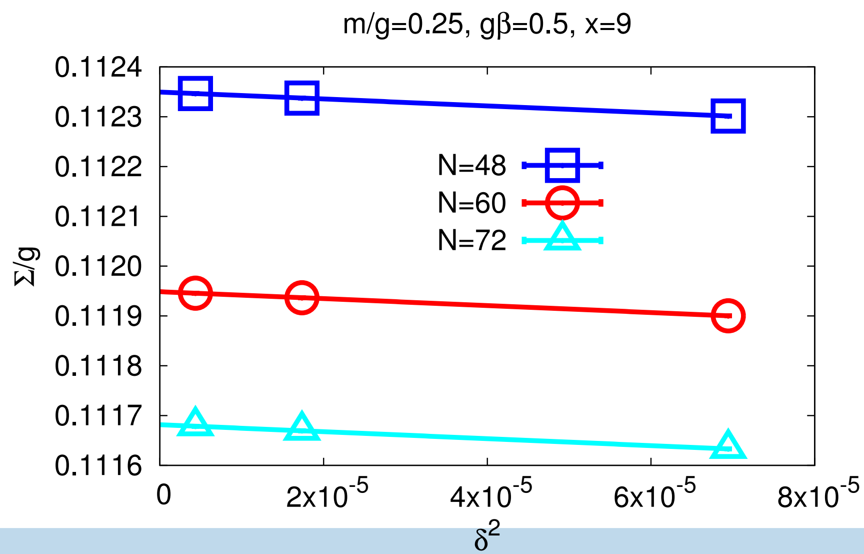

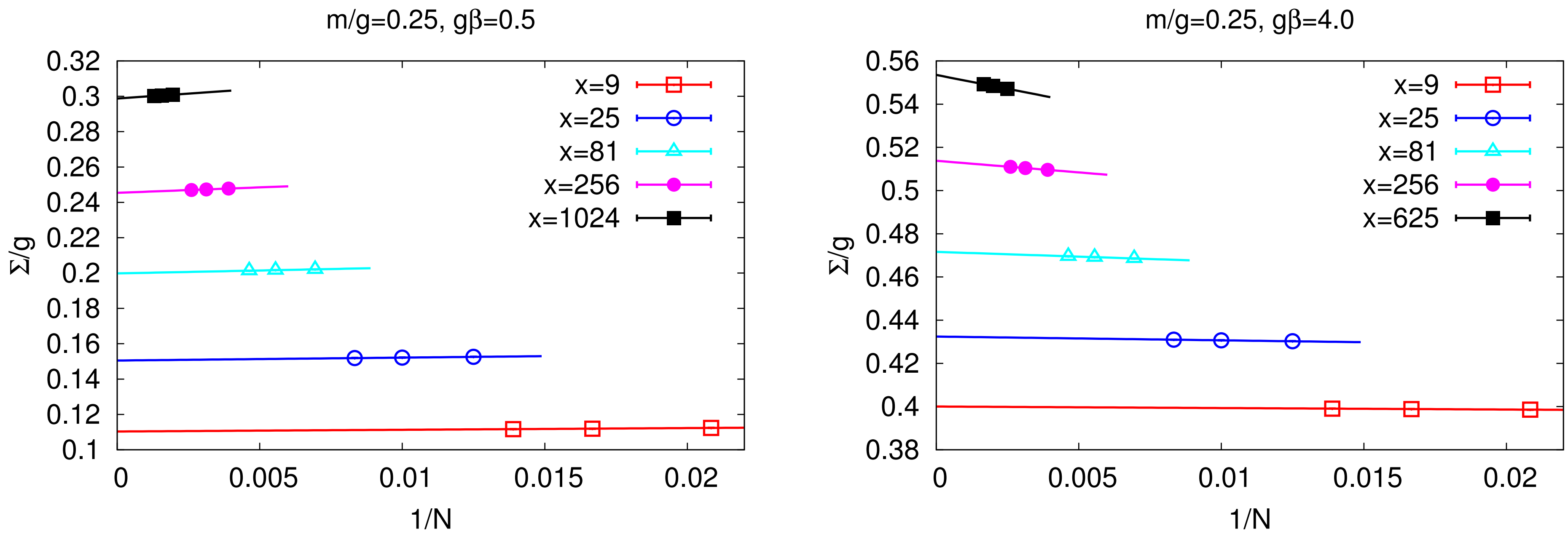

$L_{\mathrm{cut}} = 10$ – turns out to be enough, no extrapolation needed (values with $L_{\mathrm{cut}} = 8$ and $L_{\mathrm{cut}} = 12$ identical up to our precision).

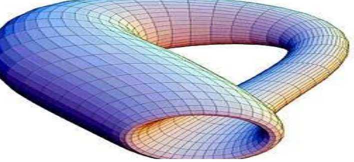

Thermal case – continuum extrapolation ($N_f = 1$)

Fitting Ansätze for continuum extrapolation:

- linear+log

$$\Sigma_{\rm subtr}(m/g,x) = \Sigma^{(1)}_{\rm subtr}(m/g) + \frac{a^{(1)}(m/g)}{\sqrt{x}}\log(x) + \frac{b^{(1)}(m/g)}{\sqrt{x}},$$

- quadratic+log

$$\Sigma_{\rm subtr}(m/g,x) = \Sigma^{(2)}_{\rm subtr}(m/g) + \frac{a^{(2)}(m/g)}{\sqrt{x}}\log(x) + \frac{b^{(2)}(m/g)}{\sqrt{x}} + \frac{c^{(2)}(m/g)}{x},$$

- cubic+log

$$\Sigma_{\rm subtr}(m/g,x) = \Sigma^{(3)}_{\rm subtr}(m/g) + \frac{a^{(3)}(m/g)}{\sqrt{x}}\log(x) + \frac{b^{(3)}(m/g)}{\sqrt{x}} + \frac{c^{(3)}(m/g)}{x} + \frac{d^{(3)}(m/g)}{x^{3/2}}$$

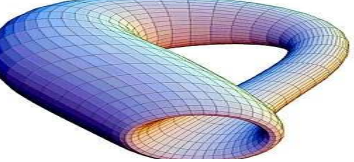

Thermal case – continuum extrapolation ($N_f = 1$)

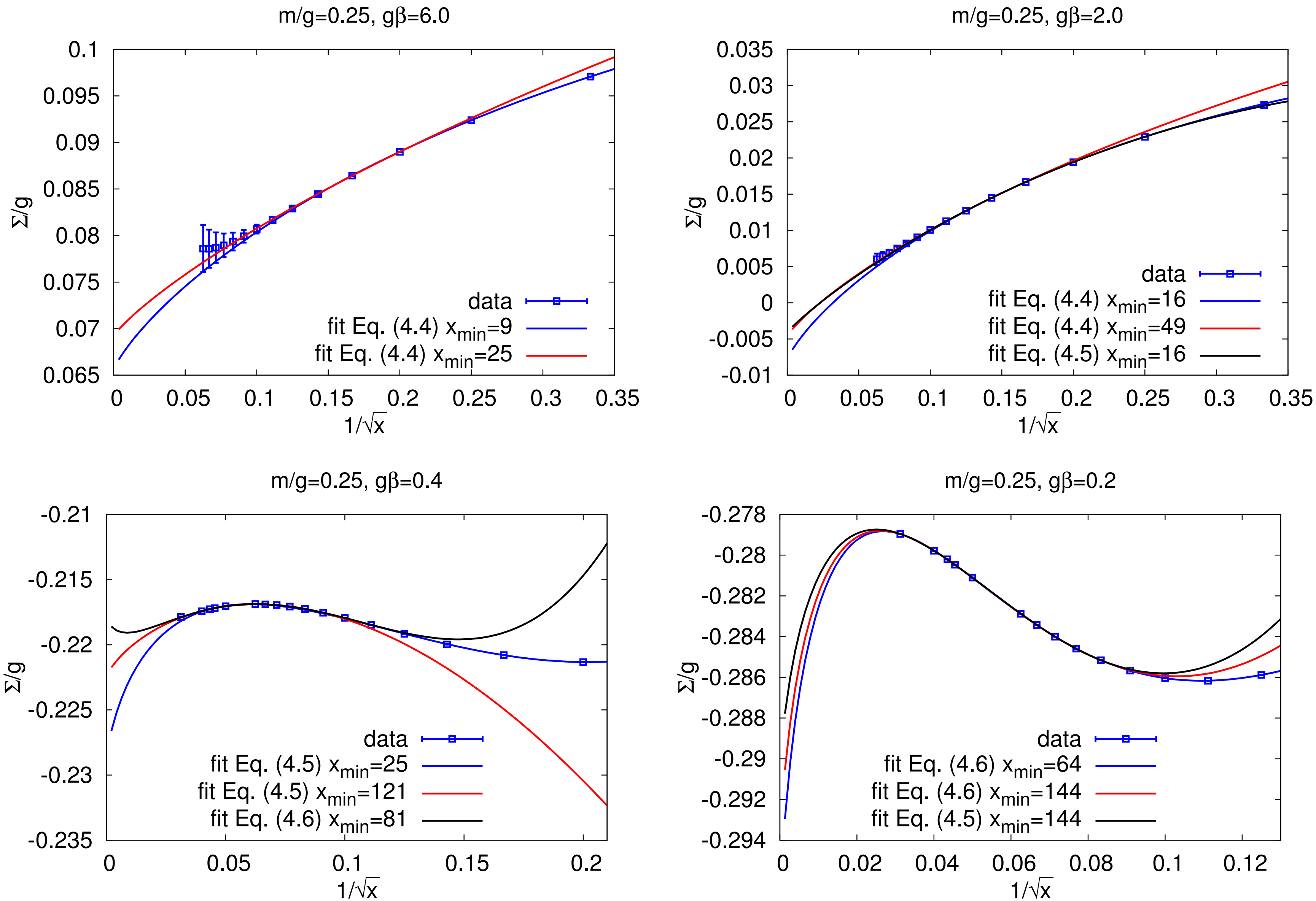

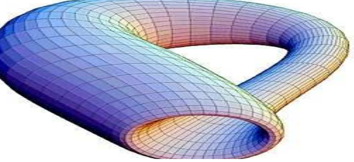

Temperature dependence ($N_f = 1$)

MASSLESS CASE

without flux truncation

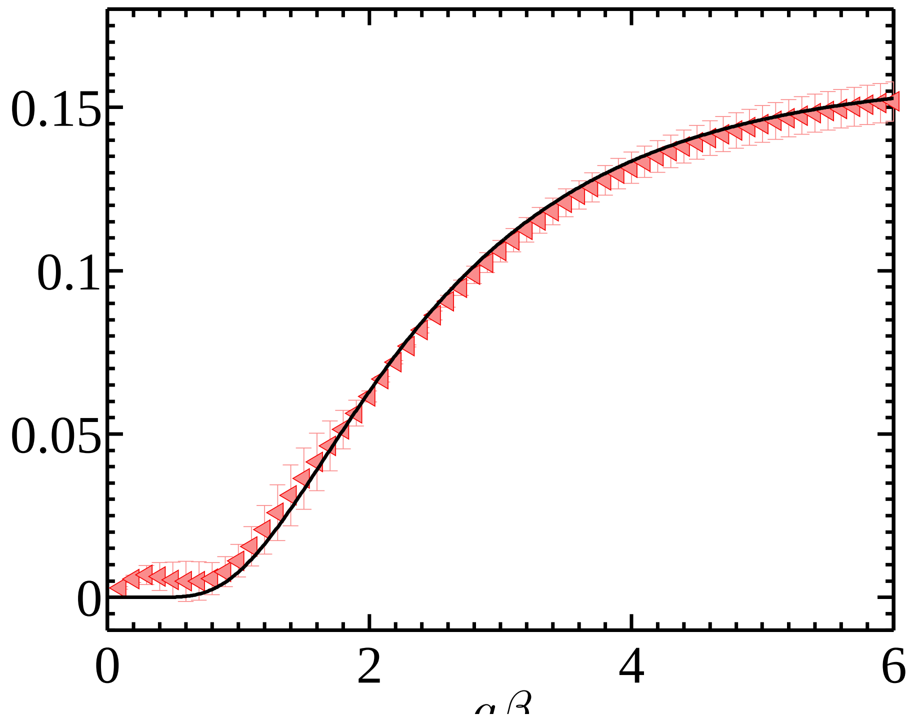

without/with flux truncation

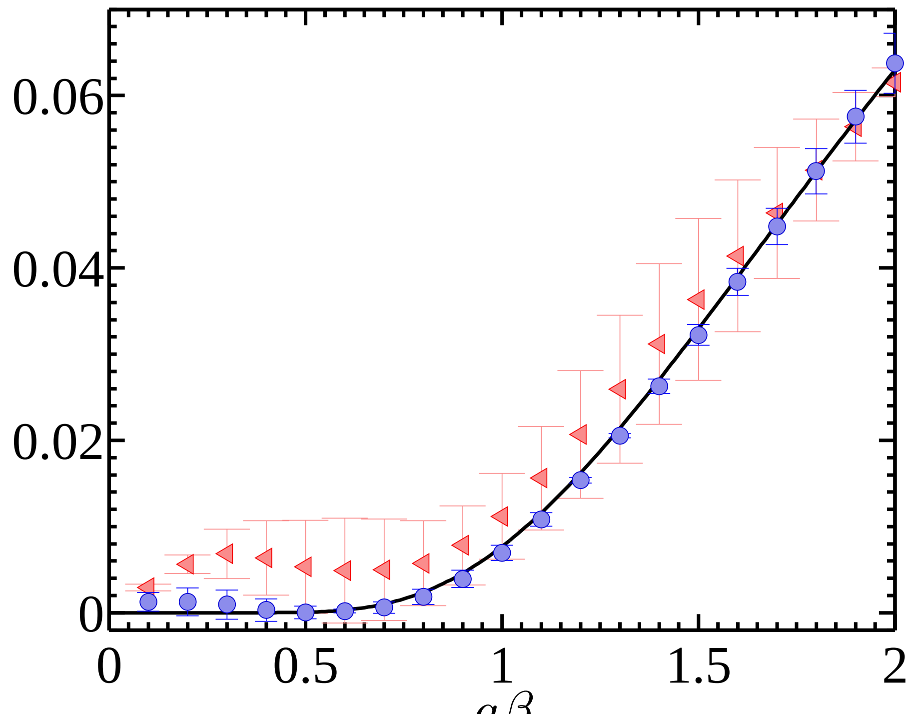

Analytical result from: [I. Sachs, A. Wipf, "Finite Temperature Schwinger Model," Helv. Phys. Acta 65, 652 (1992), arXiv:1005.1822 [hep-th]]

MASSIVE CASE

$m/g = 0.125$ $m/g = 0.5$

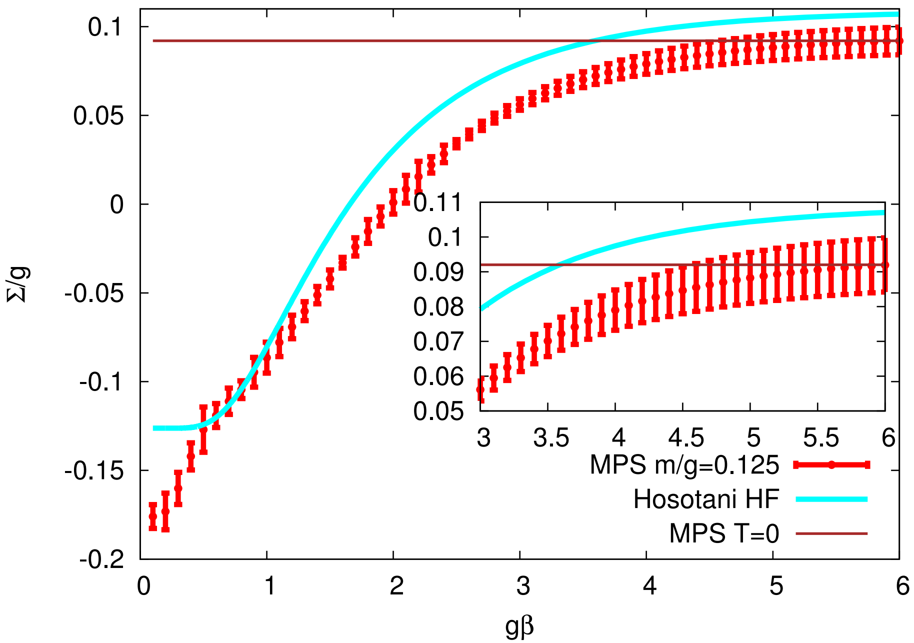

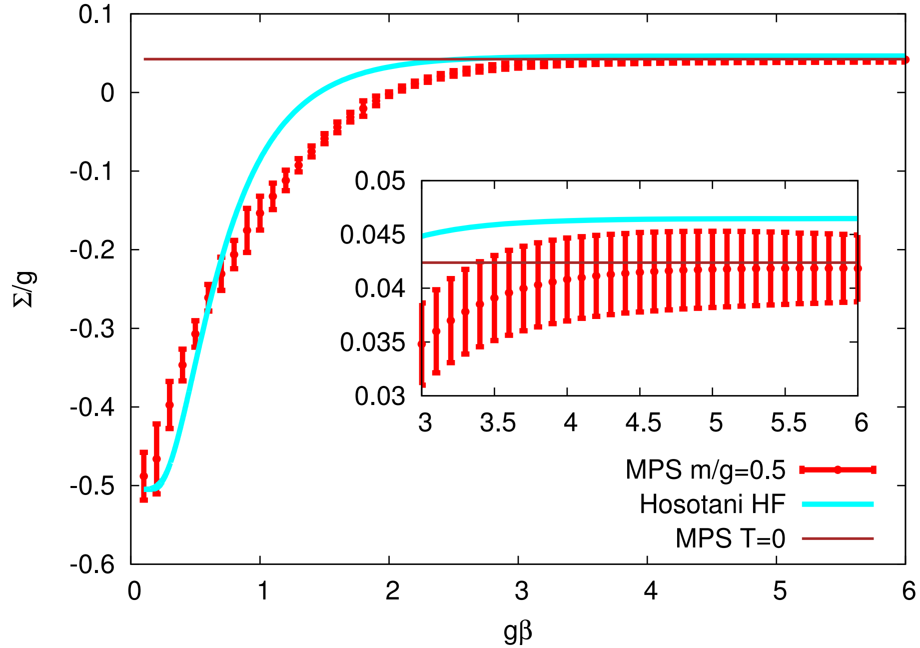

Reference curve (generalized Hartree-Fock approximation): [Y. Hosotani and R. Rodriguez, "Bosonized massive N flavor Schwinger model," J. Phys. A **31** (1998) 9925]